PB 207 103

MIXING HEIGHTS, WIND SPEEDS, AND POTENTIAL FOR URBAN AIR POLLUTION THROUGHOUT THE CONTIGUOUS UNITED STATES

Reproduced by
NATIONAL TECHNICAL
INFORMATION SERVICE
Springfield, Va. 22151

U. S. ENVIRONMENTAL PROTECTION AGENCY

BIBLIOGRAPHIC DATA SHEET	1. Report No. AP-101	2.	3. Recipient's Accession No.
4. Title and Subtitle Mixing Heights, Wind Speeds, and Potential for Urban Air Pollution Throughout the Contiguous United States			5. Report Date January 1972 6.
7. Author(s) George C. Holzworth			8. Performing Organization Rept. No.
9. Performing Organization Name and Address ENVIRONMENTAL PROTECTION AGENCY Office of Air Programs Division of Meteorology Research Triangle Park, North Carolina			10. Project/Task/Work Unit No. 11. Contract/Grant No.
12. Sponsoring Organization Name and Address Same.			13. Type of Report & Period Covered 14.

15. Supplementary Notes

16. Abstracts

A rough allowance was made for effects of the urban "heat Island" on the morning mixing heights. The morning and afternoon times coincide approximately with those of maximum and secondary minimum concentrations of slow-reacting pollutants in cities. These calculations illustrate the typical large diurnal variation in atmospheric dispersion. Twenty charts present seasonal and annual, and morning and afternoon mean mixing heights and wind speeds. A model of some general dispersion features over urban areas is described in which the normalized pollutant concentration averaged over a city is a function of mixing height, wind speed, and city size. Frequency values of mixing height by wind speed are used with the model to calculate average normalized concentration frequencies for each weather station. Thirty charts present isopleth analyses of seasonal and annual, and morning and afternoon normalized pollutant concentrations that were exceeded 10,25, and 50 percent of the time for specified city sizes.

17. Key Words and Document Analysis. 17a. Descriptors

Air pollution
Forecasting
Mathematical models
Urban areas
Meteorology
Wind velocity
Dispersing

17b. Identifiers/Open-Ended Terms

Air pollution forecasting
Episodes

17c. COSATI Field/Group 13B

18. Availability Statement	19. Security Class (This Report)	21. No. of Pages
Unlimited	UNCLASSIFIED	~~130~~ 126
	20. Security Class (This Page) UNCLASSIFIED	22. Price

MIXING HEIGHTS, WIND SPEEDS, AND POTENTIAL FOR URBAN AIR POLLUTION THROUGHOUT THE CONTIGUOUS UNITED STATES

George C. Holzworth
Division of Meteorology

ENVIRONMENTAL PROTECTION AGENCY
Office of Air Programs
Research Triangle Park, North Carolina

January 1972

The author is a meteorologist on assignment to the Environmental Protection Agency from the National Oceanic and Atmospheric Administration, U. S. Department of Commerce.

The AP series of reports is issued by the Office of Air Programs, Environmental Protection Agency, to report the results of scientific and engineering studies, and information of general interest in the field of air pollution. Information reported in this series includes coverage of Air Program intramural activities and of cooperative studies conducted in conjunction with state and local agencies, research institutes, and industrial organizations. Copies of AP reports are available free of charge as supplies permit from the Office of Technical Information and Publications, Office of Air Programs, Environmental Protection Agency, Research Triangle Park, North Carolina 27711.

For sale by the Superintendent of Documents, U.S. Government Printing Office, Washington, D.C., 20402 - Price $1.00

Office of Air Programs Publication No. AP-101

ACKNOWLEDGMENTS

Many staff members of the Division of Meteorology, which is under the direction of Robert A. McCormick, have contributed substantially to this study. In particular, the perceptive suggestions of Francis Pooler, Jr., and Kenneth L. Calder were indispensable. Extensive in-house automatic data processing was executed admirably by Adrian Busse. It has been a pleasure also to work with Richard Davis and Raymond Barr, of the National Climatic Center, who were instrumental in the preparation of the basic tabulations for this study.

CONTENTS

	Page
LIST OF FIGURES	v
LIST OF TABLES	x
ABSTRACT	xi
KEY WORDS	xi
INTRODUCTION	1
BASIC PARAMETERS: MIXING HEIGHT AND WIND SPEED	3
Concepts and Computation Methods	3
Tabulations and Availability	4
Mean Mixing Height and Wind Speeds	4
URBAN DISPERSION MODEL	9
POTENTIAL FOR URBAN AIR POLLUTION	13
Fifty-Percentile Concentrations	13
Twenty-Five-Percentile Concentrations	15
Ten-Percentile Concentrations	16
EPISODE-DAYS OF HIGH METEOROLOGICAL POTENTIAL	19
Episodes Lasting 2 Days or Longer	20
Episodes Lasting 5 Days or Longer	22
Forecast Episodes	22
SUMMARY AND CONCLUSIONS	23
APPENDIX A. NCC TABULATIONS OF MIXING HEIGHT AND WIND SPEED	97
APPENDIX B. ALLOWANCE FOR P-, C-, AND M-TYPE MIXING HEIGHTS AND WIND SPEEDS	107
APPENDIX C. DERIVATION OF URBAN DISPERSION MODEL	113
REFERENCES	117

LIST OF FIGURES

Figure		Page
1	Isopleths (m x 10^2) of mean *annual morning* mixing heights (see Table B-1 for data)	26
2	Isopleths (m x 10^2) of mean *winter morning* mixing heights (see Table B-1 for data)	27
3	Isopleths (m x 10^2) of mean *spring morning* mixing heights (see Table B-1 for data)	28
4	Isopleths (m x 10^2) of mean *summer morning* mixing heights (see Table B-1 for data)	29
5	Isopleths (m x 10^2) of mean *autumn morning* mixing heights (see Table B-1 for data)	30
6	Isopleths (m x 10^2) of mean *annual afternoon* mixing heights (see Table B-1 for data)	31
7	Isopleths (m x 10^2) of mean *winter afternoon* mixing heights (see Table B-1 for data)	32
8	Isopleths (m x 10^2) of mean *spring afternoon* mixing heights (see Table B-1 for data)	33
9	Isopleths (m x 10^2) of mean *summer afternoon* mixing heights (see Table B-1 for data)	34
10	Isopleths (m x 10^2) of mean *autumn afternoon* mixing heights (see Table B-1 for data)	35
11	Isopleths (m sec^{-1}) of mean *annual* wind speed averaged through the *morning* mixing layer (Figure 1)	36
12	Isopleths (m sec^{-1}) of mean *winter* wind speed averaged through the *morning* mixing layer (Figure 2)	37
13	Isopleths (m sec^{-1}) of mean *spring* wind speed averaged through the *morning* mixing layer (Figure 3)	38
14	Isopleths (m sec^{-1}) of mean *summer* wind speed averaged through the *morning* mixing layer (Figure 4)	39
15	Isopleths (m sec^{-1}) of mean *autumn* wind speed averaged through the *morning* mixing layer (Figure 5)	40
16	Isopleths (m sec^{-1}) of mean *annual* wind speed averaged through the *afternoon* mixing layer (Figure 6)	41
17	Isopleths (m sec^{-1}) of mean *winter* wind speed averaged through the *afternoon* mixing layer (Figure 7)	42
18	Isopleths (m sec^{-1}) of mean *spring* wind speed averaged through the *afternoon* mixing layer (Figure 8)	43
19	Isopleths (m sec^{-1}) of mean *summer* wind speed averaged through the *afternoon* mixing layer (Figure 9)	44
20	Isopleths (m sec^{-1}) of mean *autumn* wind speed averaged through the *afternoon* mixing layer (Figure 10)	45
21	Data and isopleths (sec m^{-1}) of *median annual morning* $\bar{\chi}/Q$ values (see text) for 10- (upper numerals and dashed isopleths) and 100-km (lower numerals and solid isopleths) city sizes	46
22	Data and isopleths (sec m^{-1}) of *median winter morning* χ/Q values (see text) for 10- (upper numerals and dashed isopleths and 100-km (lower numerals and solid isopleths) city sizes	47
23	Data and isopleths (sec m^{-1}) of *median spring morning* $\bar{\chi}/Q$ values (see text) for 10- (upper numerals and dashed isopleths) and 100-km (lower numerals and solid isopleths) city sizes	48
24	Data and isopleths (sec m^{-1}) of *median summer morning* $\bar{\chi}/Q$ values (see text) for 10- (upper numerals and dashed isopleths) and 100-km (lower numerals and solid isopleths) city sizes	49
25	Data and isopleths (sec m^{-1}) of *median autumn morning* $\bar{\chi}/Q$ values (see text) for 10- (upper numerals and dashed isopleths) and 100-km (lower numerals and solid isopleths) city sizes	50
26	Data and isopleths (sec m^{-1}) of *median annual afternoon* χ/Q values (see text) for 10- (upper numerals) and 100-km (lower numerals and solid isopleths) city sizes	51
27	Data and isopleths (sec m^{-1}) of *median winter afternoon* $\bar{\chi}/Q$ values (see text) for 10- (upper numerals) and 100-km (lower numerals and solid isopleths) city sizes	52

28 Data and isopleths (sec m^{-1}) of *median spring afternoon* χ/Q values (see text) for 10- (upper numerals) and 100-km (lower numerals and solid isopleths) city sizes 53
29 Data and isopleths (sec m^{-1}) of *median summer afternoon* χ/Q values (see text) for 10- (upper numerals) and 100-km (lower numerals and solid isopleths) city sizes 54
30 Data and isopleths (sec m^{-1}) of *median autumn afternoon* χ/Q values (see text) for 10- (upper numerals) and 100-km (lower numerals and solid isopleths) city sizes 55
31 Data and isopleths (sec m^{-1}) of upper *quartile annual morning* χ/Q values (see text) for 10- (upper numerals and dashed isopleths) and 100-km (lower numerals and solid isopleths) city sizes 56
32 Data and isopleths (sec m^{-1}) of upper *quartile winter morning* χ/Q values (see text) for 10- (upper numerals and dashed isopleths) and 100-km (lower numerals and solid isopleths) city sizes 57
33 Data and isopleths (sec m^{-1}) of upper *quartile spring morning* χ/Q values (see text) for 10- (upper numerals and dashed isopleths) and 100-km (lower numerals and solid isopleths) city sizes 58
34 Data and isopleths (sec m^{-1}) of upper *quartile summer morning* χ/Q values (see text) for 10- (upper numerals and dashed isopleths) and 100-km (lower numerals and solid isopleths) city sizes 59
35 Data and isopleths (sec m^{-1}) of upper *quartile autumn morning* χ/Q values (see text) for 10- (upper numerals and dashed isopleths) and 100-km (lower numerals and solid isopleths) city sizes 60
36 Data and isopleths (sec m^{-1}) of upper *quartile annual afternoon* χ/Q values (see text) for 10- (upper numerals) and 100-km (lower numerals and solid isopleths) city sizes 61
37 Data and isopleths (sec m^{-1}) of upper *quartile winter afternoon* χ/Q values (see text) for 10- (upper numerals and dashed isopleths) and 100-km (lower numerals and solid isopleths) city sizes 62
38 Data and isopleths (sec m^{-1}) of upper *quartile spring afternoon* χ/Q values (see text) for 10- (upper numerals) and 100-km (lower numerals and solid isopleths) city sizes 63
39 Data and isopleths (sec m^{-1}) of upper *quartile summer afternoon* χ/Q values (see text) for 10- (upper numerals) and 100-km (lower numerals and solid isopleths) city sizes 64
40 Data and isopleths (sec m^{-1}) of upper *quartile autumn afternoon* χ/Q values (see text) for 10- (upper numerals) and 100-km (lower numerals and solid isopleths) city sizes 65
41 Data and isopleths (sec m^{-1}) of upper *decile annual morning* χ/Q values (see text) for 10- (upper numerals and dashed isopleths) and 100-km (lower numerals and solid isopleths) city sizes 66
42 Data and isopleths (sec m^{-1}) of upper *decile winter morning* χ/Q values (see text) for 10- (upper numerals and dashed isopleths) and 100-km (lower numerals and solid isopleths) city sizes 67
43 Data and isopleths (sec m^{-1}) of upper *decile spring morning* χ/Q values (see text) for 10- (upper numerals and dashed isopleths) and 100-km (lower numerals and solid isopleths) city sizes 68
44 Data and isopleths (sec m^{-1}) of upper *decile summer morning* χ/Q values (see text) for 10- (upper numerals and dashed isopleths) and 100-km (lower numerals and solid isopleths) city sizes 69
45 Data and isopleths (sec m^{-1}) of upper *decile autumn morning* χ/Q values (see text) for 10- (upper numerals and dashed isopleths) and 100-km (lower numerals and solid isopleths) city sizes 70
46 Data and isopleths (sec m^{-1}) of upper *decile annual afternoon* χ/Q (see text) for 10- (upper numerals and dashed isopleths) and 100-km (lower numerals and solid isopleths) city sizes 71
47 Data and isopleths (sec m^{-1}) of upper *decile winter afternoon* χ/Q values (see text) for 10- (upper numerals and dashed isopleths) and 100-km (lower numerals and solid isopleths) city sizes 72

48 Data and isopleths (sec m^{-1}) of upper *decile spring afternoon* $\bar{\chi}/Q$ values (see text) for 10- (upper numerals) and 100-km (lower numerals and solid isopleths) city sizes 73
49 Data and isopleths (sec m^{-1}) of upper *decile summer afternoon* $\bar{\chi}/Q$ values (see text) for 10- (upper numerals and 100-km (lower numerals and solid isopleths) city sizes 74
50 Data and isopleths (sec m^{-1}) of upper *decile autumn afternoon* $\bar{\chi}/Q$ values (see text) for 10- (upper numerals and dashed isopleths) and 100-km (lower numerals and solid isopleths) city sizes 75
51 Isopleths of total number of episode-days in 5 years with mixing heights $\leq$ *500 m*, wind speeds $\leq$ *2.0 m sec*$^{-1}$, and no significant precipitation (see text) – for episodes lasting at least *2 days*. Numerals on left and right give total number of episodes and episode-days, respectively. Season with greatest number of episode-days indicated as W (winter), SP (spring), SU (summer), or A (autumn) 76
52 Isopleths of total number of episode-days in 5 years with mixing heights $\leq$ *500 m*, wind speeds $\leq$ *4.0 m sec*$^{-1}$, and no significant precipitation (see text) – for episodes lasting at least *2 days*. Numerals on left and right give total number of episodes and episode-days, respectively. Season with greatest number of episode-days indicated as W (winter), SP (spring), SU (summer), or A (autumn) 77
53 Isopleths of total number of episode-days in 5 years with mixing heights $\leq$ *500 m*, wind speeds $\leq$ *6.0 m sec*$^{-1}$, and no significant precipitation (see text) – for episodes lasting at least *2 days*. Numerals on left and right give total number of episodes and episode-days, respectively. Season with greatest number of episode-days indicated as W (winter), SP (spring), SU (summer), or A (autumn) 78
54 Isopleths of total number of episode-days in 5 years with mixing heights $\leq$ *1000 m*, wind speeds $\leq$ *2.0 m sec*$^{-1}$, and no significant precipitation (see text) – for episodes lasting at least *2 days*. Numerals on left and right give total number of episodes and episode-days, respectively. Season with greatest number of episode-days indicated as W (winter), SP (spring), SU (summer), or A (autumn) 79
55 Isopleths of total number of episode-days in 5 years with mixing heights $\leq$ *1000 m*, wind speeds $\leq$ *4.0 m sec*$^{-1}$, and no significant precipitation (see text) – for episodes lasting at least *2 days*. Numerals on left and right give total number of episodes and episode-days, respectively. Season with greatest number of episode-days indicated as W (winter), SP (spring), SU (summer), or A (autumn) 80
56 Isopleths of total number of episode-days in 5 years with mixing heights $\leq$ *1000 m*, wind speeds $\leq$ *6.0 m sec*$^{-1}$, and no significant precipitation (see text) – for episodes lasting at least *2 days*. Numerals on left and right give total number of episodes and episode-days, respectively. Season with greatest number of episode-days indicated as W (winter), SP (spring), SU (summer), or A (autumn) 81
57 Isopleths of total number of episode-days in 5 years with mixing heights $\leq$ *1500 m*, wind speeds $\leq$ *2.0 m sec*$^{-1}$, and no significant precipitation (see text) – for episodes lasting at least *2 days*. Numerals on left and right give total number of episodes and episode-days, respectively. Season with greatest number of episode-days indicated as W (winter), SP (spring), SU (summer), or A (autumn) 82
58 Isopleths of total number of episode-days in 5 years with mixing heights $\leq$ *1500 m*, wind speeds $\leq$ *4.0 m sec*$^{-1}$, and no significant precipitation (see text) – for episodes lasting at least *2 days*. Numerals on left and right give total number of episodes and episode-days, respectively. Season with greatest number of episode-days indicated as W (winter), SP (spring), SU (summer), or A (autumn) 83
59 Isopleths of total number of episode-days in 5 years with mixing heights $\leq$ *1500 m*, wind speeds $\leq$ *6.0 m sec*$^{-1}$, and no significant precipitation (see text) – for episodes lasting at least *2 days*. Numerals on left and right give total number of episodes and episode-days, respectively. Season with greatest number of episode-days indicated as W (winter), SP (spring), SU (summer), or A (autumn) 84

60 Isopleths of total number of episode-days in 5 years with mixing heights ⩽ *2000 m*, wind speeds ⩽ *2.0 m sec*$^{-1}$, and no significant precipitation (see text) – for episodes lasting at least *2 days*. Numerals on left and right give total number of episodes and episode-days, respectively. Season with greatest number of episode-days indicated as W (winter), SP (spring), SU (summer), or A (autumn) 85

61 Isopleths of total number of episode-days in 5 years with mixing heights ⩽ *2000 m*, wind speeds ⩽ *4.0 m sec*$^{-1}$, and no significant precipitation (see text) – for episodes lasting at least *2 days*. Numerals on left and right give total number of episodes and episode-days, respectively. Season with greatest number of episode-days indicated as W (winter), SP (spring), SU (summer), or A (autumn) 86

62 Isopleths of total number of episode-days in 5 years with mixing heights ⩽ *2000 m*, wind speeds ⩽ *6.0 m sec*$^{-1}$, and no significant precipitation (see text) – for episodes lasting at least *2 days*. Numerals on left and right give total number of episodes and episode-days, respectively. Season with greatest number of episode-days indicated as W (winter), SP (spring), SU (summer), or A (autumn) 87

63 Isopleths of total number of episode-days in 5 years with mixing heights ⩽ *500 m*, wind speeds ⩽ *4.0 m sec*$^{-1}$, and no significant precipitation (see text) – for episodes lasting at least *5 days*. Numerals on left and right give total number of episodes and episode-days, respectively. Season with greatest number of episode-days indicated as W (winter), SP (spring), SU (summer), or A (autumn) 88

64 Isopleths of total number of episode-days in 5 years with mixing heights ⩽ *500 m*, wind speeds ⩽ *6.0 m sec*$^{-1}$, and no significant precipitation (see text) – for episodes lasting at least *5 days*. Numerals on left and right give total number of episodes and episode-days, respectively. Season with greatest number of episode-days indicated as W (winter), SP (spring), SU (summer), or A (autumn) 89

65 Isopleths of total number of episode-days in 5 years with mixing heights ⩽ *1000 m*, wind speeds ⩽ *4.0 m sec*$^{-1}$, and no significant precipitation (see text) – for episodes lasting at least *5 days*. Numerals on left and right give total number of episodes and episode-days, respectively. Season with greatest number of episode-days indicated as W (winter), SP (spring), SU (summer), or A (autumn) 90

66 Isopleths of total number of episode-days in 5 years with mixing heights ⩽ *1000 m*, wind speeds ⩽ *6.0 m sec*$^{-1}$, and no significant precipitation (see text) – for episodes lasting at least *5 days*. Numerals on left and right give total number of episodes and episode-days, respectively. Season with greatest number of episode-days indicated as W (winter), SP (spring), SU (summer), or A (autumn) 91

67 Isopleths of total number of episode-days in 5 years with mixing heights ⩽ *1500 m*, wind speeds ⩽ *4.0 m sec*$^{-1}$, and no significant precipitation (see text) – for episodes lasting at least *5 days*. Numerals on left and right give total number of episodes and episode-days, respectively. Season with greatest number of episode-days indicated as W (winter), SP (spring), SU (summer), or A (autumn) 92

68 Isopleths of total number of episode-days in 5 years with mixing heights ⩽ *1500 m*, wind speeds ⩽ *6.0 m sec*$^{-1}$, and no significant precipitation (see text) – for episodes lasting at least *5 days*. Numerals on left and right give total number of episodes and episode-days, respectively. Season with greatest number of episode-days indicated as W (winter), SP (spring), SU (summer), or A (autumn) 93

69 Isopleths of total number of episode-days in 5 years with mixing heights ⩽ *2000 m*, wind speeds ⩽ *4.0 m sec*$^{-1}$, and no significant precipitation (see text) – for episodes lasting at least *5 days*. Numerals on left and right give total number of episodes and episode-days, respectively. Season with greatest number of episode-days indicated as W (winter), SP (spring), SU (summer), or A (autumn) 94

70 Isopleths of total number of episode-days in 5 years with mixing heights $\leq$ *2000 m*, wind speeds $\leq$ *6.0 m sec*$^{-1}$, and no significant precipitation (see text) – for episodes lasting at least *5 days*. Numerals on left and right give total number of episodes and episode-days, respectively. Season with greatest number of episode-days indicated as W (winter), SP (spring), SU (summer), or A (autumn) 95

71 Isopleths of total number of forecast-days of high meteorological potential for air pollution in a 5-year period. Data are based on forecasts issued since the program began, 1 August 1960 and 1 October 1963 for eastern and western parts of the United States, respectively, through 3 April 1970 96

C-1 Variations of $\bar{\chi}/\bar{Q}$ (see text) with city size (S) for various combinations of mixing height (H) and wind speed (U) 116

LIST OF TABLES

Table		Page
1	Average Normalized Concentration, X/Q (sec m^{-1})	10
2	Episodes Lasting 5 or More Days with Wind Speed $\leq$ 2 m sec^{-1}	19
3	Rank of Reciprocals of H x U	20
A-1	Mixing Height and Wind Speed Tabulations Prepared by the National Climatic Center	99
A-2	Example of National Climatic Center Tabulation III, Daily X/Q Values	102
A-3	Example of National Climatic Center Tabulation III, Seasonal Mean Values	103
A-4	Example of National Climatic Center Tabulation II, Episodes	104
A-5	Example of National Climatic Center Tabulation I, Mixing Heights by Wind Speeds	105
B-1	Mean Seasonal and Annual Morning and Afternoon Mixing Heights (Hi) and Wind Speeds (U) for NOP and All Cases	108

ABSTRACT

The mixing-layer height and the average wind speed within the mixing layer were calculated twice for each day of a 5-year record of upper air observations at 62 National Weather Service stations in the contiguous United States. The times of day of these calculations are morning and mid-afternoon. A rough allowance was made for effects of the urban "heat island" on the morning mixing heights. The morning and afternoon times coincide approximately with those of maximum and secondary minimum concentrations of slow-reacting pollutants in cities. These calculations illustrate the typical large diurnal variation in atmospheric dispersion. Twenty charts present seasonal and annual, and morning and afternoon mean mixing heights and wind speeds.

A model of some general dispersion features over urban areas is described in which the normalized pollutant concentration averaged over a city is a function of mixing height, wind speed, and city size (distance the wind travels across the city). Frequency values of mixing height by wind speed are used with the model to calculate average normalized concentration frequencies for each weather station. Thirty charts present isopleth analyses of seasonal and annual, and morning and afternoon normalized pollutant concentrations that were exceeded 10, 25, and 50 percent of the time for specified city sizes.

The occurrence of episodes during which upper limits on mixing height and wind speed were not exceeded were determined from the daily morning and afternoon values of these parameters. Isopleths of the total number of episode-days for episodes lasting at least 2 days and at least 5 days with various limiting mixing-height and wind-speed values are presented in 20 charts.

KEY WORDS: Meteorology, air pollution forecasting, mathematical modeling, urban areas, mixing height, wind speed

MIXING HEIGHTS, WIND SPEEDS, AND POTENTIAL FOR URBAN AIR POLLUTANT THROUGHOUT THE CONTIGUOUS UNITED STATES

INTRODUCTION

Recognition that community air pollution in the United States is a growing national problem has generated interest in pertinent climatological information and an overall appraisal thereof in terms of quantitative pollution potential. As used here, the *potential* for urban air pollution refers to certain meteorological factors that generally are important in the transport and diffusion of pollutants emitted by myriad but non-trivial sources in urban complexes. While a comprehensive and uniform climatology of air pollution potential for all major urban centers would be invaluable, its preparation is precluded mainly by a lack of adequate detailed meteorological data.

The present study is based primarily upon regular measurements of temperature and winds aloft at 62 National Weather Service (NWS) stations throughout the 48 contiguous states. The spacing of these stations, which is roughly 400 kilometers (km), establishes the overall resolution of spatial analyses. Since these upper-air data provide only very general indications of real diffusion and transport patterns in the urban boundary layer, which in fact are often highly complex, the results of this study should be recognized as only a general or large-scale appraisal of community air pollution potential. It is hoped that more detailed local investigations will follow.

Although prior investigations have made noteworthy contributions to the climatology of air pollution potential, they have usually dealt only with certain aspects of the subject, often in a qualitative manner, and/or have been limited to a particular location or section of the country. For example, Korshover's (1967) study of stagnating anticyclones was categorical and was restricted to the area east of the Rockies; Hosler's (1961) low-level inversion and wind-speed frequencies and Holzworth's (1964b) maximum mixing depths each dealt mainly with the indicated parameters. Hosler (1964) presented available data according to geographic areas of the United States, but made no attempt to evaluate the combined effects of the various dispersion parameters. Such an evaluation was attempted by Holzworth (1964a), but it was based on an arbitrary classification system and only considered data for two regions. More recently a quantitative appraisal of air pollution potential has been presented (Holzworth, 1967) for a few selected locations. The same general approach will be followed in this study but will be applied to the contiguous United States. Mixing-height and wind-speed data will be presented and discussed. A simple mathematical model of urban diffusion that yields normalized pollutant concentrations averaged over a city as a function of mixing height, wind speed, and city size will be described, and frequency tables of mixing height by wind speed will be used in the model to generate frequencies of normalized pollutant concentrations for different city sizes. A brief summary of this study was presented recently by Holzworth (1970).

Figures discussed in the main body of this study are grouped together after the Summary and Conclusions; tables and figures for each appendix are grouped at the end of the respective appendices to facilitate reference to them.

BASIC PARAMETERS: MIXING HEIGHT AND WIND SPEED

CONCEPTS AND COMPUTATION METHODS

The mixing height (or depth) is defined as the height above the surface through which relatively vigorous vertical mixing occurs. The concept of a mixing layer in which the lapse rate is roughly dry adiabatic (unsaturated conditions) is well founded on general theoretical principles and on practical grounds through operational use over several years in the National Air Pollution Potential Forecasting Program (Stackpole, 1967; Gross, 1970). Commonly, mixing heights go through a large diurnal variation. Although not measured directly, they can be calculated approximately from routine meteorological measurements. This study centers on two times of the day, morning and afternoon. The morning mixing height is calculated as the height above ground at which the dry adiabatic extension of the morning minimum surface temperature plus 5°C intersected the vertical temperature profile observed at 1200 Greenwich Median Time (GMT). The minimum temperature is determined from the regular hourly airways reports from 0200 through 0600 Local Standard Time (LST). The "plus 5°C" is intended to allow roughly for the usual effects of the nocturnal and early morning urban heat island since NWS upper-air-measuring stations are located in rural or suburban surroundings. Thus, more properly, the *urban* morning mixing height was calculated. The general notion of an urban nocturnal and morning mixing layer, which in reality is often highly complex, is now fairly well established by the investigations of Duckworth and Sandberg (1954), DeMarrais (1961), Summers (1967), and Clark (1969). The value of 5°C was determined arbitrarily after inspection of urban-rural differences in minimum temperature for many locations. The individual differences varied over a large range and undoubtedly depended upon a number of factors. For general application, however, 5°C is considered a slight over-estimate of an overall average minimum temperature difference – even for existing large cities. For purposes of this report the plus 5°C is interpreted to include the effects of some surface heating shortly after sunrise. Thus, the time of the urban morning mixing height coincides approximately with that of the typical diurnal maximum concentration of slow-reacting pollutants in many cities, occurring around the morning commuter rush hours. This treatment of the urban morning mixing height undoubtedly is a gross simplification of the real situation, but it is considered reasonable for the climatological purposes of this study.

The afternoon mixing height is less complicated than the morning, but was calculated in the same way, except that instead of the minimum temperature plus 5°C, the maximum surface temperature observed from 1200 through 1600 LST was used. Urban-rural differences of maximum surface temperature were assumed negligible. The typical time of the afternoon mixing height may be considered to coincide approximately with the usual mid-afternoon minimum concentration of slow-reacting urban pollutants.

The method described for determining the height of the afternoon mixing (or boundary) layer has been compared with other methods by Hanna (1969), who found it to be the more practical. In addition, mixing heights based on accelerometer and temperature measurements made with a light aircraft during daytime have been found by McCaldin and Sholtes (1970) to be in good agreement with heights calculated as indicated herein (except that McCaldin and Sholtes' calculated heights also made allowance for temperature advection aloft).

Wind speeds for both morning and afternoon were computed as arithmetic averages of speeds observed at the surface and aloft within the mixing layer. Speeds aloft were available for 150 and 300 meters (m) above station elevation and for 500, 1000, 1500, 2000, 2500, 3000, 4000 m, etc., above sea level. To prevent wind

Preceding page blank

speeds near the same level from being used twice (e.g., as for a station at 190 m above sea level) only winds separated by at least 150 m were used. Morning wind-speed calculations were based on speeds observed aloft at 1200 GMT and an average of the surface speeds observed (regular hourly airways) from 0200 through 0600 LST. Afternoon average speeds were based on the speeds observed aloft at 0000 GMT and the average surface speed from 1200 through 1600 LST. In this report the vertically averaged wind speeds are referred to simply as wind speeds when there is no ambiguity.

In the mixing-height calculations, especially for afternoons, it was assumed implicitly that between the time of a temperature-aloft measurement and a computation time significant changes in vertical temperature structure arose only from heat input at the surface. Certainly, this is not generally true on a day-to-day basis. It is reasonable to assume that over a period of years other influences average out (e.g., that cold air advection is balanced by warm advection). The matter of marked cold air advection, however, did present a problem. For example, when the maximum surface temperature between 1200 and 1600 LST was colder than the surface temperature of the 1200 GMT sounding, the mixing height could not be calculated in the prescribed manner. Such cases were designated type C.

The occurrence of precipitation also demanded special treatment since in such situations the assumption of a dry adiabatic lapse rate in the mixing layer is questionable. Mixing heights (and wind speeds) during significant precipitation were classified as type P. Significant precipitation was defined as at least two occurrences of light or one of moderate or heavy in the regular hourly airway reports from 1000 through 2100 LST for afternoons and from 2200 through 0900 LST for mornings. In the current study, P, C, and M (missing) mixing heights and wind speeds have not been used, but allowance has been made for them (see Appendix B).

TABULATIONS AND AVAILABILITY

Morning and afternoon mixing heights and wind speeds for 62 stations were calculated and tabulated by the National Climatic Center (NCC), Environmental Data Service (EDS), of the National Oceanic and Atmospheric Administration (NOAA). The 62 stations are located by the dots of Figures 21 through 70 and are identified in Table A-1. High-speed automatic computers were used to process meteorological observations on punched cards. Most surface and upper-air observations were made from the same location and most calculations were for the 5 years, 1960 through 1964. The calculations were restricted to 5 years for economy and to pre-1965 because the required hourly surface observations were on punched cards only through 1964. For most stations all hourly surface observations through 1964 are readily available in published form (U.S. Department of Commerce) which may be useful in further and/or more detailed studies involving the tabulations. All of the tabulations, which are in three parts for each station, are too lengthy to publish here, but copies may be obtained at the cost of reproduction from the Director, NCC, EDS, NOAA, Asheville, North Carolina 28801. The NCC (formerly NWRC) tabulations are illustrated and described in detail in Appendix A.

MEAN MIXING HEIGHTS AND WIND SPEEDS

The NCC tabulations of mean non-P mixing height and wind speed were arbitrarily adjusted to allow for P, C, and M cases at each station. The adjustment was based on the assumption that mixing-height and wind-speed values for P and C cases generally would be greater than for non-P cases; M cases were rare. The manner in which the allowance was made is described in Appendix B. The effect of the allowance on the mean values depended upon the frequency of cases other than non-P, as may be seen for each station in Table B-1.

Figures 1 through 20 present isopleths of "adjusted" seasonal and annual mean mixing height and wind speed for morning and afternoon (see Table B-1 for data). The data for all isopleth analyses in this report have been included, not to emphasize precision but rather to permit those who might disagree with the analyses to prepare their own. The analyses are based on data points spaced at about 400-km intervals. We have attempted to incorporate only major topographical influences into the analyses. Thus, the large-scale nature of the analyses is in concert with the rather gross distribution, at least in terms of urban air pollution potential, of the parameters being considered. In regard to topographical influences, in mountainous regions most of the data points are located at cities in the valleys and, therefore, the analyses are most appropriate to valley locations.

Urban Morning Mixing Heights

Patterns of mean annual, winter, spring, summer, and autumn morning mixing heights are shown in Figures 1 through 5, respectively. Annually (Figure 1), the morning heights range from under 300 m to over 900 m with comparatively high values generally along the coasts and over the Great Lakes. This phenomenon is due essentially to high relative humidities and/or low cloudiness, which inhibit formation of intense radiation inversions. It is more pronounced along the Gulf and Atlantic Coasts than the Pacific because Gulf and Atlantic coastal waters are warmer and provide a more copious supply of moisture to the atmosphere than those of the Pacific. Another interesting feature of Figure 1 is the ridge of higher heights extending north-northwestward from central New Mexico through western Montana with comparatively low heights on either side.

The pattern of annual morning heights is very similar to those of the individual seasons, and seasonal variations generally are not large. However, a noticeable exception occurs along the central Gulf Coast where the highest value on any of the morning charts, 1300 m, occurs at Burwood, Louisiana, in summer (Figure 4). Winter and spring values are about half of those of summer and autumn due to the very warm and moist air there in summer and autumn.

The summer season has the lowest and most widespread low mixing heights, with a large area over the western high plateau having heights less than 200 m. The lowest seasonal mean height of 109 m occurs at Ely, Nevada. Such low morning mixing heights are caused by intense radiation inversions whose formation is enhanced by dry, thin (low-density) air. In both summer and autumn, a very large portion of the contiguous 48 states is covered by morning mixing heights under 400 m. The smallest area covered by mixing heights under 400 m occurs in spring.

Afternoon Mixing Heights

Patterns of mean annual, winter, spring, summer, and autumn afternoon mixing heights are displayed in Figures 6 through 10, respectively. The general pattern of afternoon heights, as shown by the annual chart (Figure 6), is opposite to that for mornings (Figure 1); i.e., afternoon heights are relatively low along the Pacific, Gulf, and Atlantic Coast lines, and in the vicinity of the Great Lakes. This pattern is due primarily to the ameliorating effect of large water bodies on maximum surface temperatures. Consequently, diurnal variations along coast lines tend to be considerably less than over inland areas. Annually, the extreme diurnal variation occurs over the southern Rockies where morning heights of a few hundred meters are replaced in the afternoon by heights well above 2 km.

While the pattern of annual afternoon heights may be seen clearly in each of the seasonal patterns, the seasonal variation of the values is much greater for afternoons than for mornings. However, because of the

steadying influence of the oceans, most of this variation occurs at inland locations. Afternoon mean heights along coast lines are remarkably steady throughout the seasons. As may be expected, lower afternoon heights occur in winter (Figure 7) when they range from less than 600 m at northerly latitudes to over 1400 m over the southern Rockies. Highest afternoon heights occur in summer (Figure 9) when they reach 4 km over the central Rockies. In contrast, summer values along the California Coast are slightly less than in winter, resulting in extreme height gradients over California. Similarly in the East, summer heights over the Appalachians are greater than in winter but vary little along the coast, resulting in large afternoon height gradients across the Atlantic seaboard in summer. Actually, these gradients are likely to be greater than indicated by the analyses of available data. The patterns and values of mean afternoon heights in spring and autumn (Figures 8 and 10), the transition months, closely resemble those of the annual mean.

The mean afternoon mixing heights presented here correspond to the estimates of mean maximum mixing depths presented previously by Holzworth (1964b). In comparing the two sets of data, it will be noticed that, while the isopleth patterns are similar, the values in the current study are for the most part considerably higher than in the earlier study. This is believed to be the result of two main factors. The earlier study used mean temperatures based on soundings taken at 0300 GMT (i.e., for time zones in the United States varying between 1900 and 2200 LST). At these early evening hours temperatures at levels near the upper part of the afternoon mixing layer are practically unchanged from afternoon (neglecting advection, etc., in the mean) since radiational cooling aloft has only been under way for a short time. Thus, the dry adiabatic extrapolation of the surface maximum temperature first intersects the evening temperature profile at a lower height than it would for a temperature sounding taken near sunrise (e.g., 1200 GMT). This is significant although the diurnal temperature variation near the top of the afternoon mixing layer may be only 1 or 2°C. Secondly, the earlier study used previously prepared monthly mean temperature profiles and maximum surface temperatures that included precipitation cases. In such cases vertical temperature profiles tend to be more stable (neglecting condensation) and maximum surface temperatures colder, resulting in lower afternoon mixing heights than in non-precipitation cases.

Morning Wind Speeds

Isopleths of mean annual, winter, spring, summer, and autumn *morning* wind speeds are depicted in Figures 11 through 15, respectively. It should be understood that, in this report, "mean wind speeds" refer to annual and seasonal means of arithmetic averages of observed speeds within each mixing layer. The general pattern and values of mean annual speeds (Figure 11) are much like those of the individual seasons. Annually, faster speeds occur over the southern portion of the middle tier of states, over Montana, and along the Gulf and Atlantic coastlines; slower speeds are located over the central and southern Rockies, in and near major valleys of Pacific Coast states, and in a broad area extending southwestward from the central Appalachians. The fastest mean annual speeds reach almost 8 m sec^{-1}, whereas the slowest are around 2 m sec^{-1}.

Although the annual pattern of morning speeds is similar to that for the seasons, there are certain seasonal features worthy of mention. In the western half of the 48 states the largest area of slow speeds (e.g., less than 4.0 m sec^{-1}) exists in winter (Figure 12), whereas in the East it exists in summer (Figure 14). At most locations the fastest speeds occur in spring (Figure 13). But noteworthy exceptions are found over Montana, along the north Atlantic seaboard, and in the vicinity of the eastern Great Lakes where the fastest speeds occur in winter. The area of fast winds along the Atlantic Coast and the finger of fast speeds reaching westward over the Great Lakes in winter appear to be associated with high morning mixing heights (Figure 2), which in turn are enhanced by cloudiness associated with cold air outbreaks over the lakes and with storms along the Atlantic Coast.

Afternoon Wind Speeds

Isopleths of mean annual, winter, spring, summer, and autumn *afternoon* speeds are shown in Figures 16 through 20, respectively. In general these patterns are similar to those for mornings, except the afternoon speeds are about 1 to 2 m sec^{-1} faster.

URBAN DISPERSION MODEL

While the mixing-height and wind-speed data provide an opportunity for qualitative appraisal of the large-scale features of meteorological potential for community air pollution, the value of any interpretation of the data will be enhanced considerably if it is in quantitative terms. A quantitative interpretation can be achieved by use of a mathematical model of dispersion over urban areas.

The model to be used here gives the average normalized concentration ($\bar{\chi}/Q$) (i.e., the concentration (χ) averaged over a city and normalized for uniform average area emission rate (Q), as a function of mixing height (H), wind speed (U), and along-wind distance (S) across the city). All units are in meters, seconds, and grams except where indicated otherwise. The main assumptions are:

1. Steady-state conditions prevail.
2. Emissions occur at ground level and are uniform over the city.
3. Pollutants are nonreactive.
4. Lateral diffusion can be neglected.
5. Vertical diffusion from each elemental source conforms to unstable conditions and concentrations follow a Gaussian distribution out to a defined travel time that is a function of H. Thereafter, a uniform vertical distribution of pollutant occurs as a result of further dispersion within the mixing layer.

The model treats the city source as a continuous series of infinitely long cross-wind line sources, much as Lucas (1958) did, with pollutants confined within the mixing layer. As indicated in assumption 5, the model requires two equations according to whether *none* or *some* of the pollutants emitted at ground level achieve a uniform vertical distribution within the mixing layer before being transported beyond the downwind edge of the city. These equations are developed in Appendix C as equations 6 and 9, respectively, and may be written as

$$\bar{\chi}/Q = 3.994(S/U)^{0.115} \tag{6a}$$

for $(S/U) \leq 0.471H^{1.130}$ (i.e., when *no* pollutants achieve a uniform vertical distribution), and

$$\bar{\chi}/Q = 3.613H^{0.130} + \frac{S}{2HU} - \frac{0.088UH^{1.260}}{S} \tag{9a}$$

for $(S/U) \geq 0.471H^{1.130}$ (i.e., when *some* pollutants achieve a uniform vertical distribution). For most cases the term with coefficient 0.088 is very small and can be neglected.

Table 1 presents the values of $\bar{\chi}/Q$ as a function of H, U, and S. As pointed out in Appendix C, the variation of $\bar{\chi}/Q$ with S is practically linear for cities larger than 10 km. Therefore, the data in Table 1 are given for only two city sizes, 10 and 100 km (i.e., distance the wind travels across the city).

Preceding page blank

In Table 1 the dashed line separates $\bar{X}/\bar{Q}$ values to the lower right for which H has absolutely no effect for a 10-km city (i.e., all pollutants emitted over a 10-km city are transported beyond the downwind edge of the city before any uniform vertical distribution is achieved within the mixing layer; equation 6a is used). Actually for a given wind speed $\bar{X}/\bar{Q}$ is practically constant (whole number accuracy) for mixing heights somewhat lower than those for which there is absolutely no effect. This happens because only a small portion of all emissions (i.e., those from near the upwind edge of the city) are affected by the mixing layer before passing beyond the city. In Table 1 this effect can also be seen for a 100-km city, even though equation 6a is not applicable for a 100-km city for the largest mixing height and wind speed values considered.

Table 1. AVERAGE NORMALIZED CONCENTRATION, $\bar{X}/\bar{Q}$ (sec m^{-1})

City size,	Mixing height,	Wind speed, m sec^{-1}									
km	m	0.75	1.5	2.5	3.5	4.5	5.5	7.0	9.0	11.0	13.0
10	125	60	33	23	18	16	14	12	11	10	10
100	125	540	273	167	121	96	79	64	51	43	38
10	375	26	17	13	12	11	10	10	9	9	9
100	375	186	97	61	46	37	32	27	23	20	18
10	625	19	14	11	11	10	10	9	9	9	9
100	625	115	62	40	31	26	23	20	17	16	14
10	875	16	12	11	10	10	10	9	9	9	9
100	875	85	47	32	25	21	19	17	15	14	13
10	1250	14	12	11	10	10	9	9	9	9	9
100	1250	62	36	25	21	18	16	15	14	13	12
10	1750	13	11	10	10	10	9	9	9	9	9
100	1750	48	29	21	18	16	15	14	13	12	12
10	2250	13	11	10	10	10	9	9	9	9	9
100	2250	39	25	19	16	15	14	13	12	12	11
10	2750	12	11	10	10	10	9	9	9	9	9
100	2750	34	22	17	15	14	13	13	12	12	11
10	3250	12	11	10	10	10	9	9	9	9	9
100	3250	31	21	16	15	14	13	12	12	11	11
10	3750	12	11	10	10	10	9	9	9	9	9
100	3750	28	19	16	14	13	13	12	12	11	11
10	4500	12	11	10	10	10	9	9	9	9	9
100	4500	26	18	15	14	13	13	12	12	11	11

[a] Dashed line separates values to lower right for which the mixing height has absolutely no effect on $\bar{X}/\bar{Q}$ for a 10-km city.

An interesting feature of the model is that the larger the city size, the larger the effect an incremental change in U or H has on $\bar{\chi}/Q$ (see Table 1). This effect is especially large at comparatively small values of U and H, and clearly illustrates the importance of representative data in describing the meteorological potential for air pollution during critical situations. It also indicates that for daily forecasting purposes the input data must be very precise if forecasts are to be reasonably accurate.

Another noteworthy characteristic of the model is that the smaller the values of H and U, and the larger the value of S, the smaller the relative difference between $\bar{\chi}/Q$ values for this model and those for a "box" model where $(\bar{\chi}/Q)_{Box} = 1/2\ (S/HU)$. Thus, for H = 125 m, U = 0.75 m sec^{-1} and S = 100 km; $\bar{\chi}/Q$ = 540 sec m^{-1} (Table 1) and $(\bar{\chi}/Q)_{Box}$ = 533 sec m^{-1}. This correspondence does not hold, however, for more common values of H, U, and S.

Although the model presented here is rather simple in comparison to the great complexities of atmospheric dispersion and pollutant emissions in urban areas, it is in concert with the general nature of the independent parameters and the spacing of the locations for which mixing height and wind speed are available. As such, it provides a means of quantitatively appraising the *general* meteorological potential for community air pollution. Obviously, the results of this study will be enhanced by more detailed studies of each local situation.

This model is essentially the same as that for which Miller and Holzworth (1967) obtained good correspondence between calculated and observed average concentrations for each of several cities. The model is derived in Appendix C.

POTENTIAL FOR URBAN AIR POLLUTION

Using the frequency tabulations of mixing height by wind speed (Appendix A) as adjusted for the occurrence of precipitation (Appendix B) and the dispersion model, cumulative frequencies of average normalized concentration ($\bar{\chi}/Q$) for various city sizes were generated for each of the 62 upper air stations. From these data the $\bar{\chi}/Q$ value that was *exceeded* 10, 25, and 50 percent of the time was found for various city sizes for each station. In cases where the largest $\bar{\chi}/Q$ value (for the smallest values of H and U) occurred more frequently than the percentile value being considered, the desired values were obtained by extrapolation of the cumulative frequency curve of $\bar{\chi}/Q$. As shown in Appendix C, for a given mixing height and wind speed the variation of $\bar{\chi}/Q$ with city size is practically linear for cities larger than 10 km. Thus, the isoplethed maps of $\bar{\chi}/Q$ values that are exceeded a specified percentage of time (Figures 21 through 50) consider only two city sizes, 10 and 100 km. Where data are sparse, especially over water, the isopleth analyses have been extended reluctantly and should be considered speculative.

In the interpretation of $\bar{\chi}/Q$ it will be recalled that this quantity is the city-wide average concentration ($\bar{\chi}$) normalized for uniform average area emission rate (Q). The units of $\bar{\chi}/Q$ are sec m^{-1}, so that if Q is in micrograms m^{-2} sec^{-1}, $\bar{\chi}$ is in micrograms m^{-3}. For example, if $\bar{\chi}/Q$ = 50 sec m^{-1} and Q = 2 micrograms m^{-2} sec^{-1}, $\bar{\chi}$ (i.e., $(\bar{\chi}/Q) \times Q$) = 100 micrograms m^{-3}.

Since $\bar{\chi}/Q$ is the average concentration normalized for emission rate, it represents the *meteorological* potential for urban air pollution (i.e., non-meteorological variables for the most part are not considered). Although city size is one of the independent variables, it determines the effectiveness of the meteorological variables. Thus, the meteorological potential is dependent on city size. This dependency on city size may also enter in another way. For example, the heat generated by very large cities may cause morning mixing heights to be higher than for smaller cities. Such an effect would be most noticeable for the rarer extremes of very low mixing heights. Because of uncertainties about these effects and because of the approximate manner in which mixing heights are estimated, especially for mornings, these effects have not been included in this study. They should be considered, however, in more detailed studies.

The $\bar{\chi}/Q$ data presented here may be applied most readily by comparing values for different parts of the country and by projecting current measured pollutant concentrations in proportion to increases in $\bar{\chi}/Q$ values with city size.

FIFTY-PERCENTILE CONCENTRATIONS

Morning

Figures 21 through 25 show data and isopleths of theoretical $\bar{\chi}/Q$ for 10- and 100-km cities that are exceeded on 50 percent of all mornings annually, and in winter, spring, summer, and autumn, respectively. *Morning* refers to the few hours centered near the morning commuter rush hours, which roughly coincide with the diurnal maximum concentration of slow-reacting pollutants in many urban areas.

Preceding page blank

Annually (Figure 21), the highest 50-percentile morning concentrations (i.e., χ/Q) occur over southwestern Oregon where for 10-km cities a value of almost 40 sec m^{-1} is indicated. When such small cities grow to 100 km, the concentration is expected to exceed 300 sec m^{-1}, an increase by a factor of about eight. Concentrations of roughly half those in southwestern Oregon are centered over Arizona and Wyoming. These areas of high concentrations are due not only to the occurrence of slow winds (Figure 11) but also to low mixing heights (Figure 1), as indicated in Table 1. Such comparisons should be made cautiously, however, since mixing height and wind speed frequency distributions at many stations are often anything but normal. East of the Rockies, the annual median concentrations for 10-km cities vary between only 9 and 13 sec m^{-1}; for 100-km cities the values are generally three to five times greater, except along much of the Atlantic and Gulf Coasts where the factor is two to three. Assuming the current size of New York City is 50 km, the interpolated median morning χ/Q value is 13 sec m^{-1}; when that city grows to 100 km the median value will increase to only 19 sec m^{-1}. If New York City were located a few hundred miles to the southwest, the annual median concentration for a 100-km city would be around 50 sec m^{-1}. Along the southern California Coast, the annual median value for a 60-km city (approximate size of Los Angeles) is 41 sec m^{-1}, which increases to 63 sec m^{-1} for a 100-km city. In terms of annual median morning χ/Q values for 100-km cities, the meteorological potential along the southern California Coast is about three times that along the mid-Atlantic Coast.

The seasonal patterns of median concentration for mornings are much like the annual pattern. In general the smallest χ/Q values occur in winter (Figure 22) over the eastern half of the United States and in spring (Figure 23) over the western half of the country. For most locations, the largest values occur in summer and/or autumn (Figures 24 and 25), the area of greatest values in the East being further south and having slightly larger values in autumn than in summer.

Afternoon

Figures 26 through 30 show theoretical χ/Q values that are exceeded on 50 percent of all afternoons annually, and in winter, spring, summer, and autumn, respectively. *Afternoon* refers to the several hours centered around the usual time of daily maximum surface temperature, which in many cities roughly coincides with a typical afternoon minimum concentration of slow-reacting pollutants.

Annually (Figure 26), the median afternoon χ/Q values for a 10-km city are for the most part not much smaller than the values for morning and they are practically uniform, being either 9 or 10 sec m^{-1}. As indicated in the discussion of the model, this happens mainly because the median afternoon mixing heights are so high. Even for 100-km cities there is little variation in χ/Q, with most values being near 15 sec m^{-1}, greatest values occur near the California Coast where they are around 25 sec m^{-1}. In terms of current large cities (around 50 km in size), median afternoon χ/Q values over most of the contiguous United States are 11 to 13 sec m^{-1} and attain a maximum along the southern California Coast of only 17 sec m^{-1}. In these terms there is little variation in the meteorological potential for community air pollution.

The only seasonal pattern of afternoon median χ/Q values that is appreciably different from the annual pattern is for winter (Figure 27), and these differences are restricted to very large cities in the West. Thus, when cities in central Wyoming reach 100 km, the winter χ/Q values will exceed 55 sec m^{-1} on half the afternoons; similarly 35 sec m^{-1} will be exceeded over much of Washington, Oregon, and California. By comparison χ/Q along the southern California Coast will be around only 25 sec m^{-1}.

For the same city size, median theoretical concentrations are never greater and are usually less for afternoons than for mornings, with the differences varying from slight to large depending upon location and city size. Since the variation of χ/Q values with city size is much more rapid for mornings than afternoons, the growth

of cities will affect the meteorological potential most profoundly for mornings. The general implications for control and abatement purposes are obvious.

25-PERCENTILE CONCENTRATIONS

Morning

Figures 31 through 35 show data and isopleths of theoretical $\bar{\chi}/Q$ that are exceeded on 25 percent of all mornings annually, and in winter, spring, summer, and autumn, respectively. These patterns are similar to those for corresponding median $\bar{\chi}/Q$ charts (Figures 21 through 25), except that the upper quartile values are larger in the former, especially for 100-km cities. This happens because, as stated earlier, the rate of increase of $\bar{\chi}/Q$ with decreasing wind speed and mixing height is greater for large cities than for small ones. Also, because of the climatological variation of mixing height and wind speed, the range of $\bar{\chi}/Q$ values for both small and large cities is greater for upper quartile than for median charts. For example, annually (Figure 31), the upper quartile $\bar{\chi}/Q$ values for 10-km cities vary between 11 and 71 sec m^{-1} and for 100-km cities, between 29 and 649 sec m^{-1}. Thus, the patterns for quartile charts are more intense than for median charts. This is evident in Figures 31 through 35, where the isopleth patterns over the eastern United States are particularly clear when contrasted with the flat patterns of Figures 21 through 25.

Annually (Figure 31), the centers of highest upper quartile morning concentrations in the West are almost double the corresponding median values. In the East the increase for 100-km cities is by a factor of more than six at several locations, and there is a large area oriented along the Appalachian Mountains where the $\bar{\chi}/Q$ values for a 100-km city exceed 200 sec m^{-1}.

Seasonally, there are some rather large variations in the upper quartile values of $\bar{\chi}/Q$. In general, the values in the eastern half of the United States are equally small in winter and spring (Figures 32 and 33); they are greatest in autumn (Figure 35) by a factor of roughly three to four over winter and spring. Over the Rockies, the values are smallest in spring and summer, and greatest in autumn and winter by a factor of about two. In the far West, the values are smallest in spring, except for the southern California Coast where they are smallest in summer. Values are greatest over the northern section of the West in summer and over the southern section in autumn and winter. Some fairly large values also occur over the upper Plains during summer. It is interesting that at the upper quartile level, seasonal peak $\bar{\chi}/Q$ values in the East and West are each about 90 and 825 sec m^{-1} for 10- and 100-km cities, although they occur in different seasons, autumn and summer.

Afternoon

Figures 36 through 40 show theoretical $\bar{\chi}/Q$ values that are exceeded on 25 percent of all afternoons annually, and in winter, spring, summer, and autumn, respectively. Annually, the upper quartile concentrations for 10-km cities are practically constant, varying only between 9 and 11 sec m^{-1}. These values are almost the same as for the median concentrations. Even for 100-km cities, the upper quartile afternoon concentration at most locations is only a fraction larger than the median concentration. Annually, the largest upper quartile afternoon concentrations for 100-km cities occur over southern California with values of only 35 to 40 sec m^{-1}.

Upper quartile values of afternoon $\bar{\chi}/Q$ over the eastern United States vary slightly seasonally and spatially. In the western United States in winter, however, the concentrations for 100-km cities exceed 75 sec m^{-1} over large areas, attaining a value of 204 sec m^{-1} over central Wyoming and 116 sec m^{-1} over southwestern Oregon. While the winter patterns for 10- and 100-km cities are similar, they are much less intense for smaller cities.

Notice that in Figure 37 the isopleths over Wyoming are left incomplete not only for ease of reading but also because the extreme values may be representative of a small area.

Upper quartile charts for the other seasons are generally much like those for the annual data, except that, for 100-km cities, the χ/Q values are around 45 sec m^{-1} over southern California in summer and autumn (as well as in winter). The χ/Q values are around 45 sec m^{-1} just off the coast of Massachusetts in summer also.

TEN-PERCENTILE CONCENTRATIONS

Morning

Figures 41 through 45 show that data and isopleths of theoretical χ/Q are exceeded on 10 percent of all mornings annually, and in winter, spring, summer, and autumn, respectively. These patterns are similar to those for corresponding upper quartile $\bar{\chi}/Q$ charts (Figures 31 through 35), except that upper decile values are larger and the patterns are more intense. The increases over upper quartile and median values are generally larger in the East than in the West. For example, annually (Figure 41) at the upper decile level the higher values in the East are about equal to those in the far West, whereas at the median level (Figure 21) there is little pattern in the East but a clear maximum in the far West. Annually, the largest upper decile morning $\bar{\chi}/Q$ values exceed 80 and 800 sec m^{-1} for 10- and 100-km cities, and there are large sections of the country where 60 and 600 sec m^{-1} are exceeded. These are indeed large values (e.g., in comparison to corresponding median values). It is fortuitous that most of our very large cities are not located in areas of such high meteorological potential for community air pollution.

The relatively high χ/Q values over the upper Plains (Figure 41) were unexpected, perhaps because most cities in the area are not large and have not often experienced pollutant concentrations that generated widespread interest. However, without effective abatement efforts, this situation is bound to become worse as cities grow. Other regions that face a similar prospect show up clearly in the isopleth analyses.

The pattern of annual upper decile morning concentrations (Figure 41) is generally similar to that of each of the seasons, but with differences in magnitude. In the eastern United States the area of high $\bar{\chi}/Q$ values along the Appalachian Mountains is clearly highest in autumn (Figure 45) when, for some locations, they exceed 100 and 1000 sec m^{-1} for 10- and 100-km cities, and are almost double the values in winter (Figure 42). In the upper Plains the highest values occur in summer and the lowest in winter. Along the south Atlantic Coast, over Florida, and along the Gulf Coast the concentrations are relatively low throughout the year, but they are lowest in summer. The two regions of moderately high concentrations over the Rockies are highest in winter and autumn, lowest in spring and summer. Highest $\bar{\chi}/Q$ values over western Oregon are around 100 and 1000 sec m^{-1} for 10- and 100-km cities, and occur in summer, but values are almost as high in autumn when they extend southward through interior California. Over southern California the highest concentrations are comparatively moderate and are attained in autumn and winter.

Afternoon

Figures 46 through 50 show the theoretical $\bar{\chi}/\bar{Q}$ values that are expected to be exceeded on 10 percent of all afternoons annually, and in winter, spring, summer, and autumn, respectively. Annually (Figure 46), even at the upper decile level, there is little variation in afternoon $\bar{\chi}/\bar{Q}$ values east of the Rockies for 10- or 100-km cities, and the values are only slightly larger than at the upper quartile level. In the western United States, however,

there are two areas where the upper decile $\bar{\chi}/\bar{Q}$ values for 100-km cities exceed 50 sec m^{-1}; over Wyoming and Oregon peak values are near 150 and 100 sec m^{-1}, respectively. For more realistic city sizes, however, the values are much smaller.

Seasonally, most of the higher upper decile $\bar{\chi}/\bar{Q}$ values shown annually are accounted for in winter (Figure 47); for 10- and 100-km cities, values of 70 and 650 sec m^{-1}, respectively, are reached over Wyoming and values of a little less than half are reached over Oregon. Notice that in these two regions the isopleths are left incomplete for clarity and because the extreme values may not be generally respresentative. Nevertheless, $\chi/\bar{Q}$ values of over 100 sec m^{-1} for 50-km cities are indicated for the two western regions. East of the Rockies, in winter, there is no significant variation in $\bar{\chi}/\bar{Q}$ for 10-km cities, and for 100-km cities the variation is not large. The $\bar{\chi}/\bar{Q}$ values for autumn afternoons (Figure 50) are very similar to those shown annually (Figure 46). In spring and summer (Figures 48 and 49), there is practically no variation in $\bar{\chi}/\bar{Q}$ for 10-km cities, and even for 100-km cities the variation for the most part is rather small.

EPISODE-DAYS OF HIGH METEOROLOGICAL POTENTIAL

The classic study of the occurrence of episodes with restricted dispersion is the contribution of Korshover (1967) who based his determinations largely upon the magnitude of sea-level pressure gradients. However, his study was confined to the United States east of the Rocky Mountains because of problems inherent in the reduction of pressure to sea level for stations located in high and irregular terrain. The current study does not suffer from this limitation. Tabulations were made of episodes during which specified meteorological conditions were satisfied at each of the 62 upper air stations. This report is concerned with episodes lasting at least 2 days and episodes lasting at least 5 days with no precipitation cases and upper limits on mixing height and wind speed determined by the following matrix:

Wind speed, m sec^{-1}	Mixing height, m			
	500	1000	1500	2000
2				
4				
6				

The phrase, "episodes lasting at least 2 or 5 days," means that the conditions were satisfied in at least five or eleven consecutive computation times, respectively (e.g., morning of day 1, to afternoon of day 1, to morning of day 2, etc.). A defined precipitation event terminated an episode and was not counted as part of the episode. For the seven stations for which full 5-year tabulations were not available (Table A-1), the episode data were extrapolated to 5 years.

Figures 51 through 70 include the data for episodes lasting at least 2 and 5 days for mixing height-wind speed limits in the foregoing matrix, with four exceptions. Figures are omitted for episodes of 5 days or longer characterized by wind speeds 2.0 m sec^{-1} or less and any of the four specified mixing heights since these conditions only occurred as listed in Table 2.

Table 2. EPISODES LASTING 5 OR MORE DAYS WITH WIND SPEED $\leq$ 2.0 m sec^{-1}

Location	Mixing Heights, m			
	500	1000	1500	2000
Medford, Ore.	4 (24)[a]	9 (59)	10 (69)	10 (69)
Lander, Wyo.	2 (15)	2 (19)	2 (19)	2 (19)
Winnemucca, Nev.	0 (0)	0 (0)	1 (7)	1 (7)

[a]The first figure is the number of episodes; the number of episode-days is given in parentheses.

Preceding page blank

These episodes all occurred in winter. Each of the six most severe episodes (i.e., at Medford and Lander) was clearly associated with a quasi-stationary anticyclone.

Before discussing the episode maps, it is of interest to consider the relative severity of the various mixing height (H) and wind speed (U) limits (e.g., is an episode with $H \leq 1000$ m and $U \leq 4.0$ m sec^{-1} more severe than one of equal duration with $H \leq 1500$ m and $U \leq 2.0$ m sec^{-1}?). This can be done conveniently and roughly by ranking the reciprocal of H x U as in Table 3.

Table 3. RANK OF RECIPROCALS OF H x U

Wind speed,	Episodes at Mixing Height, m			
m sec^{-1}	500	1000	1500	2000
2	1	2	3	4
4	2	4	5	6
6	3	5	7	8

This is practically the same ranking that is obtained using χ/Q values for a city size of about 40 km or larger. The total number of episodes and episode-days for a given duration and severity ranking may be approximated by summing the occurrences for appropriate limiting conditions. For example, for episodes of 2 days or longer with a severity ranking of 2 ($H \leq 500$ m, $U \leq 4.0$ m sec^{-1}, and $H \leq 1000$ m, $U \leq 2.0$ m sec^{-1}) at Lander, Wyoming, the total number of episode-days is the sum of 154 (Figure 52, for $H \leq 500$ m, $U \leq 4.0$ m sec^{-1}) plus 94 (Figure 54, for $H \leq 1000$ m, $U \leq 2.0$ m sec^{-1}) minus 71 (Figure 51, for $H \leq 500$ m, $U \leq 2.0$ m sec^{-1}), which totals 177. This total is an underestimate, however, since episodes were determined separately for each set of mixing-height and wind-speed conditions; episodes were not determined for multiple sets of conditions that may be rated of approximately equal severity. Limiting mixing-height and wind-speed conditions of like severity have not been combined in order to show the contributions of individual component conditions and since other definitions of severity may be employed. The severity of various limiting meteorological conditions, together with various episode durations, could be ranked in terms of Duration/(H x U), but this seems to be a gross over-simplification, and is not considered further in the present study.

As mentioned, in mountainous regions most of the NWS observation data used in this study were obtained in valleys and, therefore, are most appropriate to valley locations, although such details may not be shown by the isopleth analyses.

EPISODES LASTING 2 DAYS OR LONGER

Figure 51 shows that episodes of 2 days or longer with extreme limiting conditions of $H \leq 500$ m and $U \leq 2.0$ m sec^{-1} occur at only 11 of the 62 locations, mostly in the West. It is perhaps surprising that the total number of such episode-days in 5 years is as high as 71 at Lander, Wyoming, and 52 at Medford, Oregon. Increasing the wind-speed limit to 4.0 m sec^{-1} with $H \leq 500$ m (Figure 52) results in some occurrences at almost two-thirds of the stations, although the total episode-days at many stations is small. At Lander the episode-days totaled 154, an increase of 83 over Figure 51, whereas at Medford the increase is only 3 episode-days. This happens because at Medford, with $H \leq 500$ m, episodes with $2.0 < U \leq 4.0$ m sec^{-1} occur rarely. In Figure 52, also notice the effect of relatively slow winds over California and fast winds over the middle tier of states. Figure 53 for $H \leq 500$ m and $U \leq 6.0$ m sec^{-1} shows increases over Figure 52 much as expected from the previous

discussion. The comparatively very large frequency of episode-days over southern California is due to the occurrence of persistent low mixing heights and fairly slow winds with sparse precipitation.

Considering episodes with $H \leq 1000$ m, Figure 54 shows that with $U \leq 2.0$ m sec^{-1} the pattern of episode-days is much like that of Figure 51 ($H \leq 500$ m, $U \leq 2.0$ sec^{-1}). In both figures, the very limiting conditions occur at only two stations in the East and in the West are greatest by far at Medford and Lander. Increasing the wind speed limit to 4.0 m sec^{-1} with $H \leq 1000$ m (Figure 55) results in some episode-days at all except 6 of the 62 stations. Most of these zero and other low occurrences are at stations in relatively windy regions. In Figure 55 the greatest number of episode-days in the East barely exceeds 20, whereas in the West 100 is exceeded at many locations. The greatest number of episode-days in Figure 55 is 471 at San Diego, California (isopleths incomplete in this area), and it is surprising that the values are more than twice those at nearby Santa Monica (Los Angeles). This happens because the episode criterion most often *not* satisfied at both locations is afternoon $U \leq 4.0$ m sec^{-1}, and, while afternoon wind speeds at both locations are typically near the critical value, they are usually around 1 m sec^{-1} faster at Santa Monica than at San Diego. This difference between San Diego and Santa Monica occurs on most charts where the limiting wind speed is 4.0 m sec^{-1}. The comparatively small frequency of episodes at Ely, Nevada, is also interesting. Over the central and southern Rockies the afternoon mixing heights in spring, summer, and autumn are usually so high as to largely eliminate the occurrence of low mixing-height episodes from all seasons except winter, but then the morning wind speeds (Figure 12) at Ely are considerably faster than at nearby stations. Relatively low frequencies occur at Ely on most of the episode figures. For $H \leq 1000$ m and $U \leq 6.0$ m sec^{-1} Figure 56 shows that these conditions occur at all stations. In the West, 100 episode-days is exceeded at most stations and 600 episode-days is exceeded over much of California, whereas in the East the greatest number of corresponding episode-days is 87 at Burwood, Louisiana (near New Orleans).

Figure 57 shows that for $H \leq 1500$ m and $U \leq 2.0$ m sec^{-1} the episode frequencies are very similar to those for $H \leq 1000$ m and $U \leq 2.0$ m sec^{-1} (Figure 54). Apparently for these conditions the mixing heights are less effective than wind speeds in limiting the occurrence of episodes. Figure 58 is particularly important because the limiting conditions of $H \leq 1500$ m and $U \leq 4.0$ m sec^{-1} have been used, in one form or another, as criteria in the National Air Pollution Potential Forecasting Program (Stackpole, 1967; Gross, 1970). Clearly, the meteorological potential for episodes is much greater in the West than in the East, with barely 100 episode-days at one eastern station and over 100 days at most western stations. Several western stations have more than 200 episode-days. Figure 59 shows that with $H \leq 1500$ m and $U \leq 6.0$ m sec^{-1}, episodes are quite frequent at most stations. However, the severity of such potential episodes is markedly reduced by wind speeds at 6.0 m sec^{-1}, except perhaps for very large cities.

For the greatest mixing heights considered, $H \leq 2000$ m and $U \leq 2.0$ m sec^{-1}, Figure 60 shows that in the West episode data are practically unchanged from the conditions of Figure 57 ($H \leq 1500$ m and $U \leq 2.0$ m sec^{-1}), but that in the East the number of stations meeting the criteria almost doubles. Figure 61 illustrates that episodes with $H \leq 2000$ m and $U \leq 4.0$ m sec^{-1} occur at all stations and such episode-days have a frequency greater than 100 over most of the West and over much the East. For the least limiting conditions, $H \leq 2000$ m and $U \leq 6.0$ m sec^{-1}, Figure 62 shows that the total episode-days in 5 years is less than 100 at only 12 stations and is more than 200 (i.e., 1 day in about 9) at well over half the stations.

For $H \leq 500$ and ≤ 1000 m (Figures 51 through 56) the season with the greatest number of episode-days is winter for most stations. For $H \leq 1500$ and 2000 m (Figures 57 through 62) the predominant season with the greatest number of episode-days continues to be winter in the West but shifts to autumn in the East. This is probably due in part to the more frequent occurrence of winter cyclonic storms in the East than in the West. This general effect of storminess may also be seen in the Pacific Northwest Region of Figures 58 through 62 where autumn or summer is the season with the greatest number of episode-days at several stations. As a general rule for the same limiting conditions, the average duration of episodes in the West tends to be greater than in the East.

EPISODES LASTING 5 DAYS OR LONGER

For 5-day episodes the frequencies and isoline patterns of Figures 63 through 70 are much like those with corresponding limits on H and U for 2-day episodes (Figures 51 through 62), except that 5-day episodes generally occur much less frequently. As indicated, 5-day episodes with $U \leqslant 2.0$ m sec^{-1} only occur at three stations. Five-day episodes with the *least* limiting conditions, $H \leqslant 2000$ m and $U \leqslant 6.0$ m sec^{-1} (Figure 70), did not occur once in the 7 years considered at seven stations. For the important condition of $H \leqslant 1500$ m and $U \leqslant 4.0$ m sec^{-1}, 5-day episodes (Figure 67) occur at only 24 stations, whereas 3-day episodes (Figure 58) occur at 60 stations. This difference occurs mainly in the East. In general, the discussion regarding 2-day episodes is applicable to 5-day episodes.

FORECAST EPISODES

For the most part there is fair qualitative agreement between the patterns of objectively derived episode-days with limiting conditions like those used as forecast criteria (Figure 58) and actual forecast-days of high air pollution potential (Figure 71). Notable exceptions occur, however, in the vicinity of Ely, Nevada, where the condition seems to have been relatively over-forecast and in the vicinity of Lander, Wyoming, where it seems to have been relatively under-forecast. Notice that in Figure 71 the actual forecast-days have been adjusted to a 5-year base for comparison with Figure 58. The number of derived episode-days in 5 years tends to be somewhat greater than forecast, especially in the West. This is due, at least in part, to the conservative nature of the forecasts and to the forecast requirement that meteorological conditions be met over a large area (minimum size about 75,000 square miles). In regard to the latter requirement, inspection of derived episodes indicates that they often occurred simultaneously at several adjacent stations in association with slow-moving anticyclones. Especially along the California Coast, however, episodes of limited dispersion are often confined to rather small areas.

SUMMARY AND CONCLUSIONS

This study is based upon regular surface observations and upper air measurements of temperature and wind during 5 years at 62 NWS stations in the contiguous United States. These observations have been used to derive climatological statistics on morning (after sunrise) and afternoon mixing heights over cities and vertically averaged wind speeds through the corresponding heights. The method of deriving these data is given in some detail along with sources for obtaining copies of the data in the hope that they will be used in other applications, particularly more detailed and specific studies of air pollution meteorology.

Annual and seasonal isoplethed maps of mean morning and afternoon mixing heights and wind speeds are presented. Morning mixing heights over most of the United States usually range in any season from around 300 to 800 m, with the higher values commonly found adjacent to large bodies of water. Afternoon mixing heights display a large seasonal variation. Winter values range from 600 m over northern central and northwestern states to 1400 m over the southern Rockies. In summer, the range is from 600 m along the California Coast to 4 km over the southern Rockies with relatively low heights along all coasts. Maps of mean morning wind speed generally display isopleth patterns that are similar from season to season although irregular variations occur in some areas (e.g., over the northern Rockies and from the Great Lakes eastward to the Atlantic Coast). Fastest average speeds reach 9 m sec^{-1} in spring over Oklahoma and in winter over the northern Rockies and along the middle Atlantic Coast. Slowest speeds are 2 m sec^{-1} and only occur in the far West, but morning winds of 3 m sec^{-1} or less occur in all seasons over much of California and Oregon; in summer, autumn, and winter over parts of the Rockies; and in summer over the middle Appalachians and part of Mississippi. Seasonal patterns of afternoon speeds are much like those for mornings except most afternoon speeds are around 1 to 2 m sec^{-1} faster.

A simple model of dispersion over urban areas is developed in which the theoretical city-wide average pollutant concentration ($\bar{\chi}$), normalized for uniform average area emission rate ($\bar{Q}$), is a function of mixing height, wind speed, and city size (i.e., along-wind distance across the city). For city sizes greater than 10 km, the variation of $\bar{\chi}/\bar{Q}$ with city size is practically linear. Frequency tabulations of mixing height by wind speed are used in the model to generate cumulative frequencies of $\bar{\chi}/\bar{Q}$ for each of the 62 observation locations. Isopleth maps of annual and seasonal $\bar{\chi}/\bar{Q}$ values for 10- and 100-km cities that were *exceeded* on 10, 25, and 50 percent of mornings and afternoons are presented in 30 figures. This information may be utilized most readily by comparing $\bar{\chi}/\bar{Q}$ values (for a given city size) for different areas, and for different city sizes in accordance with anticipated changes in city size and emission rates. In such evaluations, the assumptions in the model should not be overlooked and care should be exercised in interpreting between data locations.

The isoplethed $\bar{\chi}/\bar{Q}$ charts show that over the United States both large and small variations in these theoretical values may occur spatially, diurnally, and seasonally as well as with city size and for different percentile values of the cumulative frequencies. Thus, in terms of the concepts used in this study, the meteorological potential is anything but simple and is summarized only briefly. Annually, the median $\bar{\chi}/\bar{Q}$ values for mornings (Figure 21) vary from 9 to 39 sec m^{-1} for 10-km cities and from 17 to 329 sec m^{-1} for 100-km cities with comparatively low values and flat isopleth patterns east of the Rockies and clearly defined patterns in the West. At the upper quartile level the isopleths of morning annual $\bar{\chi}/\bar{Q}$ values (Figure 31) show an additional area of high values along the axis of the Appalachians, but the highest values remain in the far West centered over Oregon. In the upper decile chart of morning annual $\bar{\chi}/\bar{Q}$ values (Figure 41), the isopleth patterns are quite intense with a range of values from 16 to 95 sec m^{-1} for 10-km cities and from 96 to 890 sec m^{-1} for

100-km cities. Highest concentrations are centered over Oregon with values almost as high over Mississippi and extending northeastward along the Appalachians. A new area of relatively high values is located over the upper Plains and secondary high centers over Wyoming and Arizona persist from the median chart. In general, comparatively high morning concentrations occur over much of the West at the median, upper quartile, and upper decile levels; along the Appalachians extending into Mississippi at the upper quartile and decile levels; and over the upper Plains at the upper decile level. As a rule, the highest morning $\bar{X}/\bar{Q}$ values occur in autumn and/or summer.

For afternoons the annual chart of median $\bar{X}/\bar{Q}$ values (Figure 26) indicates that 10-km cities have a value of 9 or 10 sec m^{-1} and 100-km cities have a range only from 13 to 26 sec m^{-1}. This results in practically no isopleth pattern for 10-km cities and a very flat pattern for 100-km cities. At the upper quartile level, the afternoon annual values of $\bar{X}/\bar{Q}$ (Figure 36) are not much greater than the median values, even for 100-km cities. At the upper decile level the afternoon annual $\bar{X}/\bar{Q}$ values (Figure 46) for 10-km cities range only from 10 to 22 sec m^{-1} and for 100-km cities from 20 to 150 sec m^{-1}. While there are some clear-cut isopleth patterns for upper decile annual afternoon concentrations, these are confined mostly to the West. However, even for 100-km cities the afternoon isopleth patterns are rather flat compared with those on the corresponding morning chart. This lack of spatial variation in the afternoon concentrations occurs largely because the afternoon mixing heights are generally so high as to have little or no effect on the $\bar{X}/\bar{Q}$ values even for 100-km cities. In view of the large seasonal variation of afternoon mixing heights, it is not surprising to find that at most places the highest afternoon $\bar{X}/\bar{Q}$ values occur in winter and are considerably larger than corresponding annual values.

Morning and afternoon $\bar{X}/\bar{Q}$ charts indicate that in some areas the diurnal variations are exceptionally large, particularly at the upper decile and quartile frequencies for large cities (e.g., along the Appalachians some upper decile diurnal variations for 100-km cities exceed a factor of 25). This could happen because the more extreme morning mixing heights for large cities are underestimated. Practical allowance for such effects (for city sizes of up to 100 km) have reduced the morning $\bar{X}/\bar{Q}$ values but the values are still considerably greater than afternoon values, and they still increase with city size. Consideration of emission control strategies for preventing and alleviating the widespread occurrence of undesirable pollutant concentrations over cities should recgonize that large diurnal variations in $\bar{X}/\bar{Q}$ occur in many regions and also that the magnitude of this variation increases with city size. Added effects of morning $\bar{X}/\bar{Q}$ values should also be carefully considered in those places where recirculation of contaiminated air occurs, since such effects are not included in the dispersion model. Episodes of at least a day during which high $\bar{X}/\bar{Q}$ values may be expected are especially indicated for those areas where both the morning and afternoon values are relatively large. The more outstanding areas of such coincidence are centered in Wyoming and Oregon; they occur mainly in winter and autumn at upper decile and quartile frequencies. As cities in these areas grow, they could experience very serious air pollution problems. Other applications of the data presented in Figures 21 through 50 are readily apparent (e.g., for specific locations, and for variations of city size and emission rate). However, because of the gross nature of the urban dispersion model and the input parameters, the derived $\bar{X}/\bar{Q}$ values should be recognized as only generally representative of real situations.

Finally, this study has objectively determined the episodic occurrence of several limited dispersion conditions during 5 years at each of the 62 upper air stations. Two episode durations are included, at least 2 days and at least 5 days. The most limited dispersion conditions considered—mixing heights 500 m or less and wind speeds 2.0 m sec^{-1} or less with no significant precipitation during episodes lasting at least 5 days—occurred at only two stations (a total of six episodes and 39 episode-days). The least-limited dispersion conditions considered—mixing heights 2000 m or less and wind speeds 6.0 m sec^{-1} or less with no significant precipitation during episodes lasting at least 2 days (Figure 62)—occurred at all stations, and at San Diego and Santa Monica California, such episode-days were more common than not. Intermediate limiting conditions of mixing heights—1500 m or less and wind speeds 4.0 m sec^{-1} or less with no significant precipitation during episodes lasting at least 2 days (Figure 58)—are of interest because such criteria have been used in the National Air Pollution Potential Forecasting Program. Figure 58 shows that total episode-days with these conditions are at a

minimum through the middle tier of states with no days in 5 years at two stations. In the East, the total number of these episode-days barely exceeds 100 at one station, but in the West 100 days is exceeded at most stations and 200 days is not uncommon. Episodes with these same limiting conditions, but lasting at least 5 days (Figure 67), are extremely rare in all but the western states where 100 days in 5 years is exceeded at several stations.

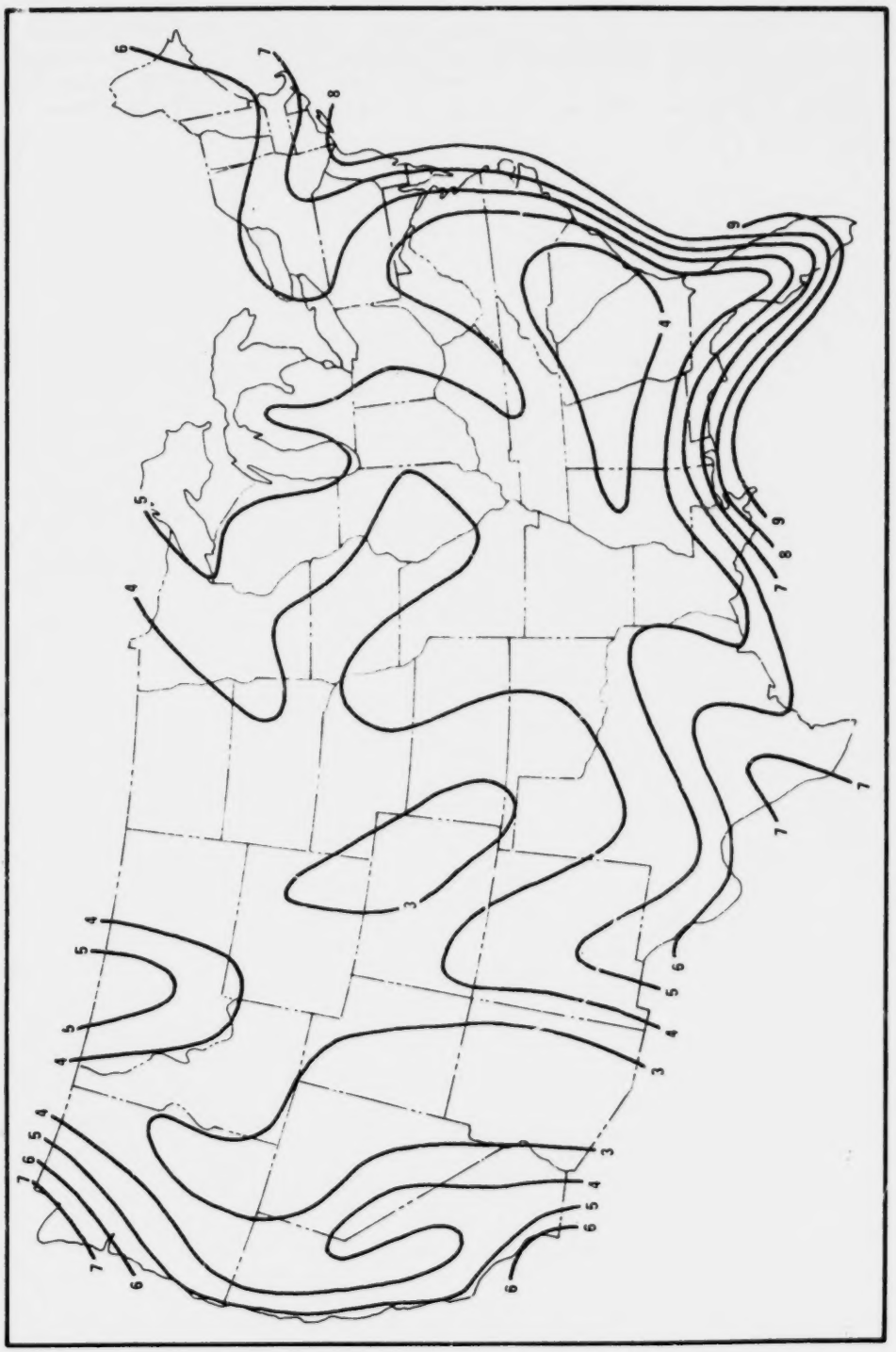

Figure 1. Isopleths (m x 10^2) of mean annual morning mixing heights (see Table B-1 for data).

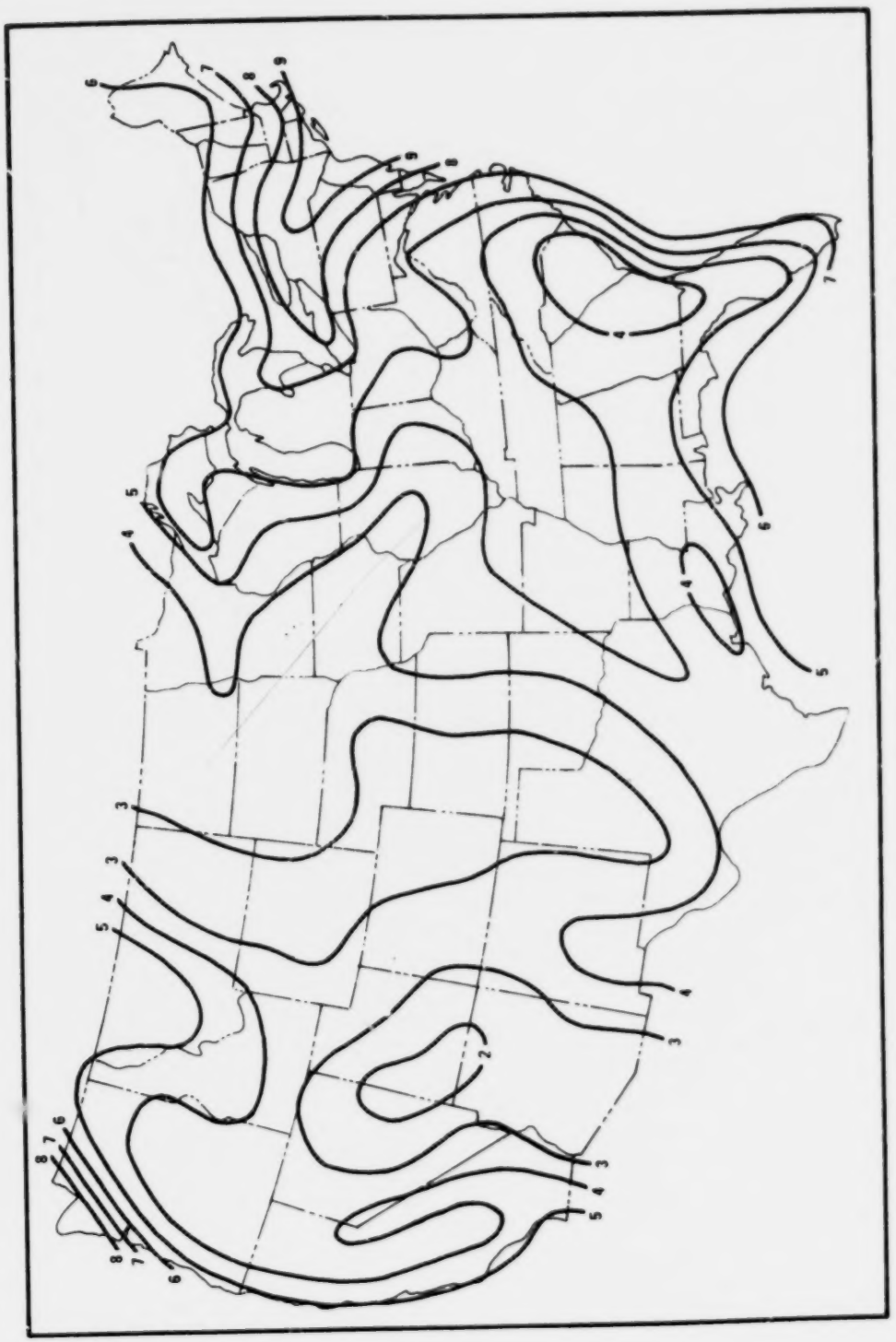

Figure 2. Isopleths (m x 10^2) of mean winter morning mixing heights (see Table B-1 for data).

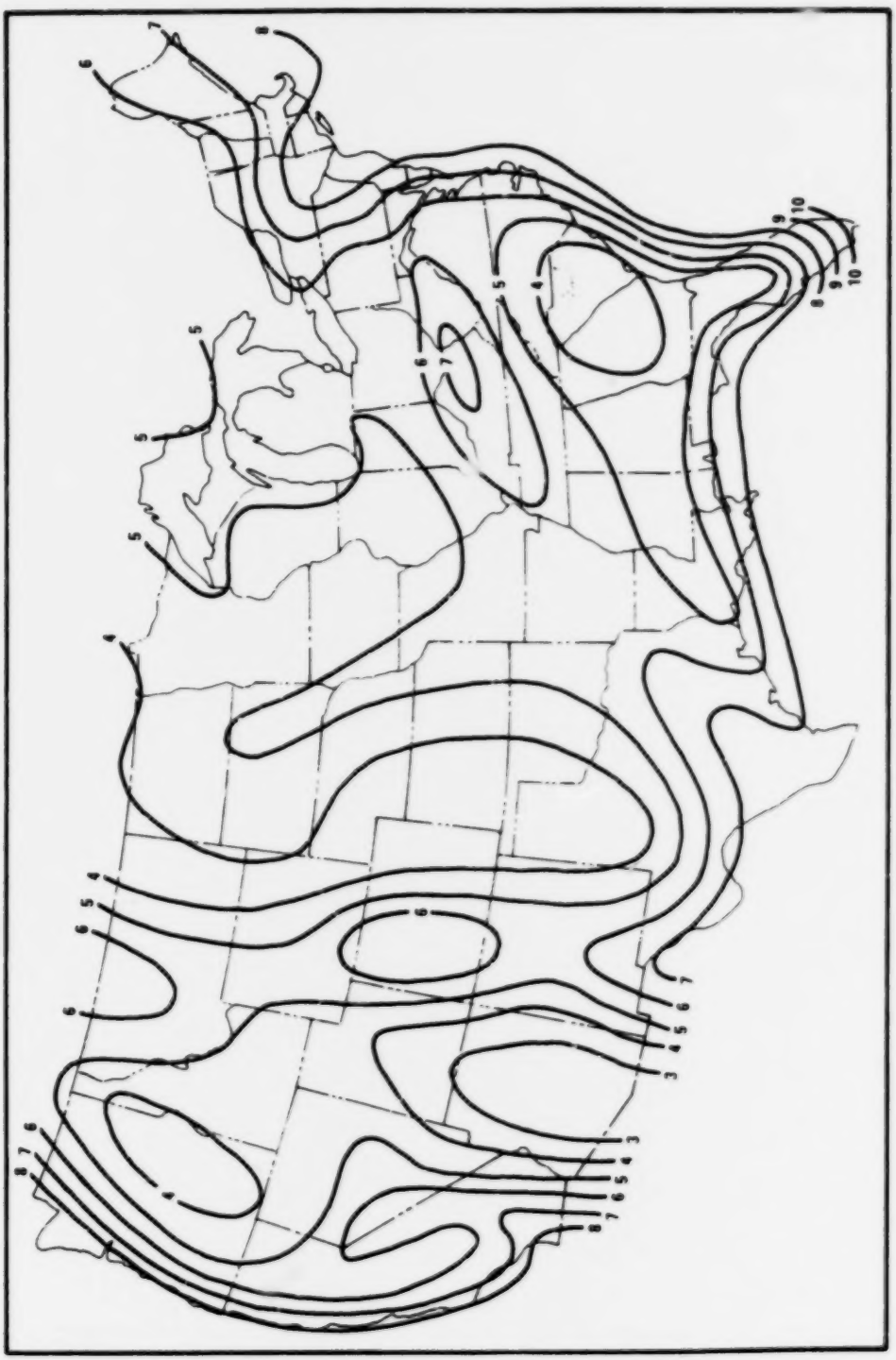

Figure 3. Isopleths (m x 10^2) of mean spring morning mixing heights (see Table B-1 for data).

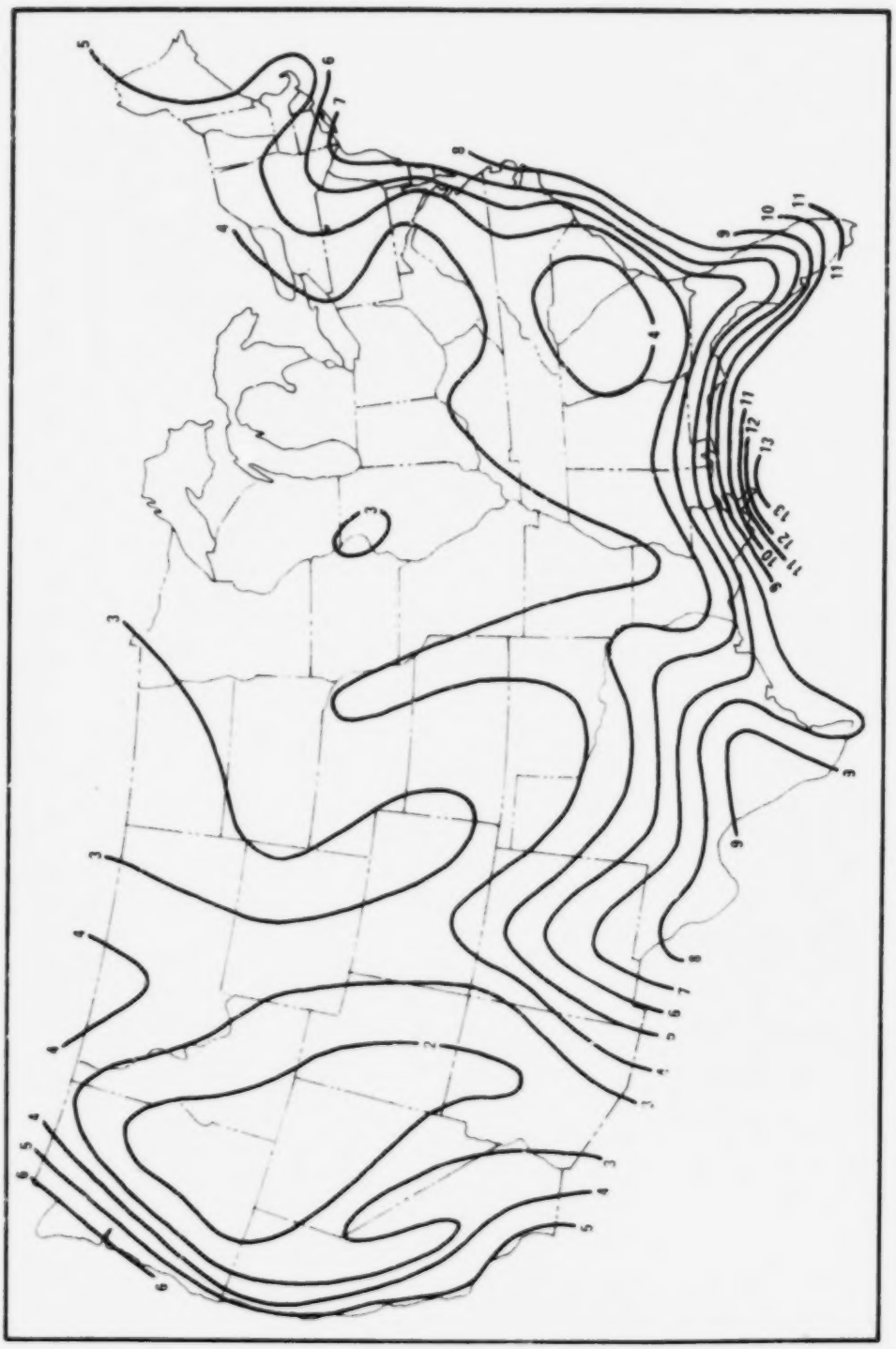

Figure 4. Isopleths (m x 10^2) of mean summer morning mixing heights (see Table B-1 for data).

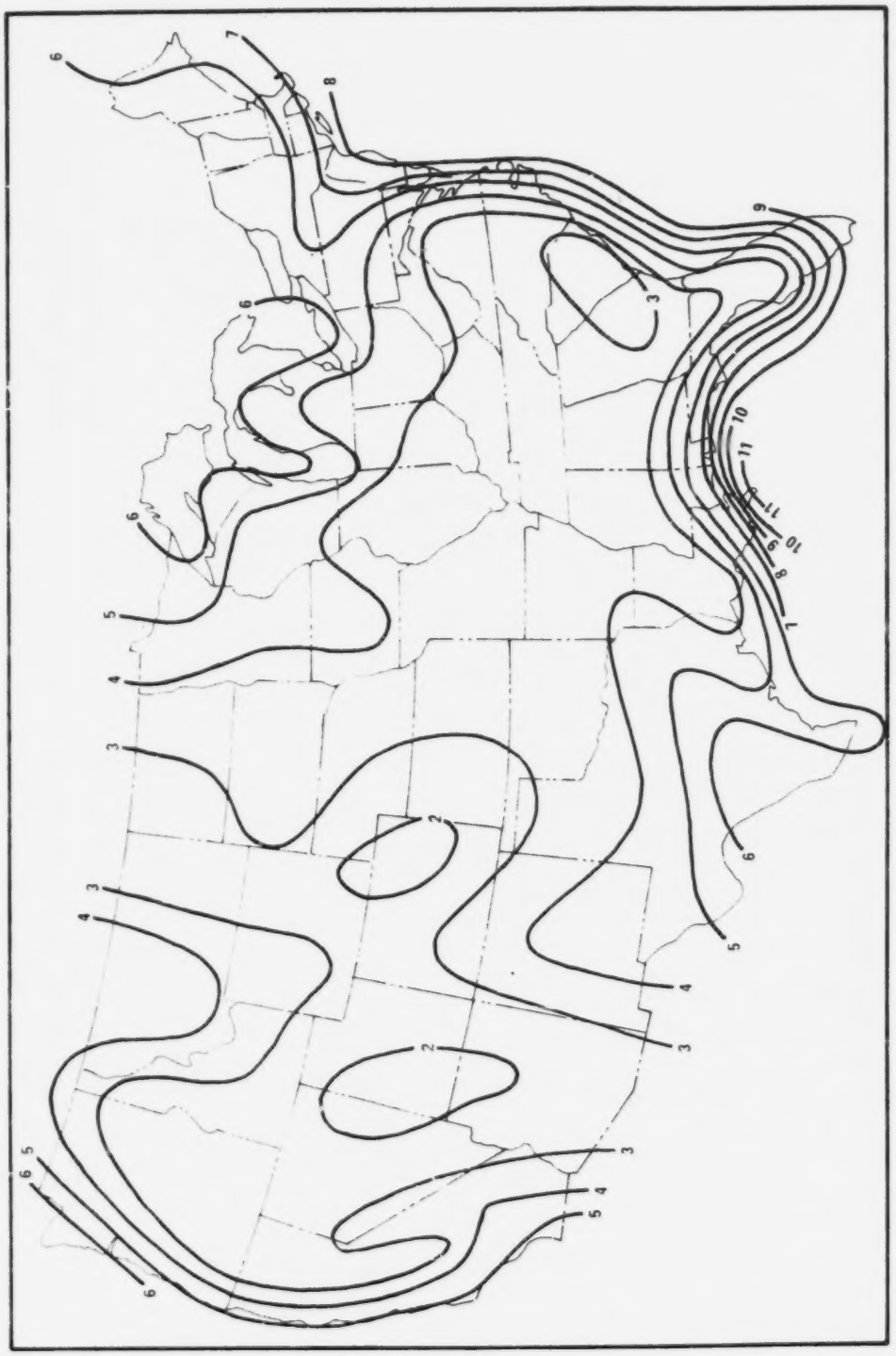

Figure 5. Isopleths (m x 10^2) of mean autumn morning mixing heights (see Table B-1 for data).

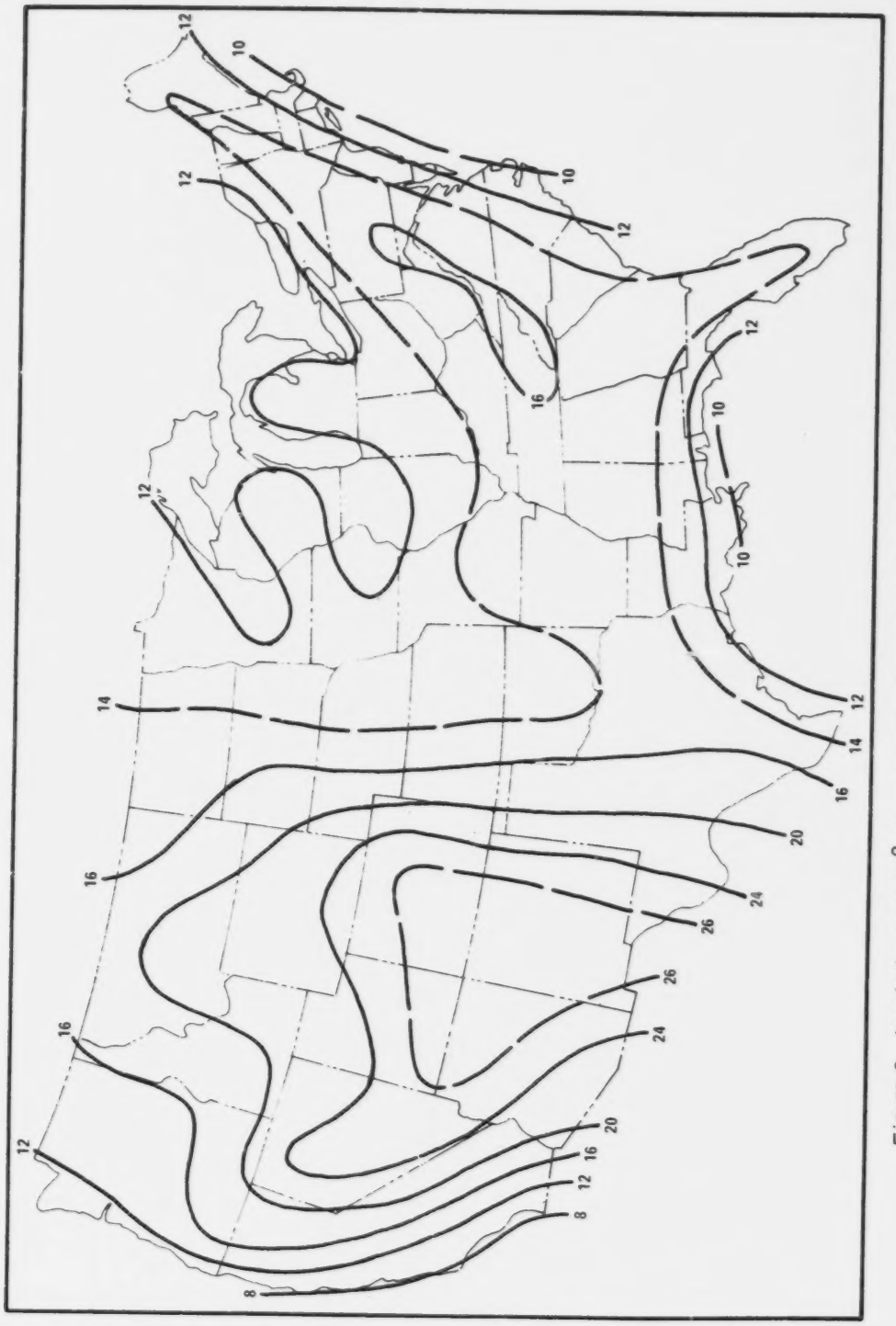

Figure 6. Isopleths (m x 10^2) of mean annual afternoon mixing heights (see Table B-1 for data).

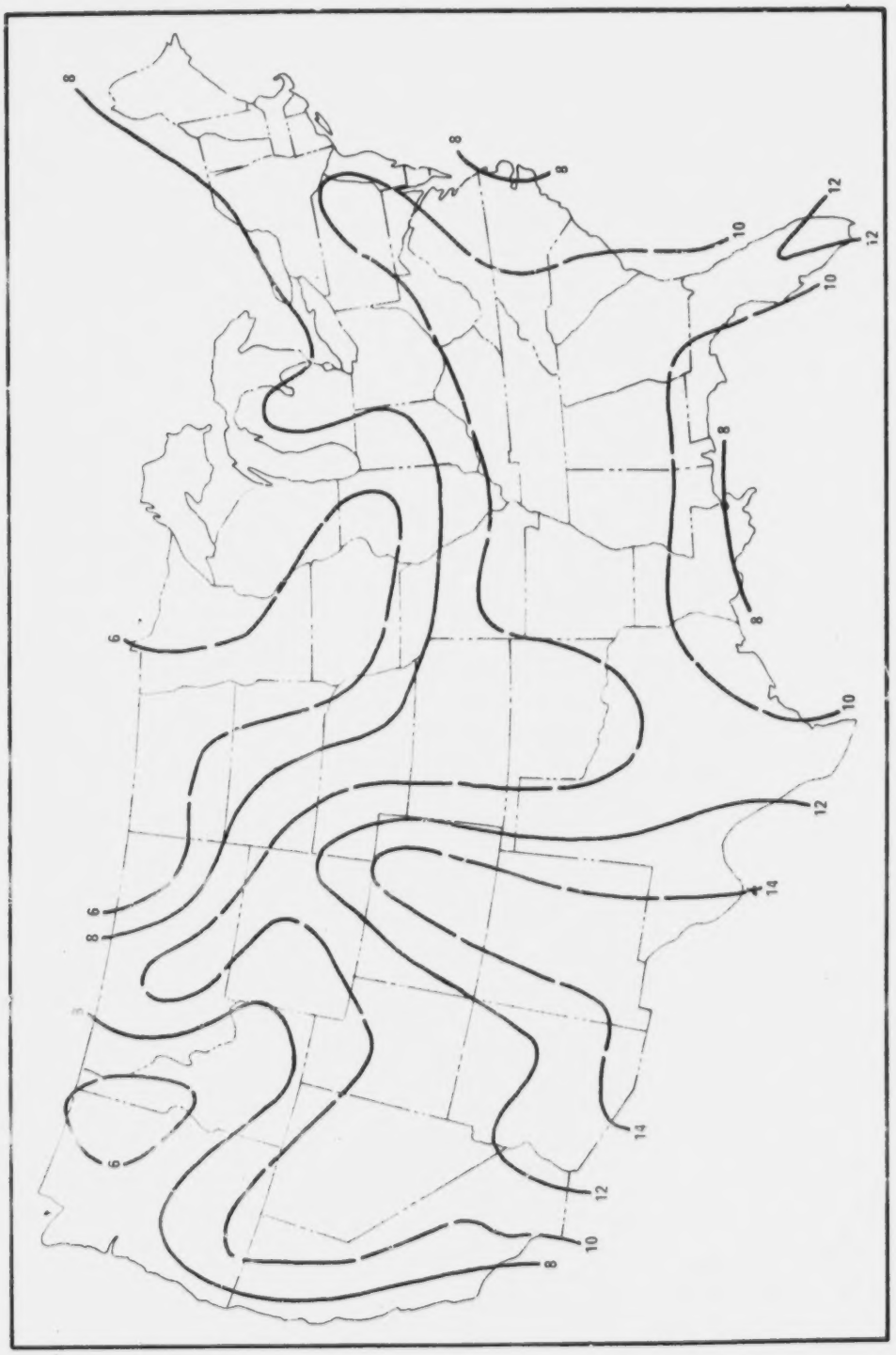

Figure 7. Isopleths ($m \times 10^2$) of mean winter afternoon mixing heights (see Table B-1 for data).

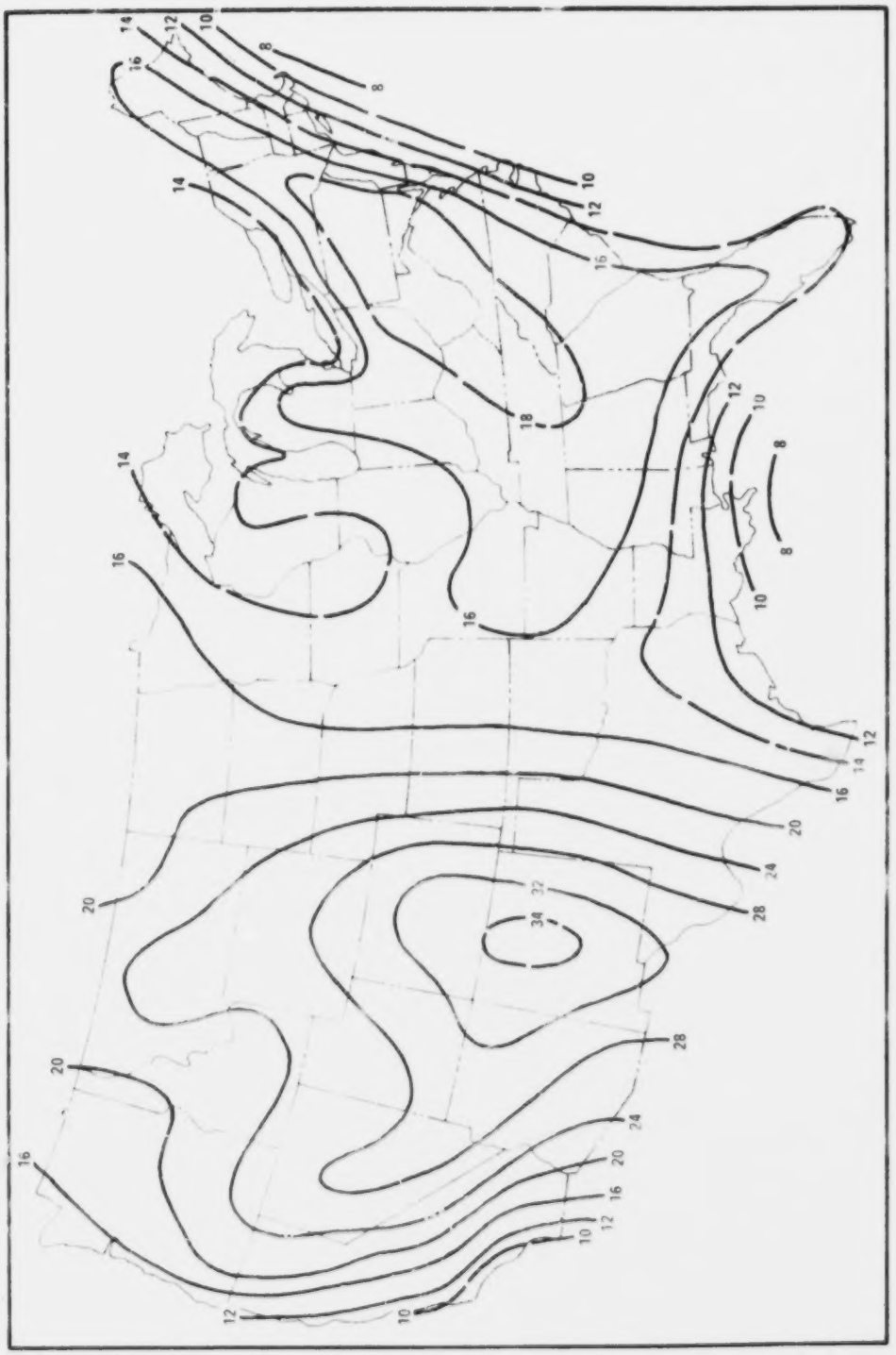

Figure 8. Isopleths ($m \times 10^2$) of mean spring afternoon mixing heights (see Table B-1 for data).

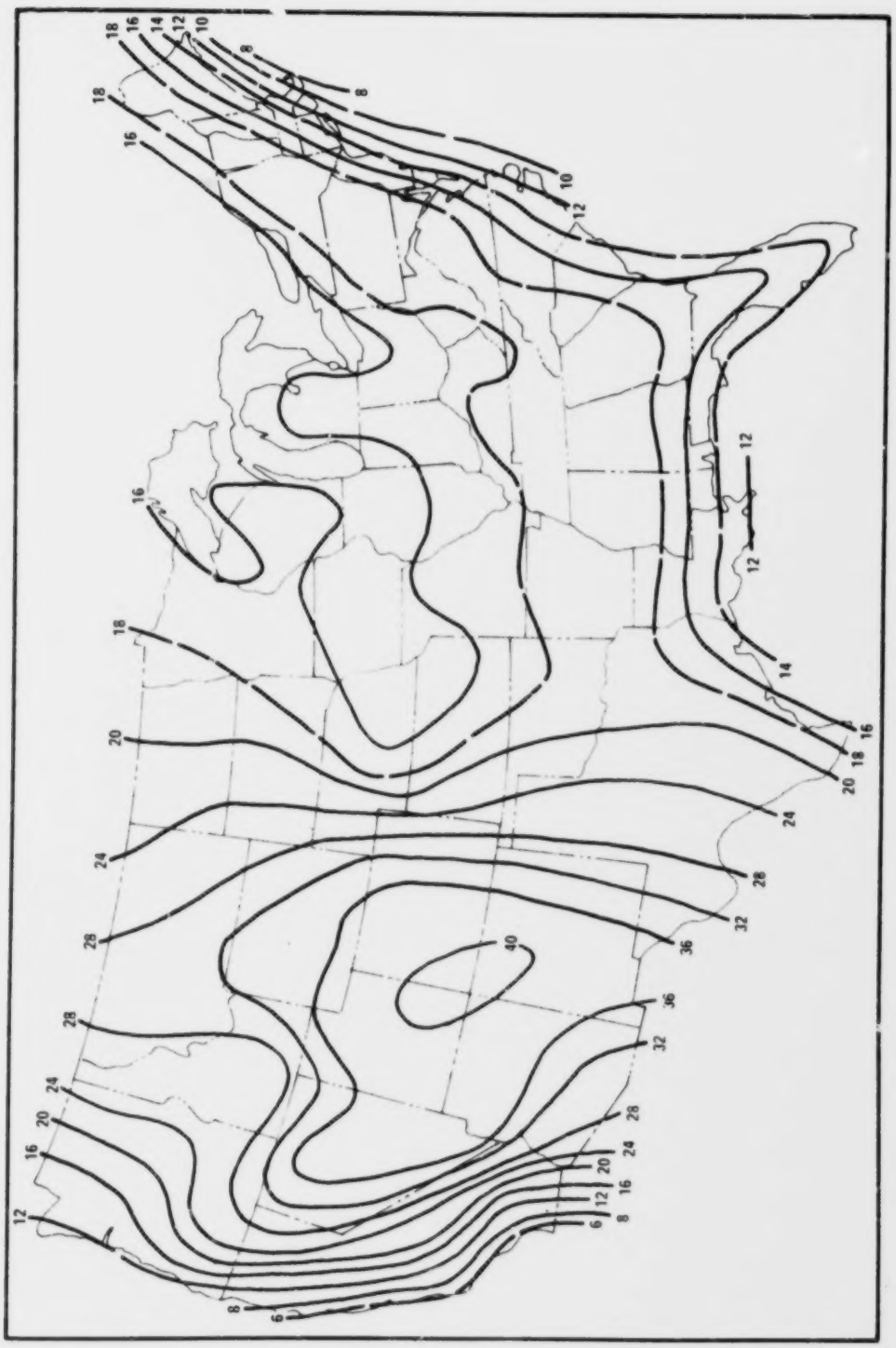

Figure 9. Isopleths ($m \times 10^2$) of mean summer afternoon mixing heights (see Table B-1 for data).

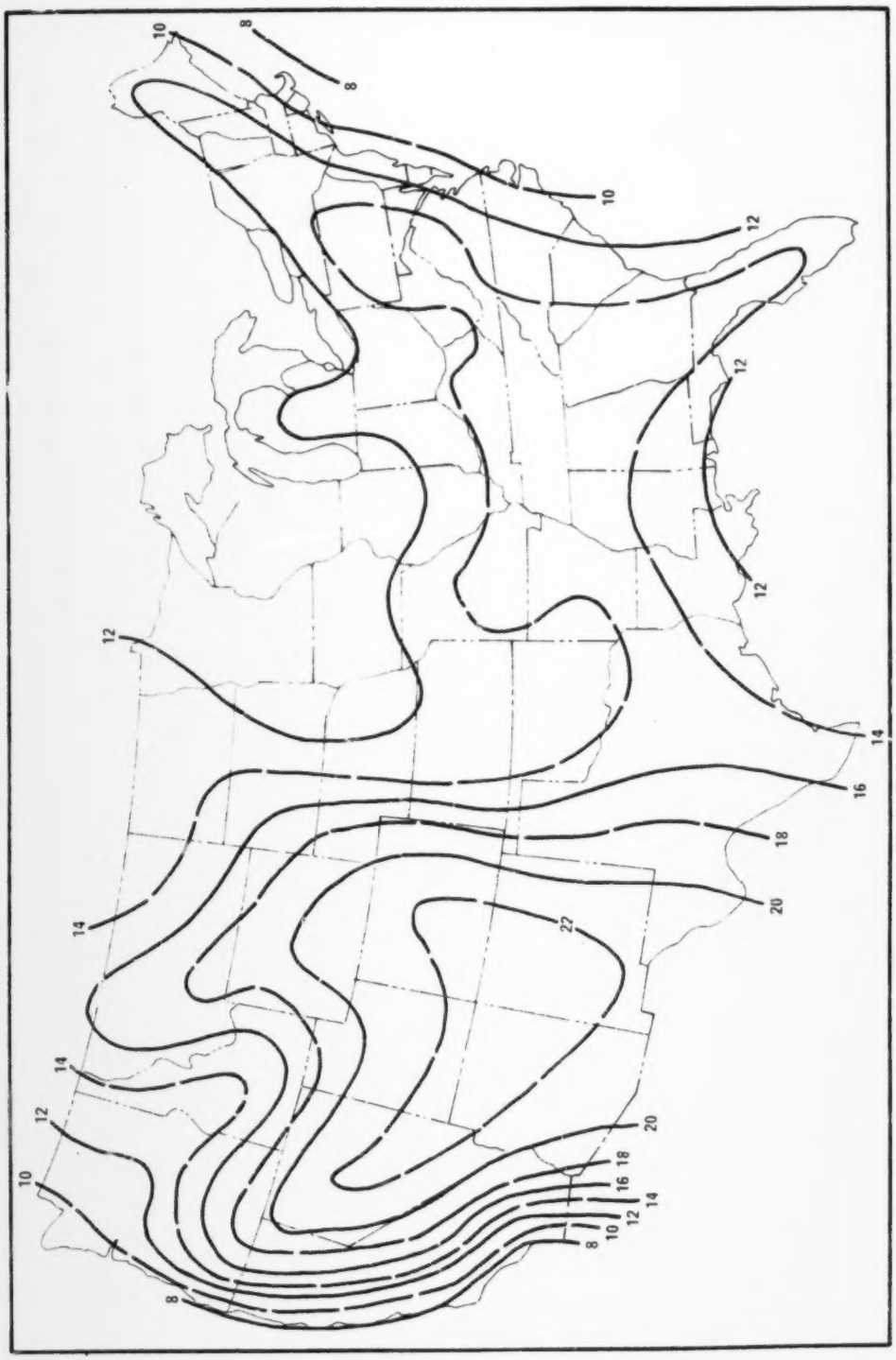

Figure 10. Isopleths (m x 10^2) of mean autumn afternoon mixing heights (see Table B-1 for data).

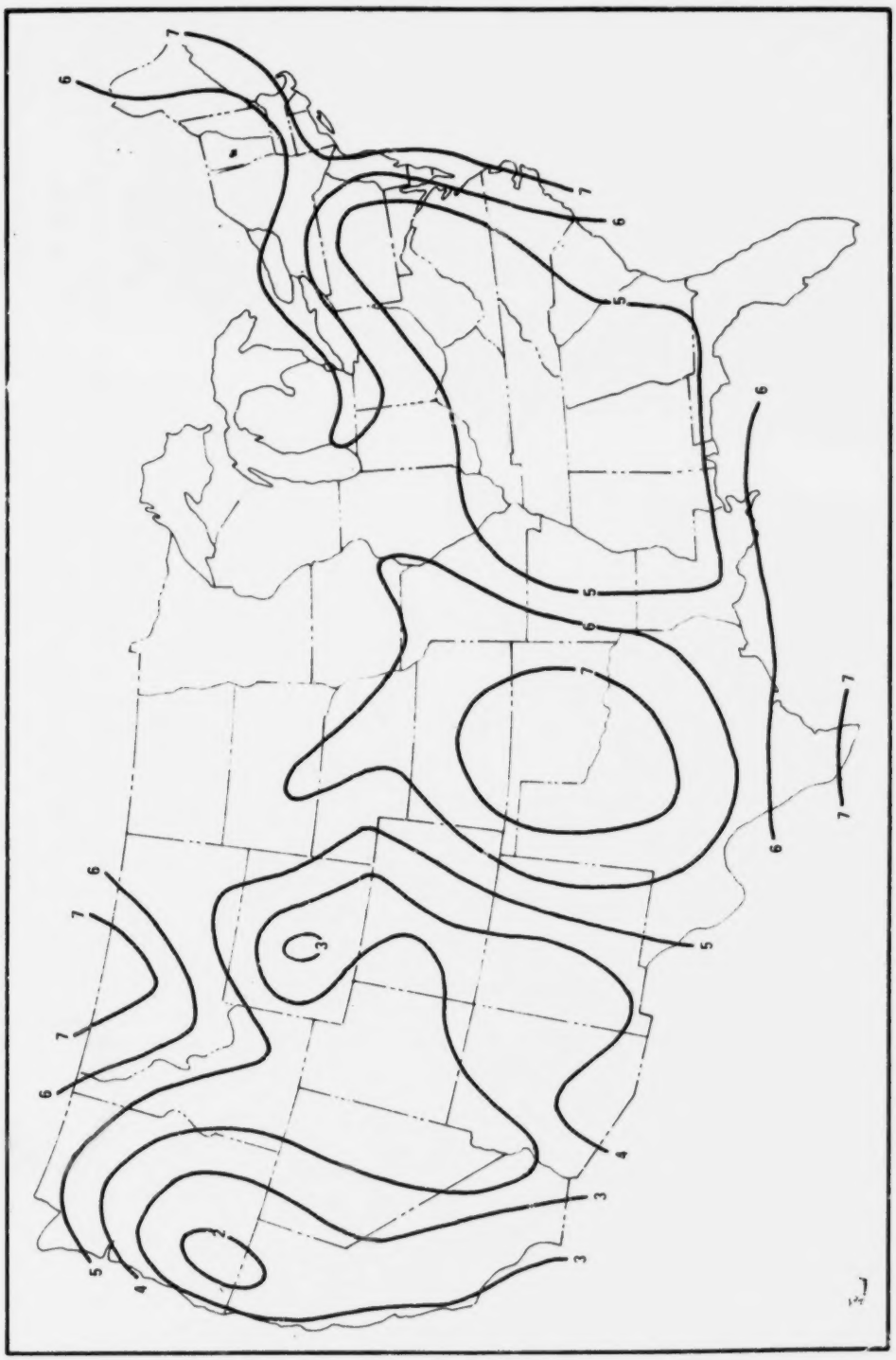

Figure 11. Isopleths (m sec^{-1}) of mean annual wind speed averaged through the morning mixing layer (Figure 1).

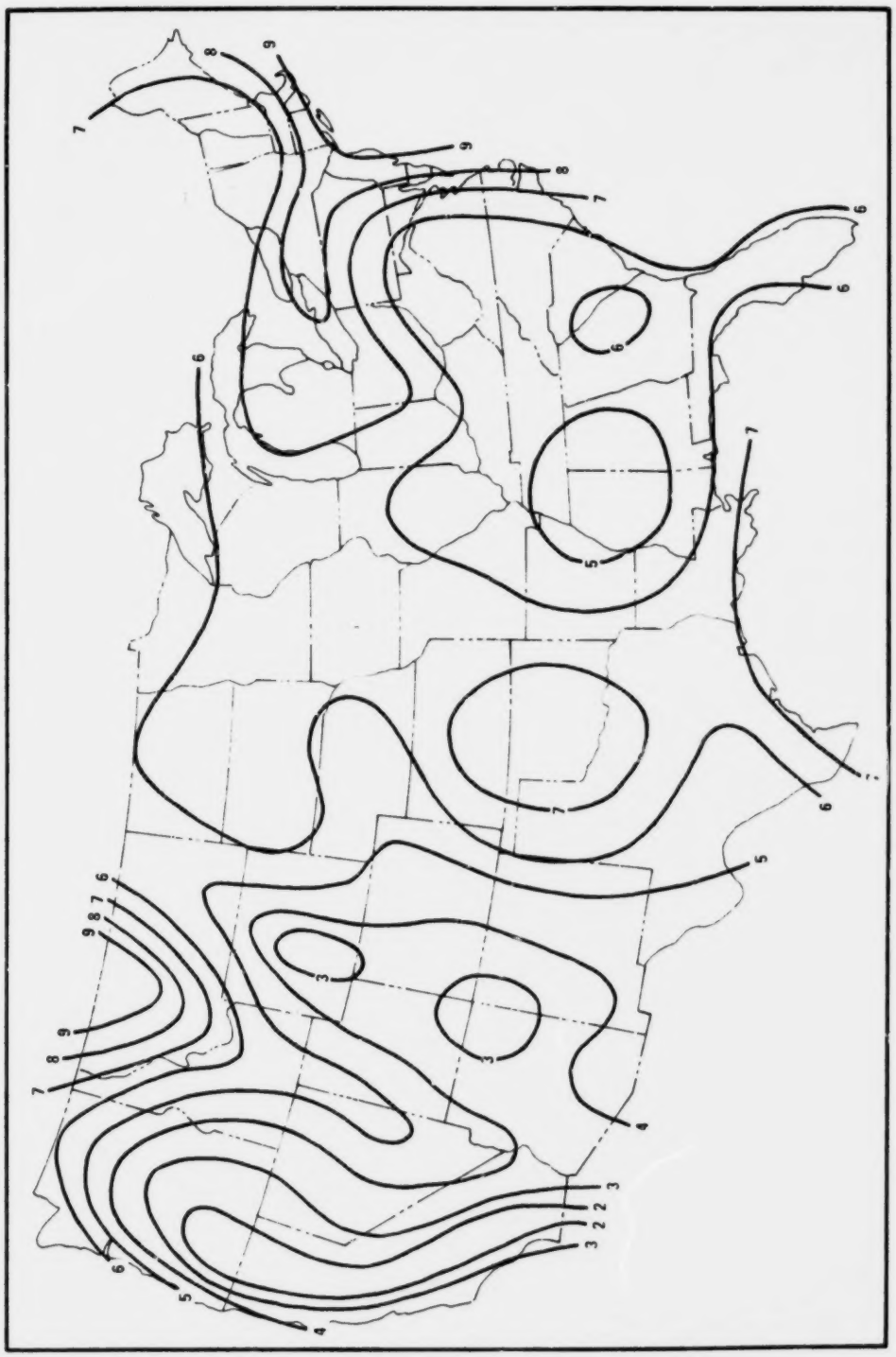

Figure 12. Isopleths (m sec^{-1}) of mean winter wind speed averaged through the morning mixing layer (Figure 2).

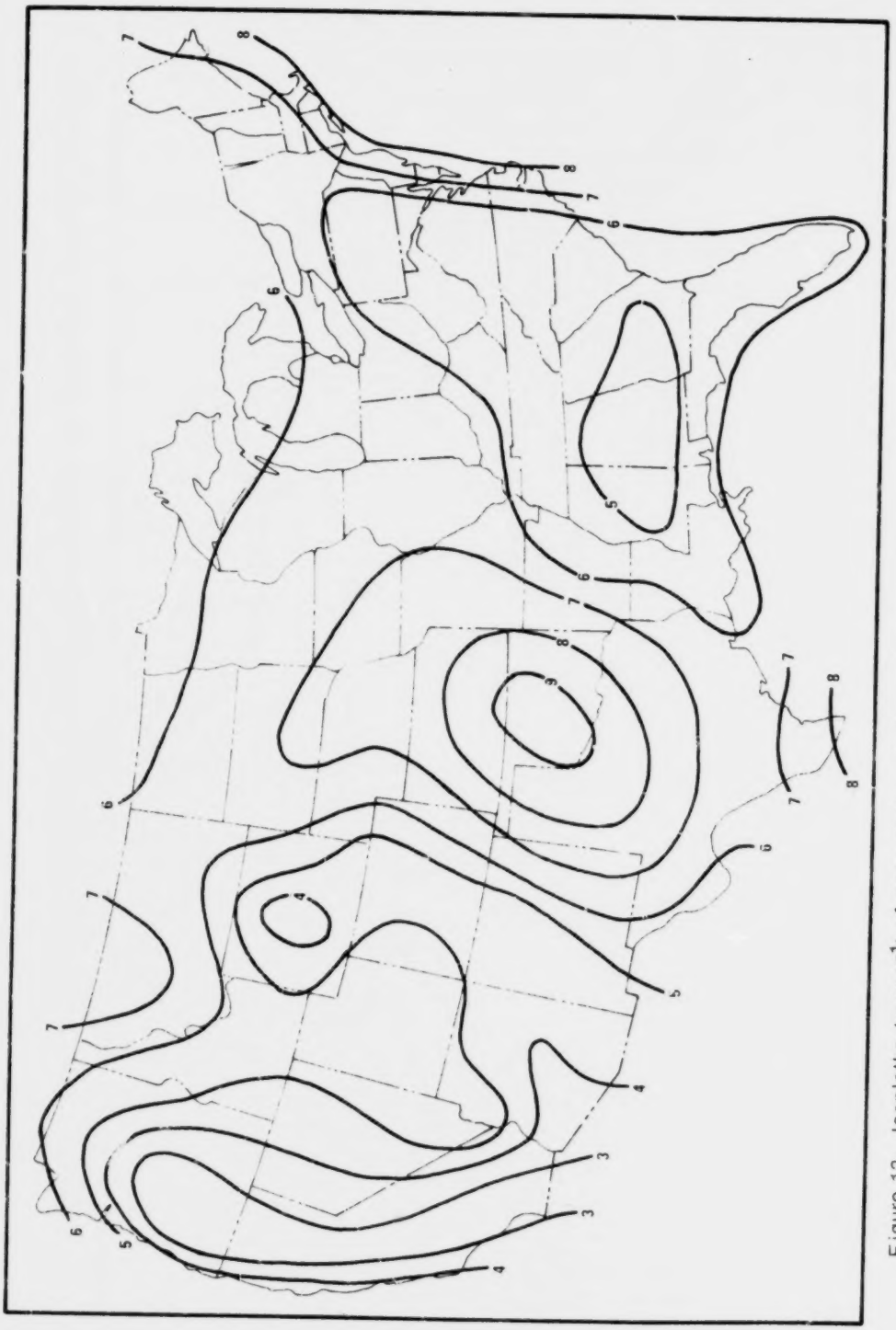

Figure 13. Isopleths (m sec^{-1}) of mean spring wind speed averaged through the morning mixing layer (Figure 3).

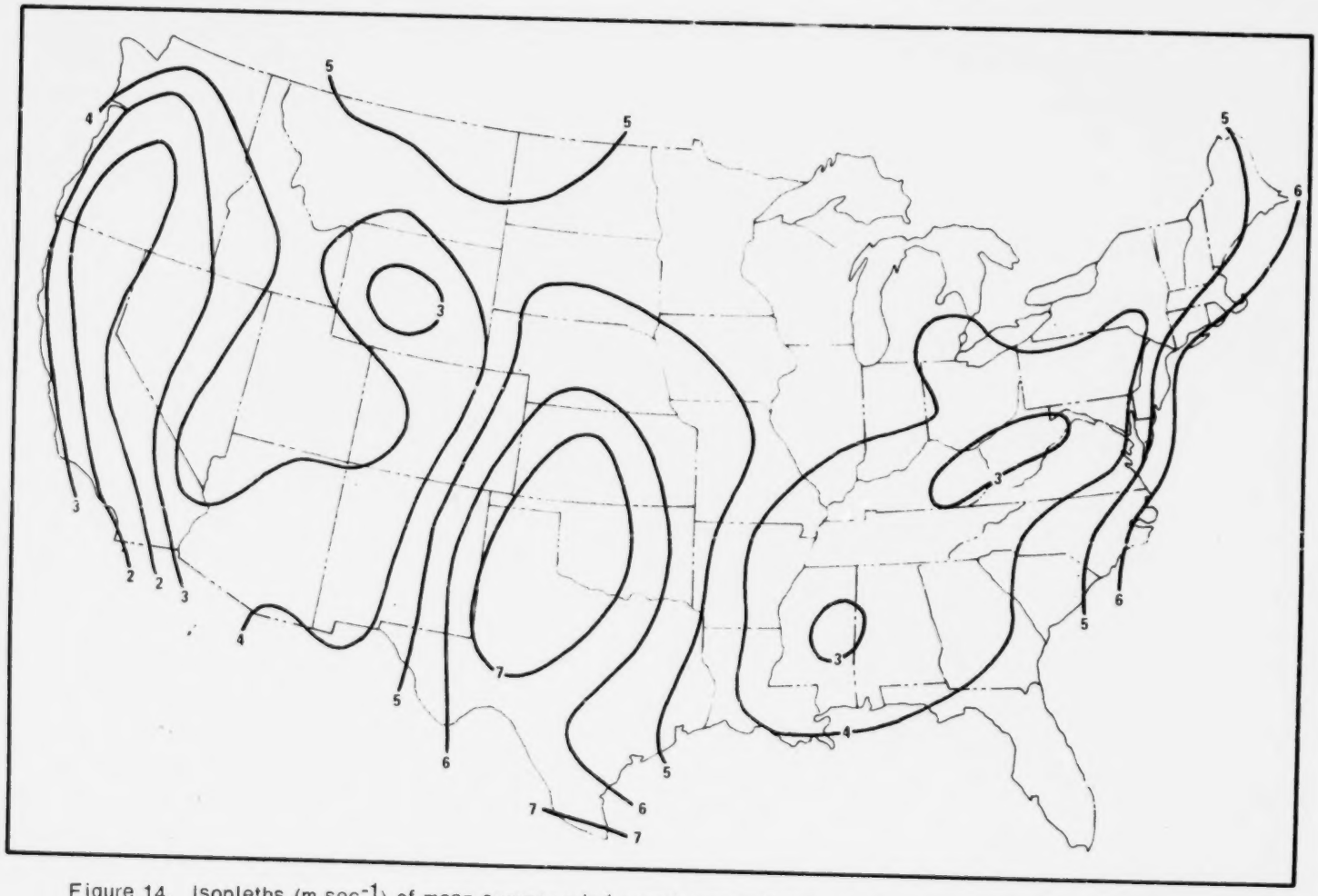

Figure 14. Isopleths (m sec^{-1}) of mean summer wind speed averaged through the morning mixing layer (Figure 4).

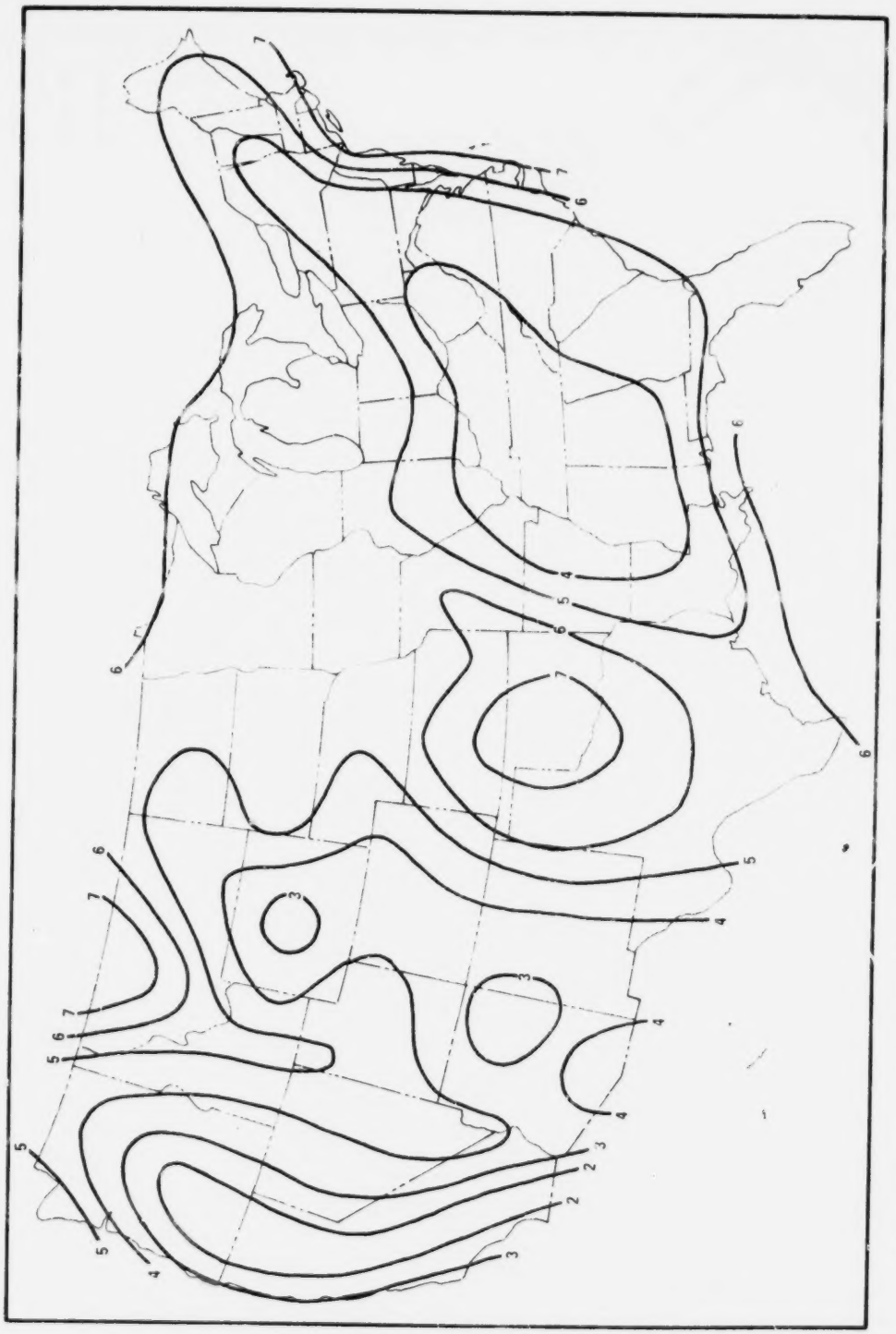

Figure 15. Isopleths (m sec^{-1}) of mean autumn wind speed averaged through the morning mixing layer (Figure 5).

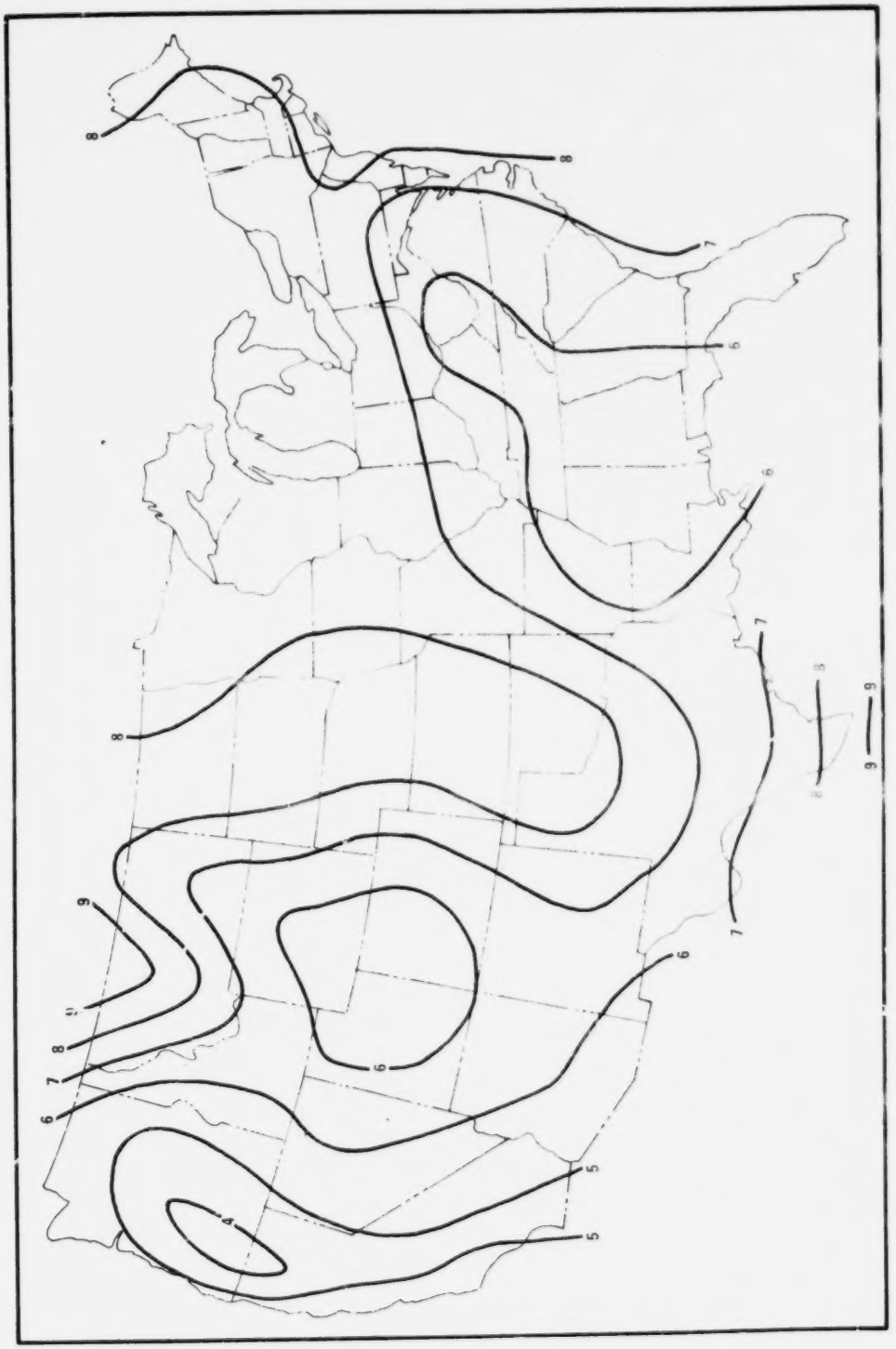

Figure 16. Isopleths (m sec^{-1}) of mean annual wind speed averaged through the afternoon mixing layer (Figure 6).

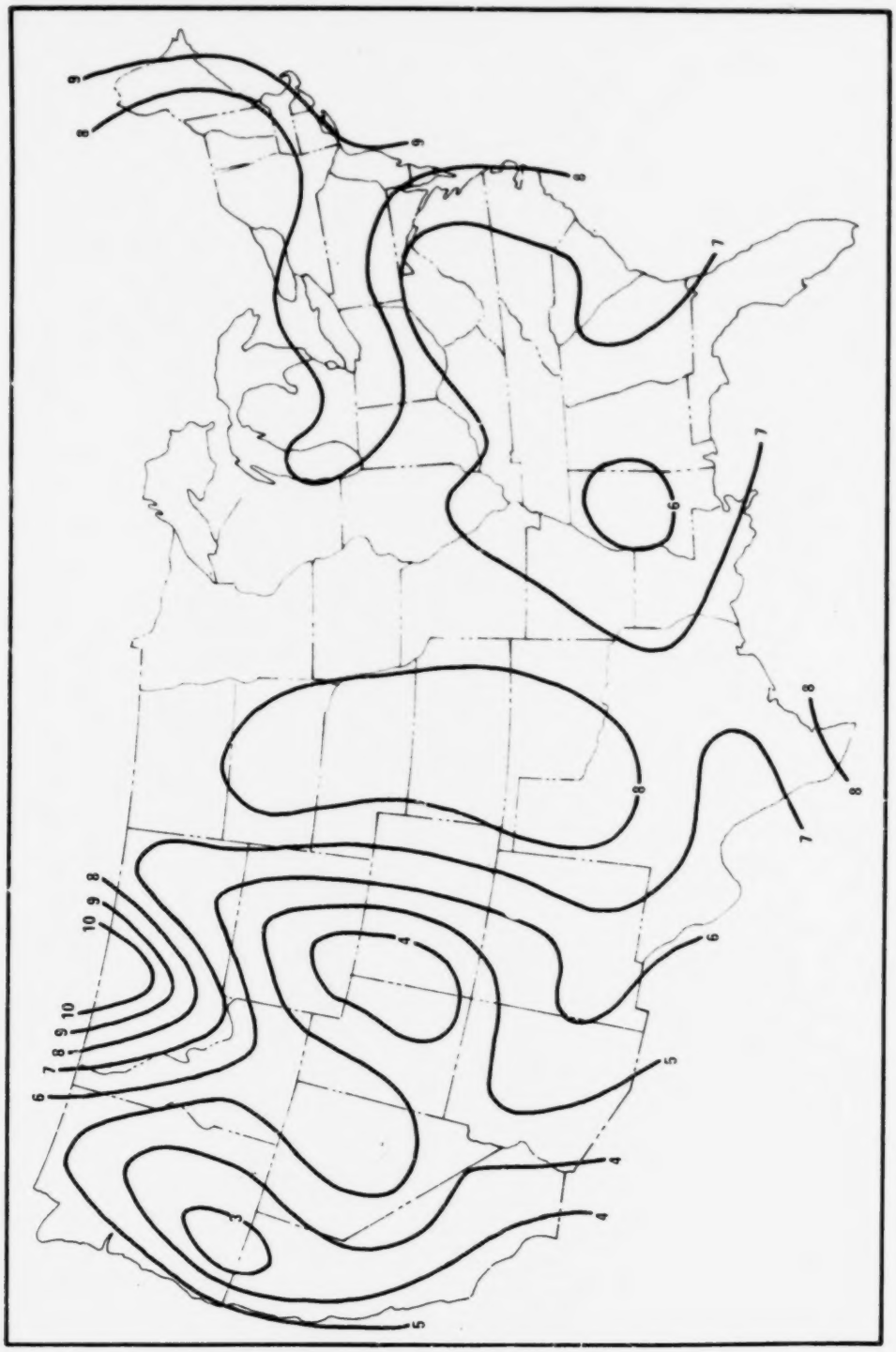

Figure 17. Isopleths (m sec^{-1}) of mean winter wind speed averaged through the afternoon mixing layer (Figure 7).

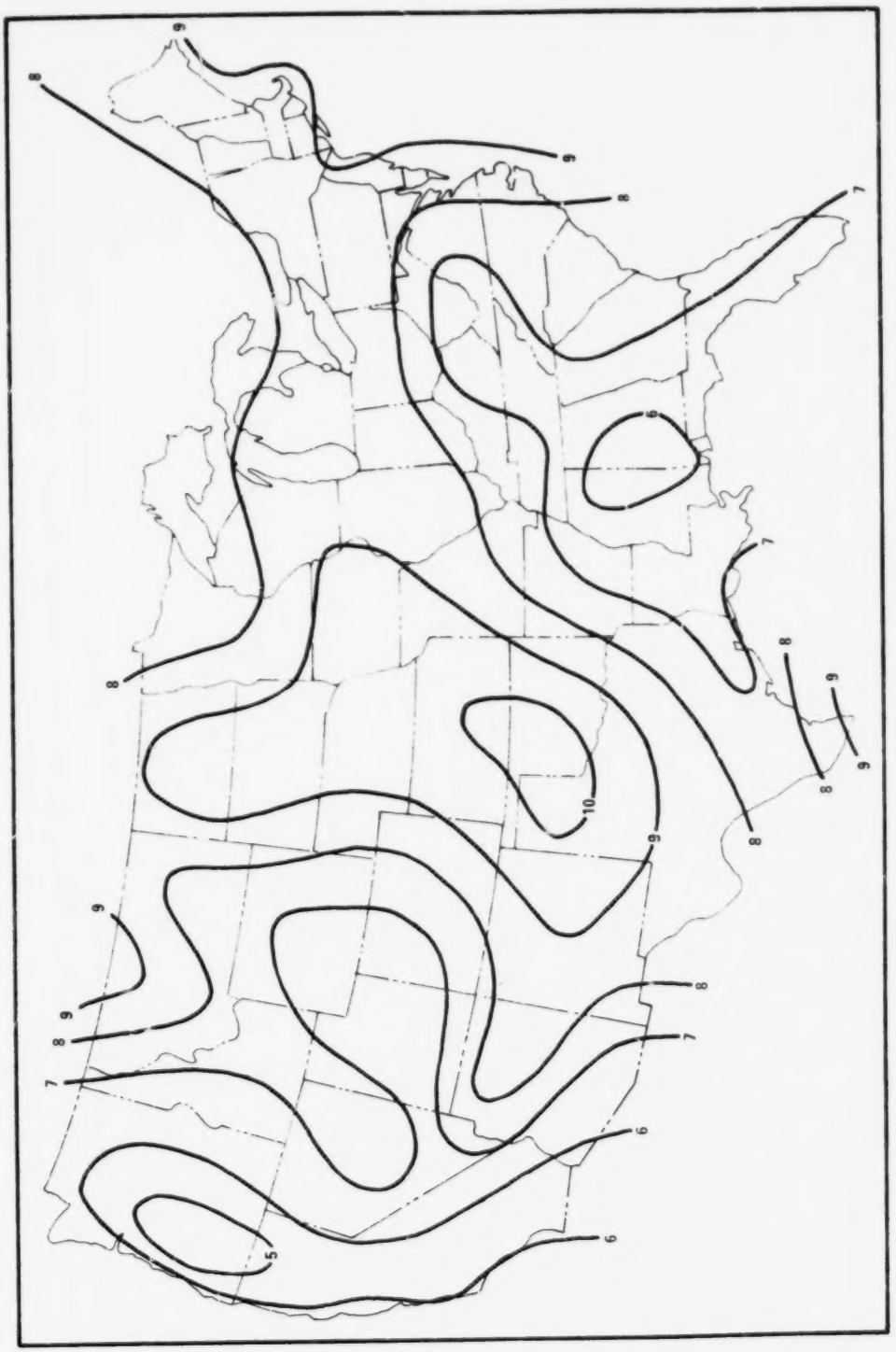

Figure 18. Isopleths (m sec^{-1}) of mean spring wind speed averaged through the afternoon mixing layer (Figure 8).

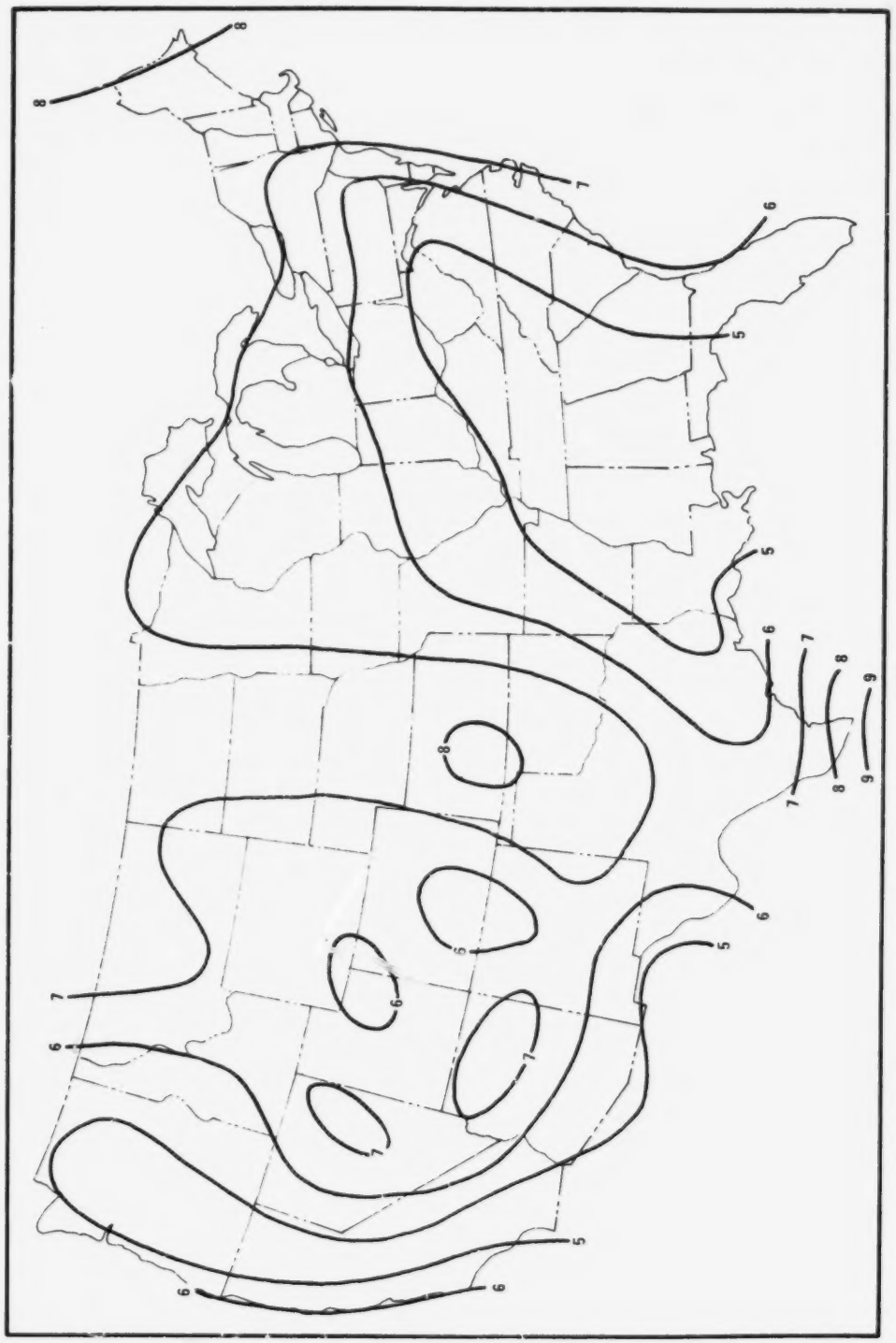

Figure 19. Isopleths (m sec^{-1}) of mean summer wind speed averaged through the afternoon mixing layer (Figure 9).

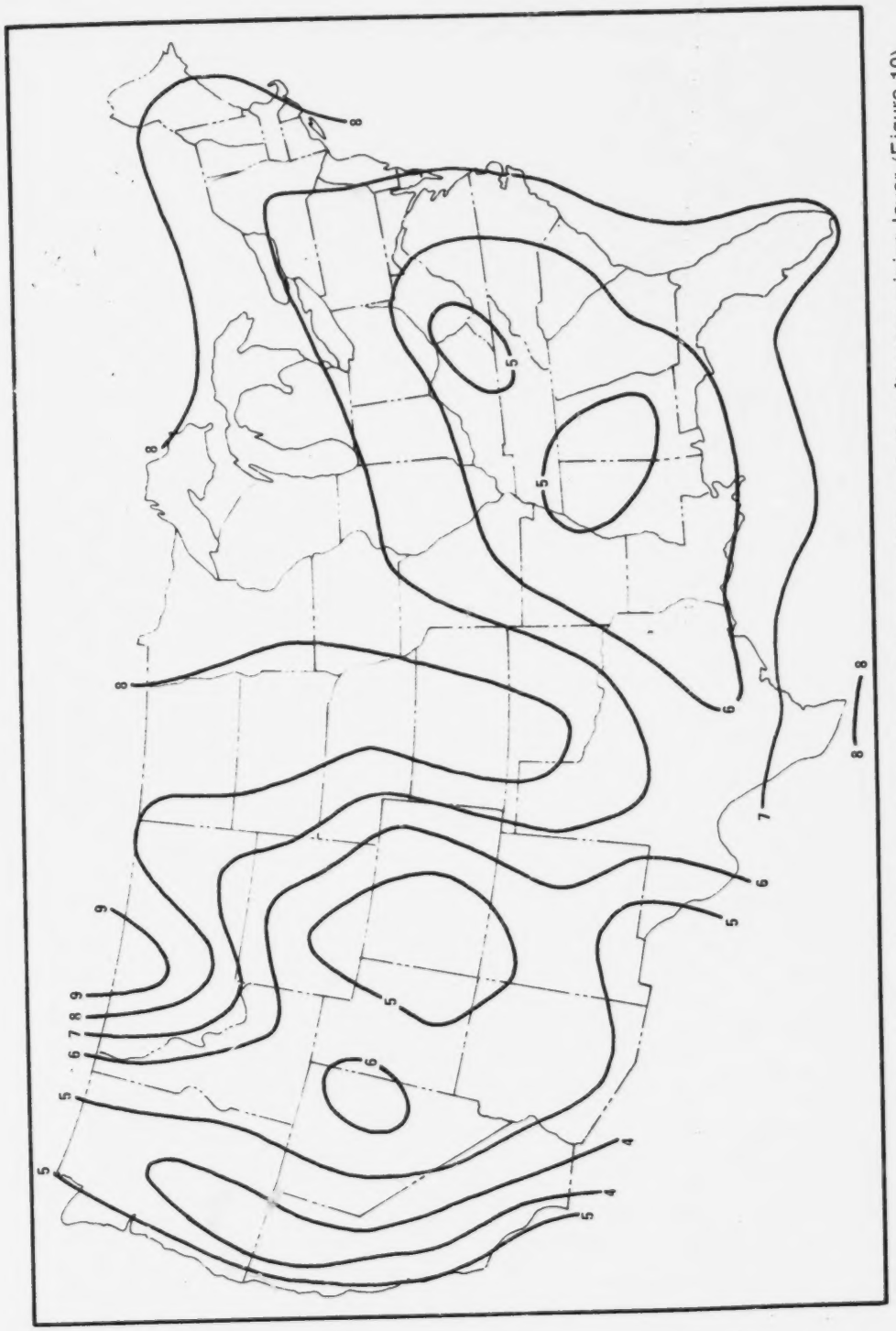

Figure 20. Isopleths (m sec^{-1}) of mean autumn wind speed averaged through the afternoon mixing layer (Figure 10).

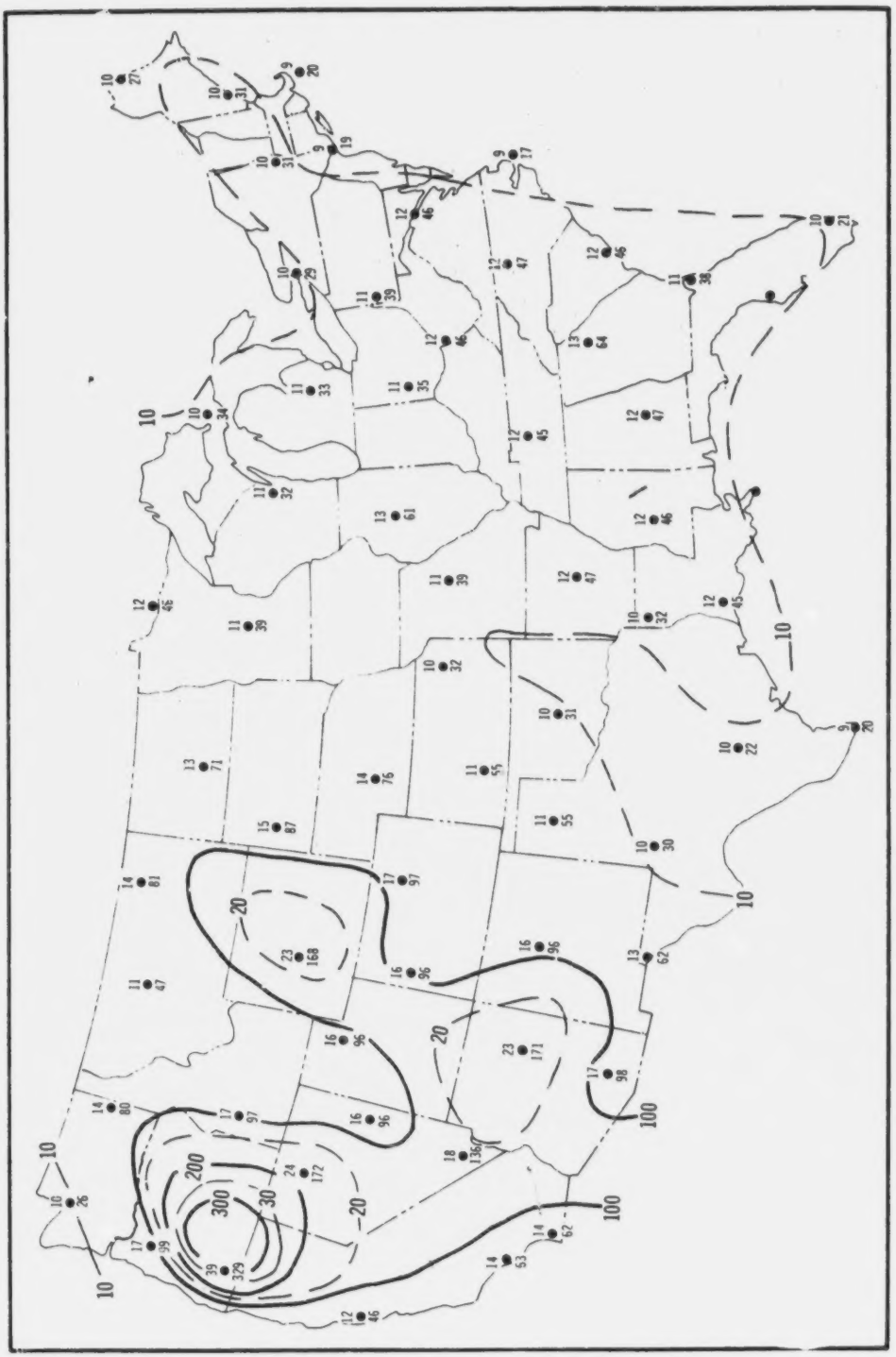

Figure 21. Data and isopleths (sec m^{-1}) of median annual morning $\overline{\chi}/\overline{Q}$ values (see text) for 10- (upper numerals and dashed isopleths) and 100-km (lower numerals and solid isopleths) city sizes.

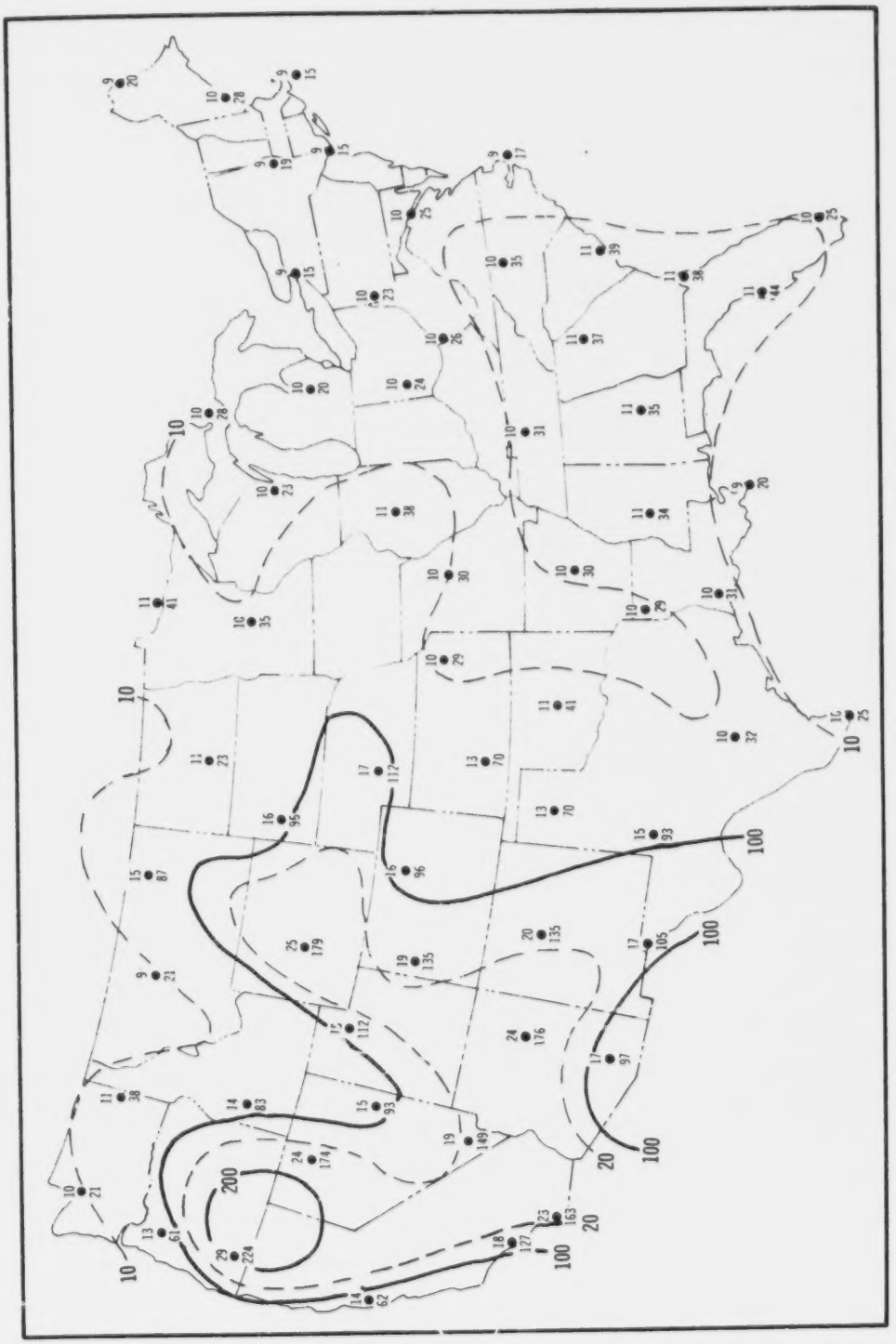

Figure 22. Data and isopleths (sec m^{-1}) of the median winter morning $\bar{\chi}/\bar{Q}$ values (see text) for 10- (upper numerals and dashed isopleths) and 100-km (lower numerals and solid isopleths) city sizes.

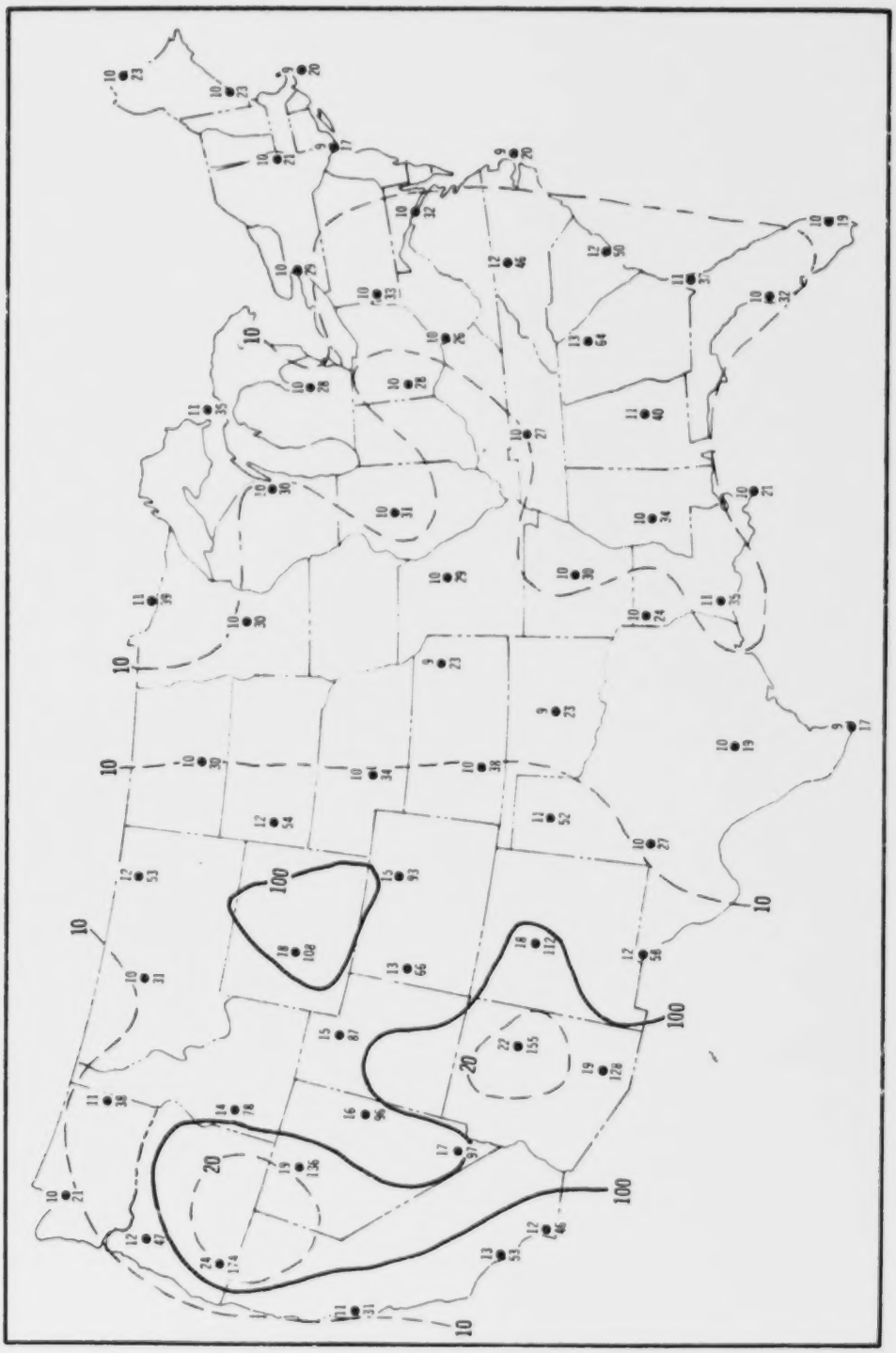

Figure 23. Data and isopleths (sec m^{-1}) of median spring morning $\bar{\chi}/\bar{Q}$ values (see text) for 10- (upper numerals and dashed isopleths) and 100-km (lower numerals and solid isopleths) city sizes.

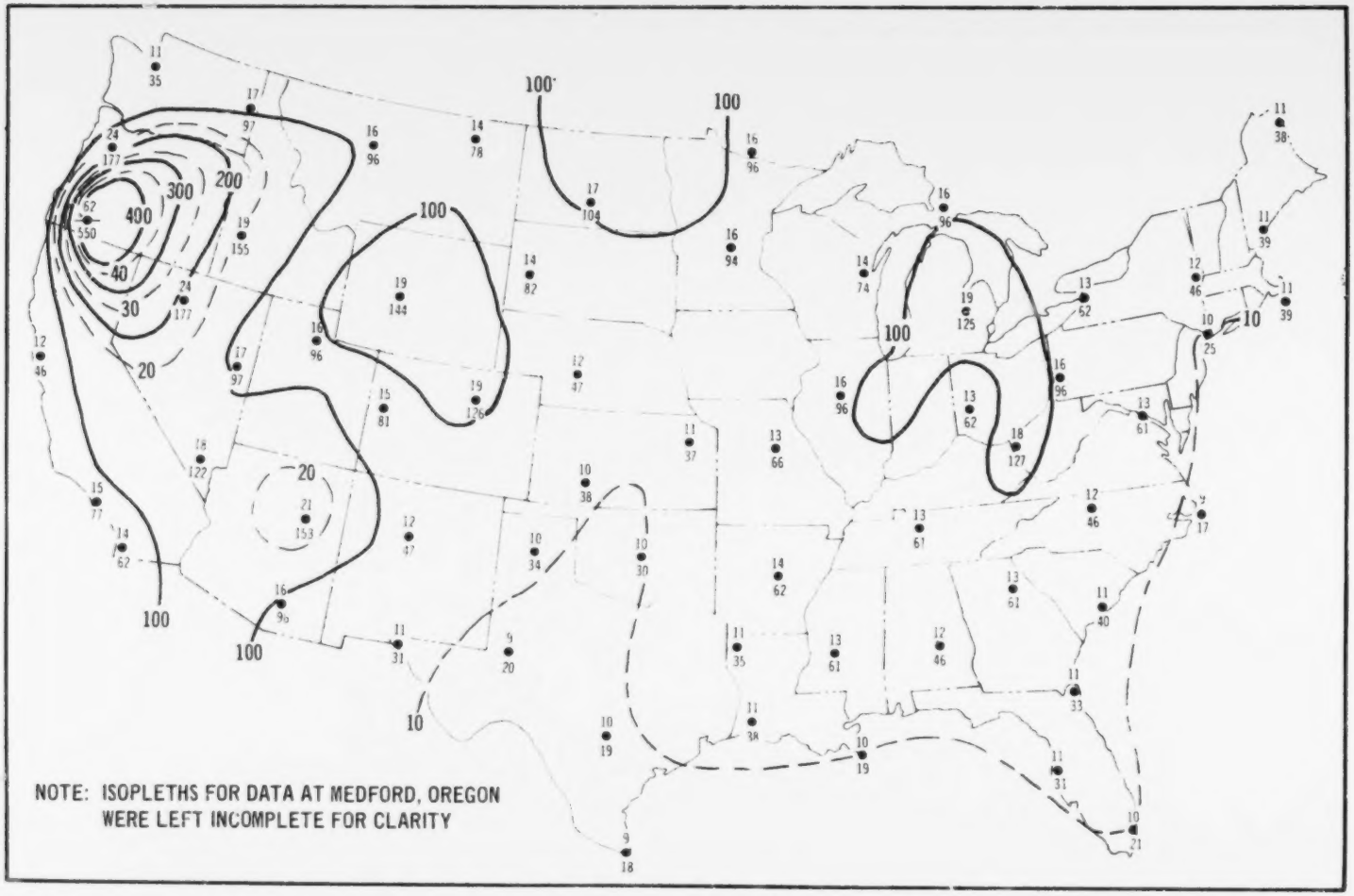

Figure 24. Data and isopleths (sec m^{-1}) of median summer morning $\bar{\chi}/\bar{Q}$ values (see text) for 10- (upper numerals and dashed isopleths) and 100-km (lower numerals and solid isopleths) city sizes.

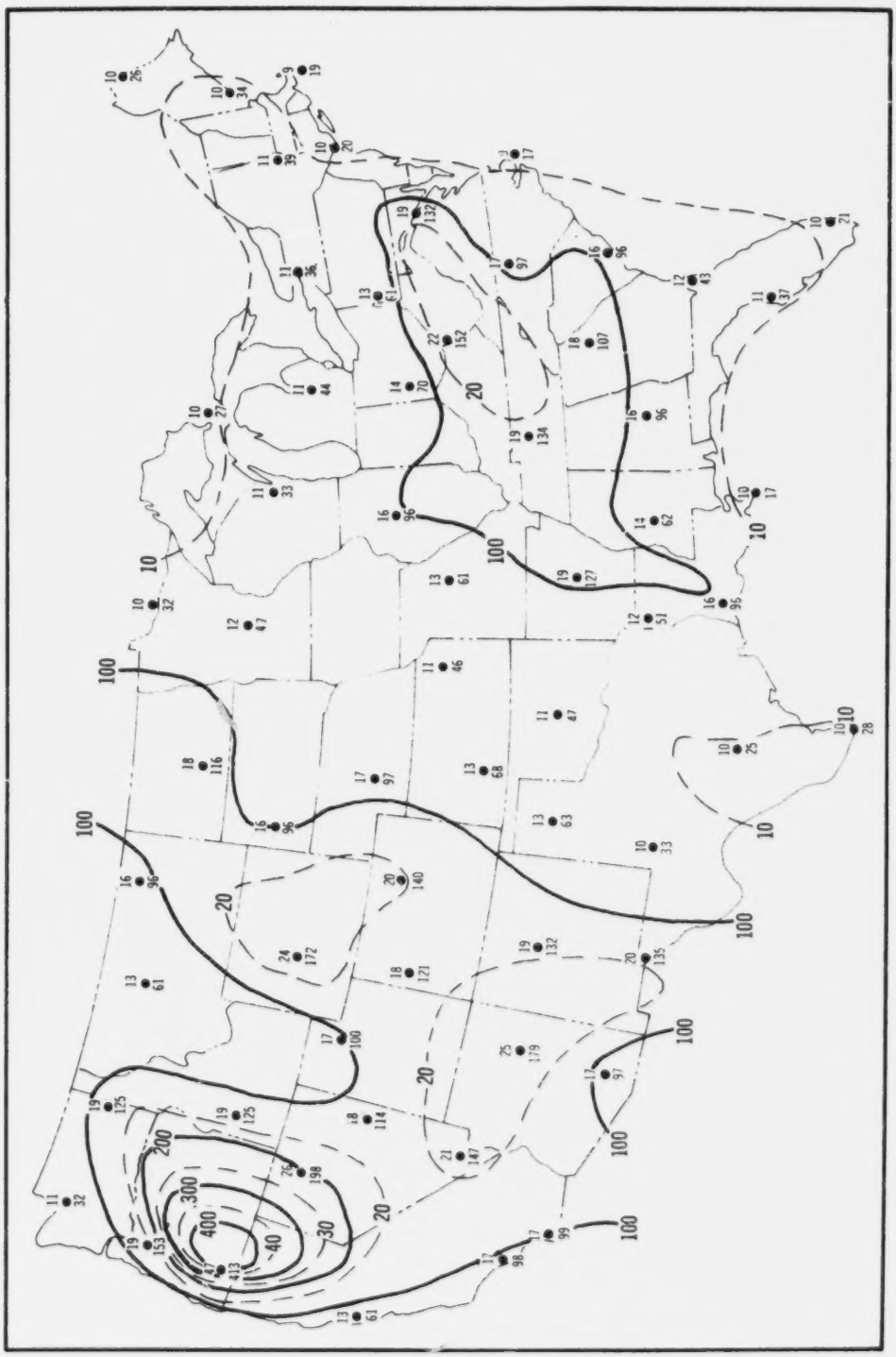

Figure 25. Data and isopleths (sec m^{-1}) of median autumn morning $\bar{\chi}/\bar{Q}$ values (see text) for 10- (upper numerals and dashed isopleths) and 100-km (lower numerals and solid isopleths) city sizes.

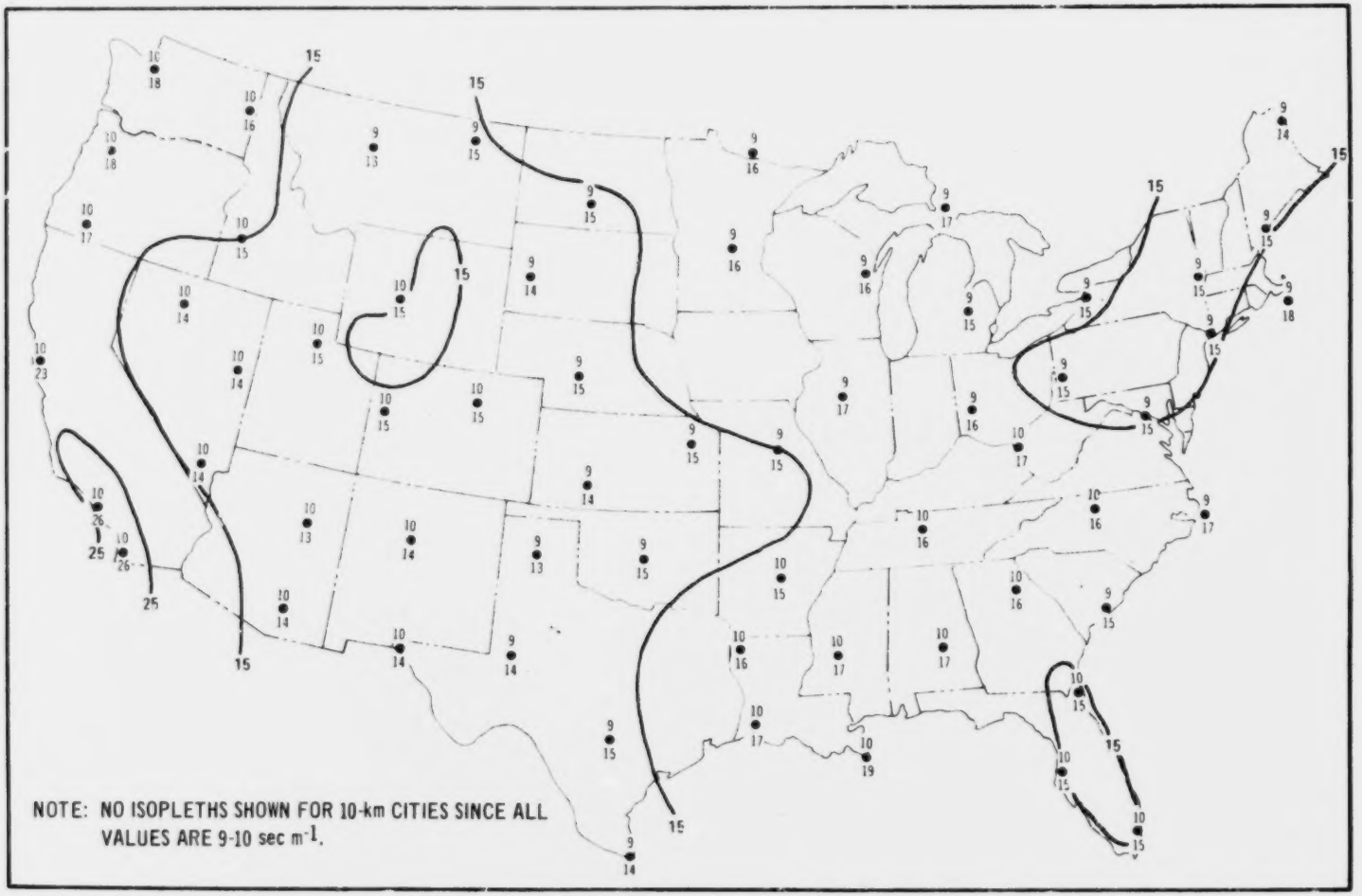

Figure 26. Data and isopleths (sec m^{-1}) of median annual afternoon $\bar{\chi}/\bar{Q}$ values (see text) for 10- (upper numerals) and 100-km (lower numerals and solid isopleths) city sizes.

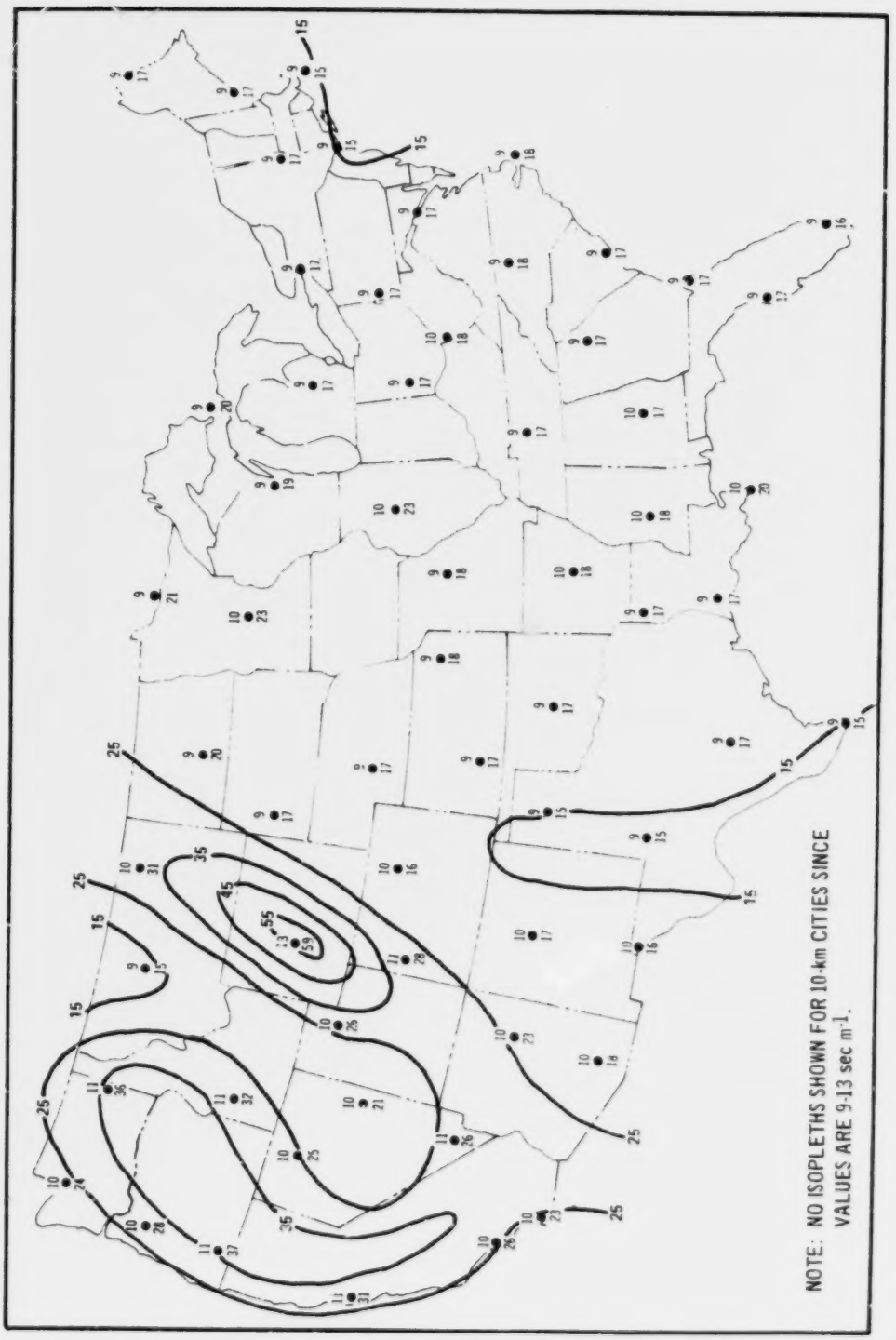

Figure 27. Data and isopleths (sec m^{-1}) of median winter afternoon $\tilde{\chi}/\bar{Q}$ values (see text) for 10- (upper numerals) and 100-km (lower numerals and solid isopleths) city sizes.

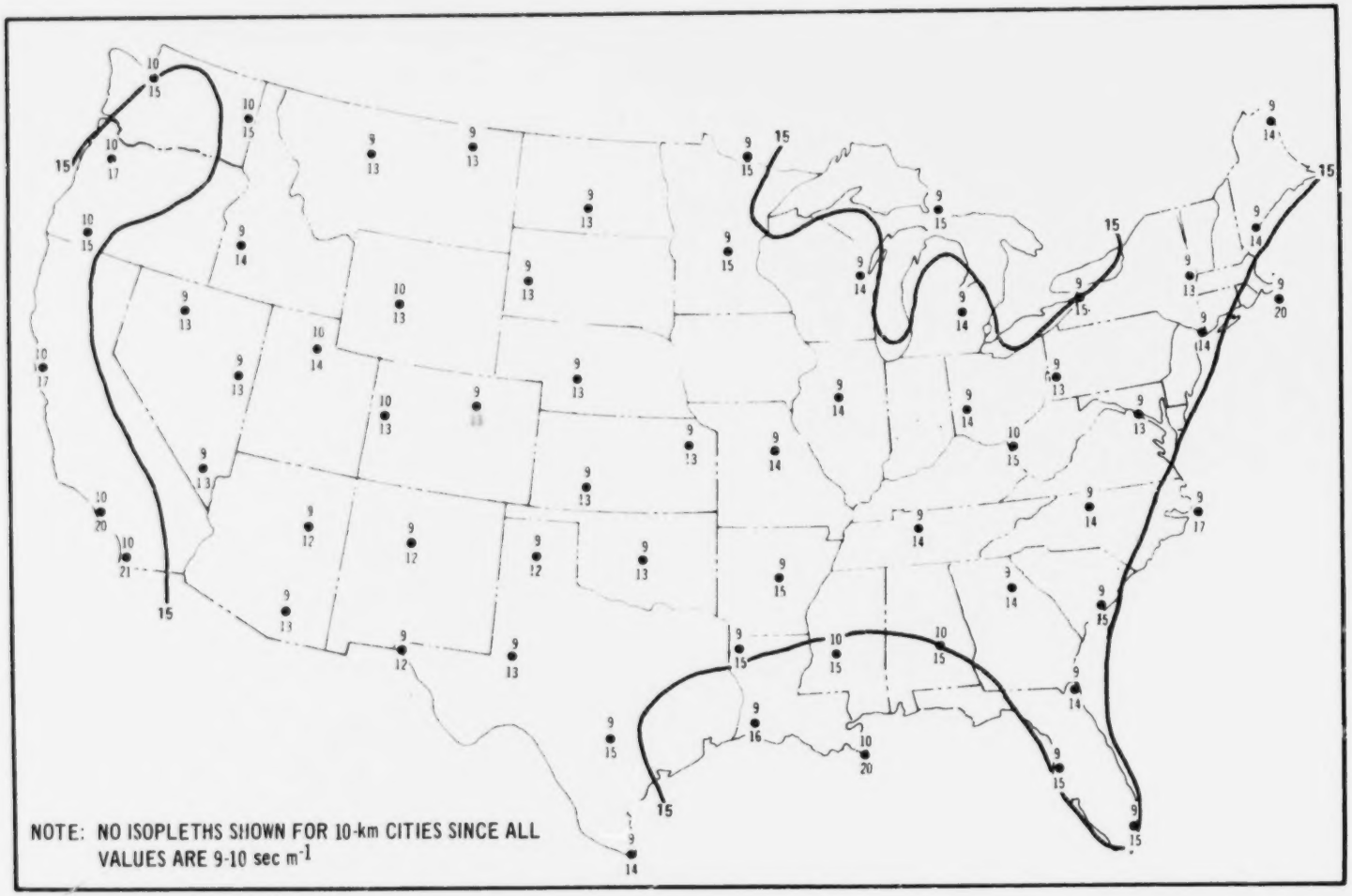

Figure 28. Data and isopleths (sec m^{-1}) of median spring afternoon $\bar{\chi}/\bar{Q}$ values (see text) for 10- (upper numerals) and 100-km (lower numerals and solid isopleths) city sizes.

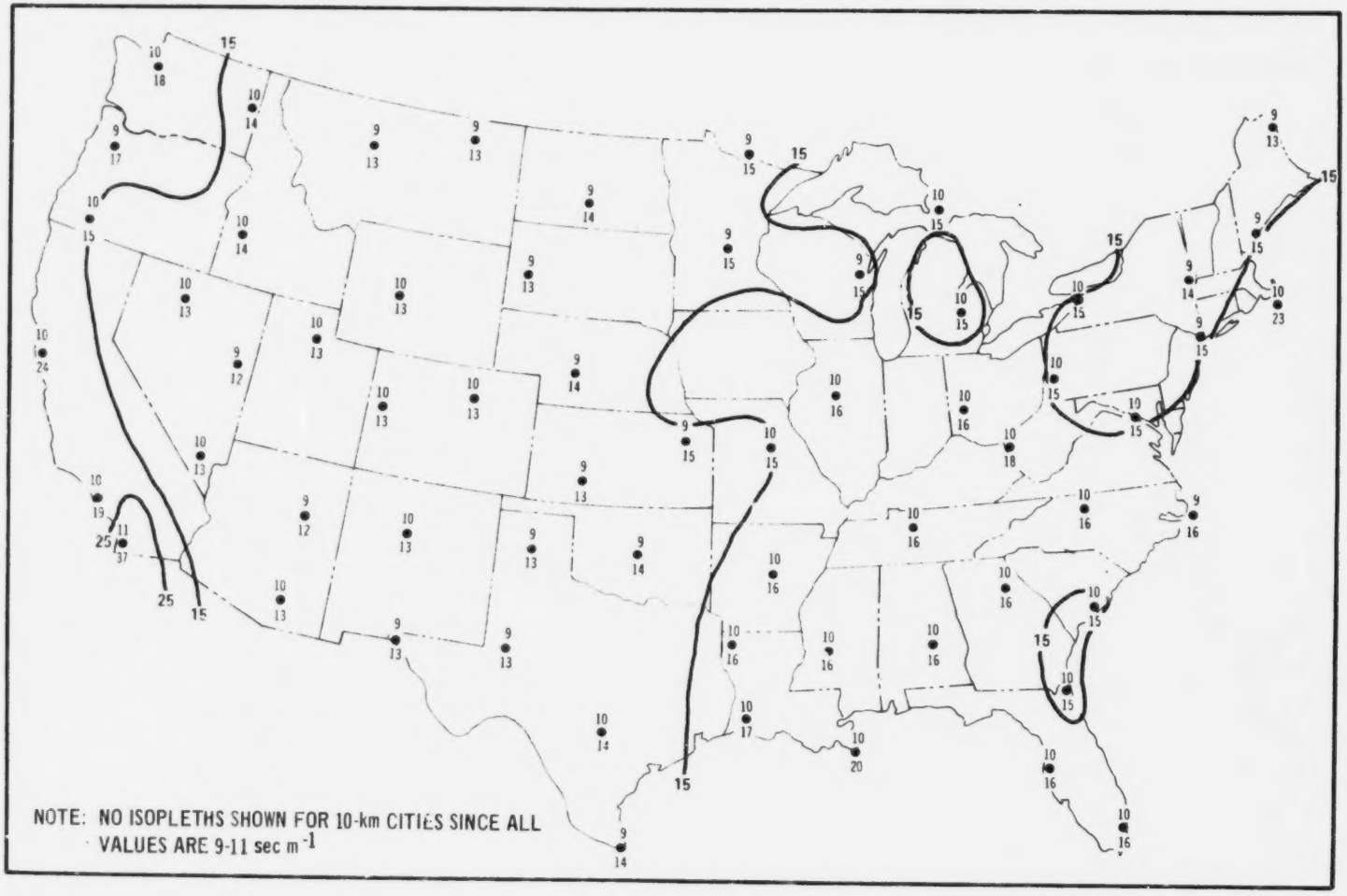

Figure 29. Data and isopleths (sec m^{-1}) of median summer afternoon $\bar{\chi}/\bar{Q}$ values (see text) for 10- (upper numerals) and 100-km (lower numerals and solid isopleths) city sizes.

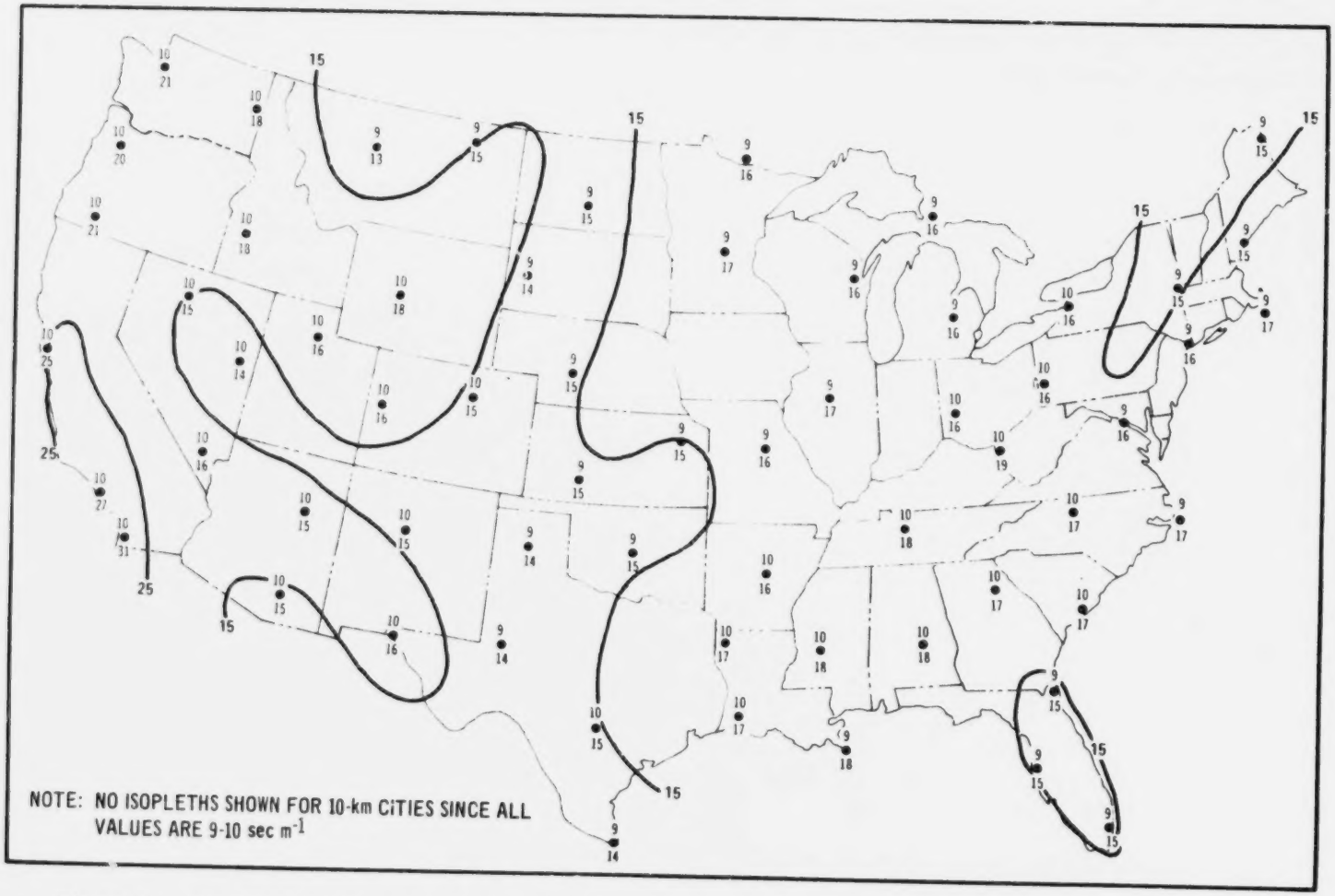

Figure 30. Data and isopleths (sec m-1) of median autumn afternoon $\tilde{\chi}/\bar{Q}$ values (see text) for 10- (upper numerals) and 100-km (lower numerals and solid isopleths) city sizes.

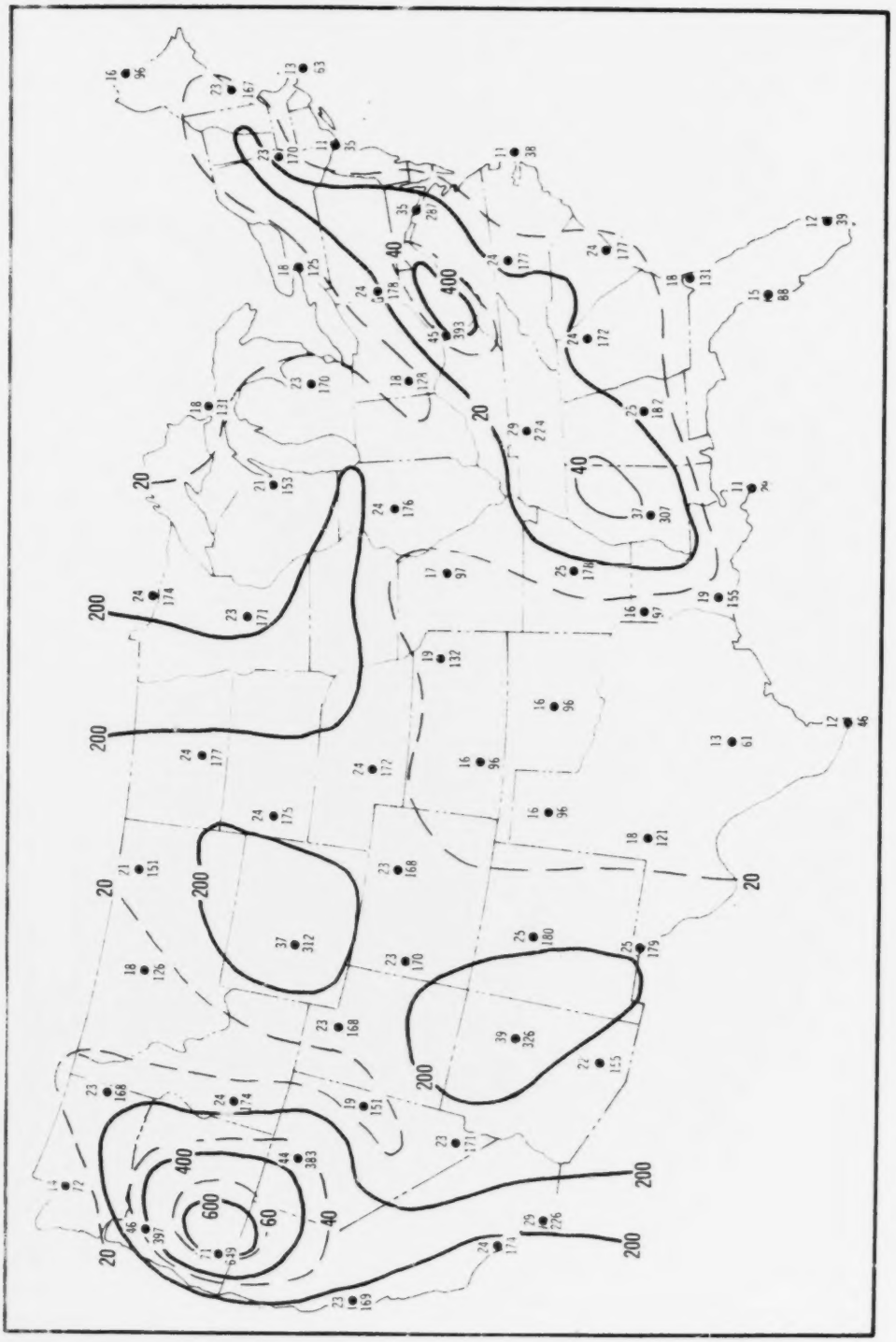

Figure 31. Data and isopleths (sec m^{-1}) of upper quartile annual morning $\bar{\chi}/\bar{Q}$ values (see text) for 10- (upper numerals and dashed isopleths) and 100-km (lower numerals and solid isopleths) city sizes.

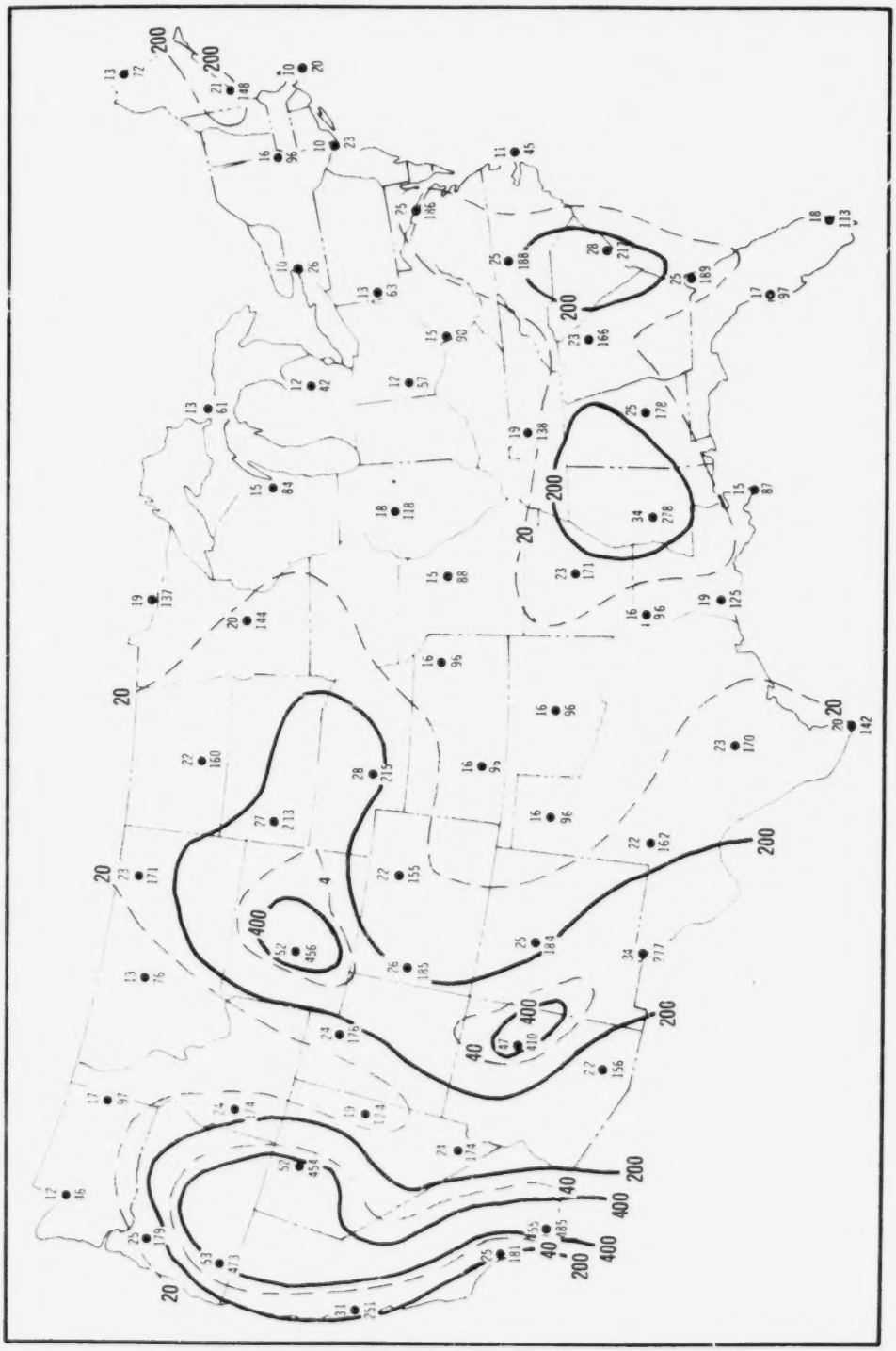

Figure 32. Data and isopleths (sec m^{-1}) of upper quartile winter morning $\bar{\chi}/\bar{Q}$ values (see text) for 10- (upper numerals and dashed isopleths) and 100-km (lower numerals and solid isopleths) city sizes.

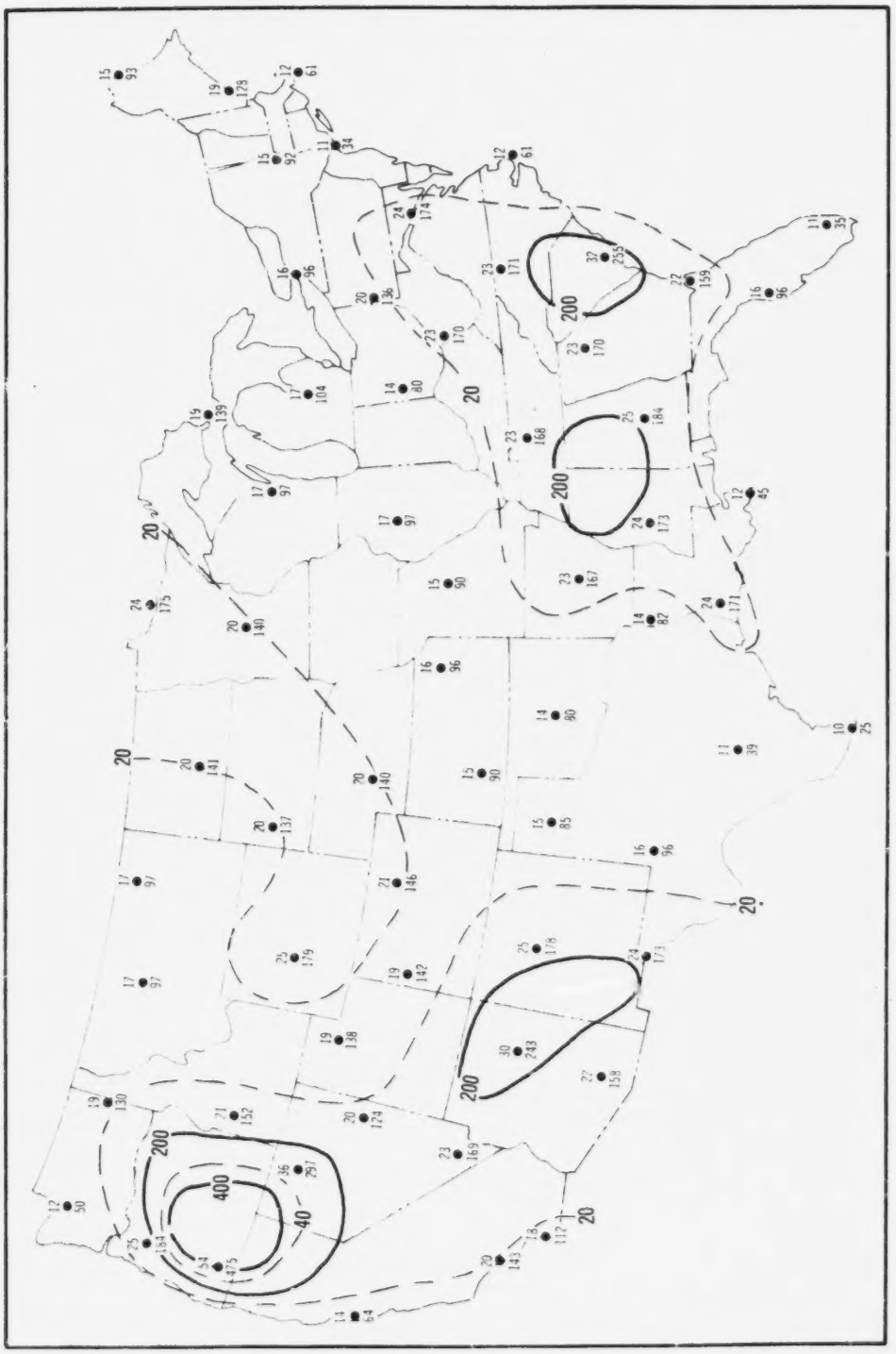

Figure 33. Data and isopleths (sec m^{-1}) of upper quartile spring morning $\bar{\chi}/\bar{Q}$ values (see text) for 10- (upper numerals and dashed isopleths) and 100-km (lower numerals and solid isopleths) city sizes.

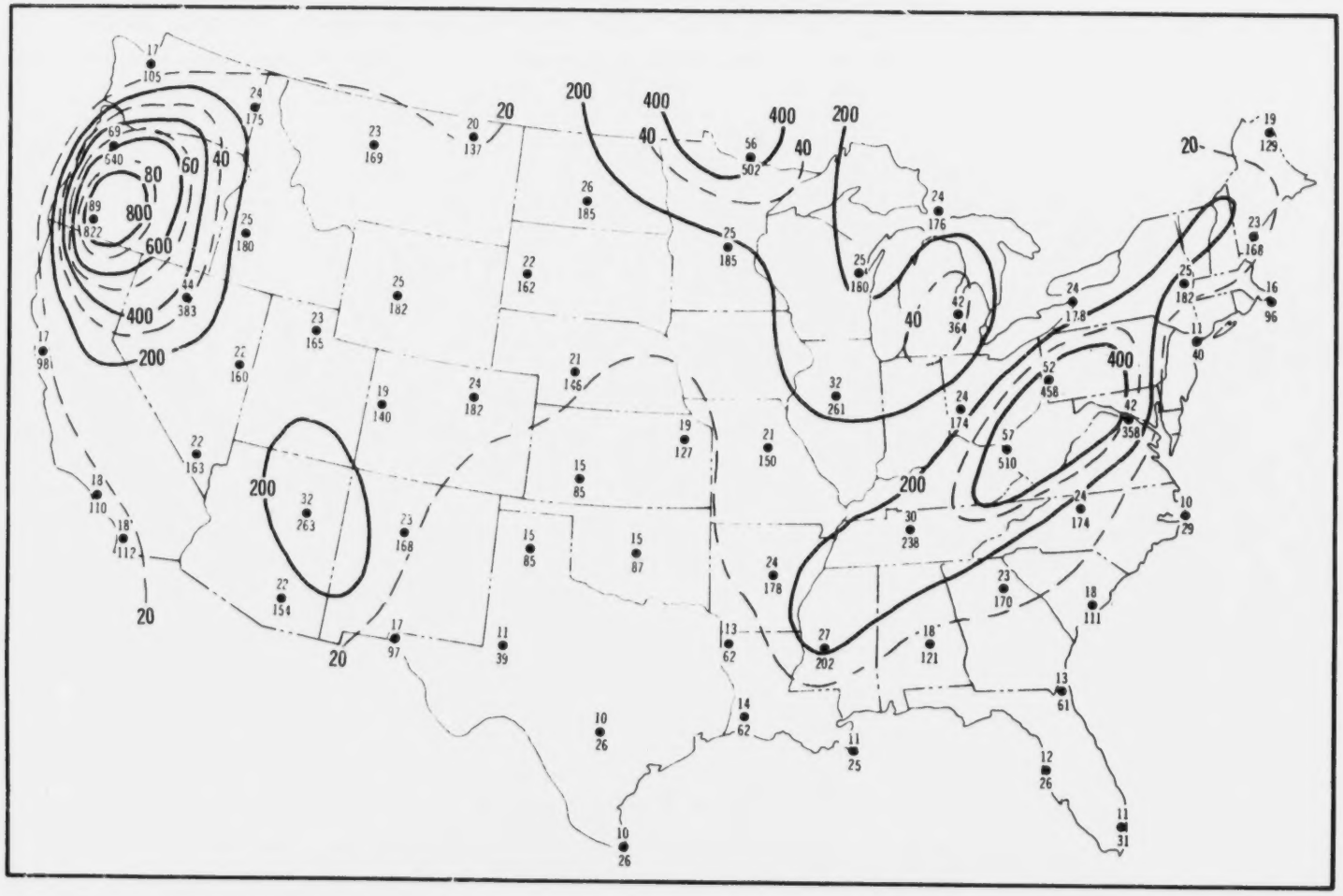

Figure 34. Data and isopleths (sec m^{-1}) of upper quartile summer morning $\bar{\chi}/\bar{Q}$ values (see text) for 10- (upper numerals and dashed isopleths) and 100-km (lower numerals and solid isopleths) city sizes.

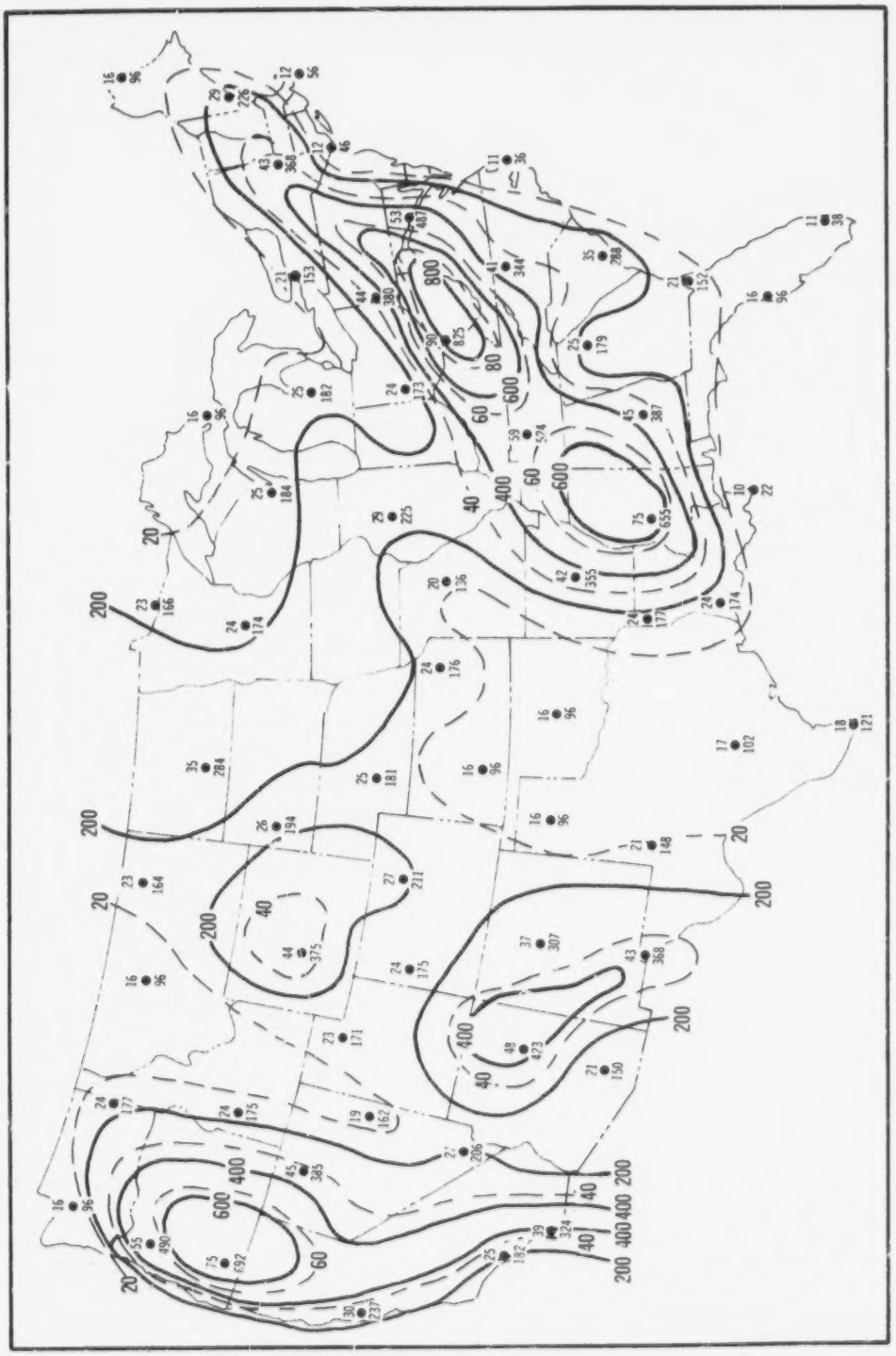

Figure 35. Data and isopleths (sec m^{-1}) of upper quartile autumn morning $\overline{\chi}/\overline{Q}$ values (see text) for 10- (upper numerals and dashed isopleths) and 100-km (lower numerals and solid isopleths) city sizes.

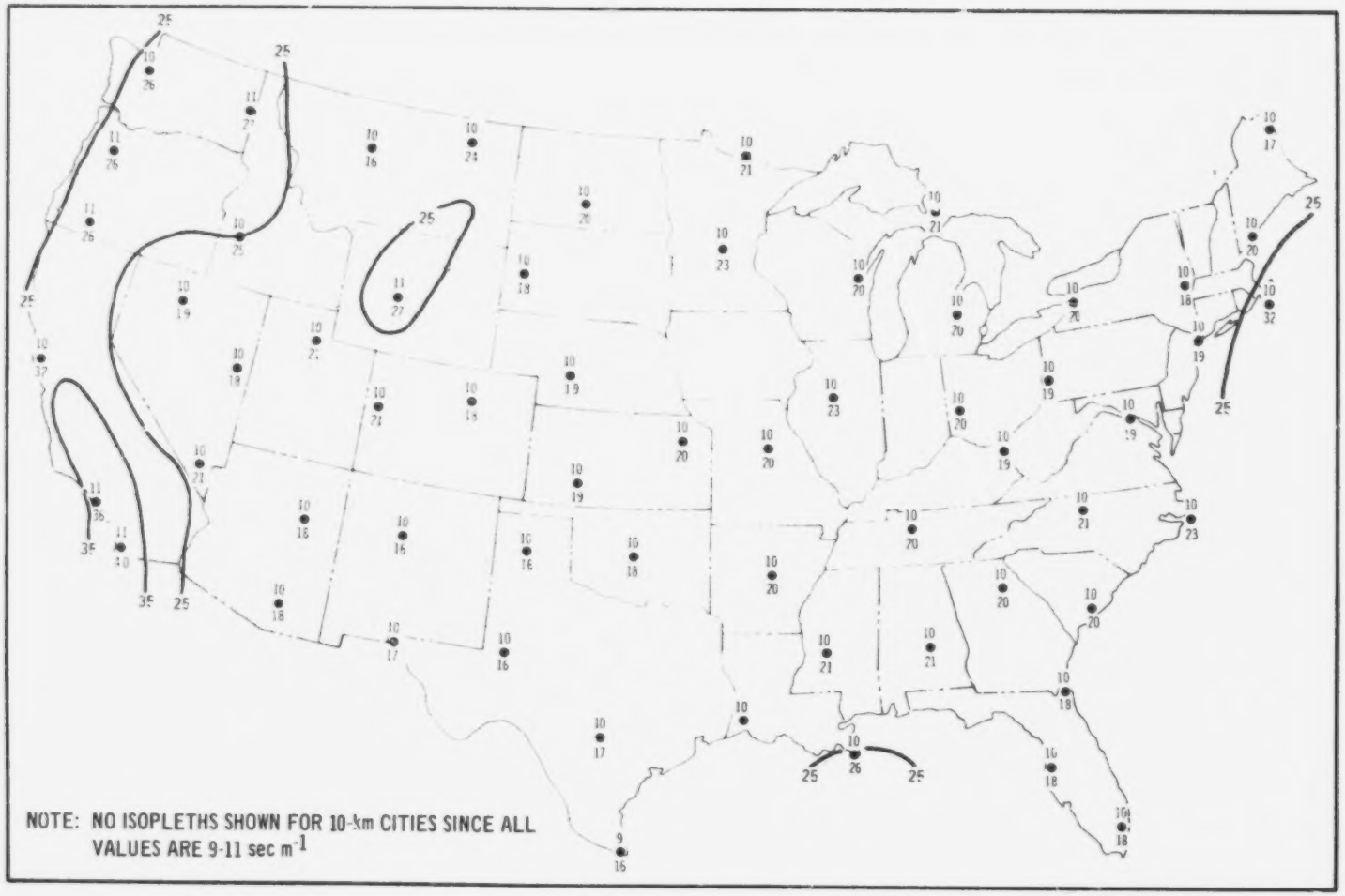

Figure 36. Data and isopleths (sec m^{-1}) of upper quartile annual afternoon $\bar{\chi}/\bar{Q}$ values (see text) for 10- (upper numerals) and 100-km (lower numerals and solid isopleths) city sizes.

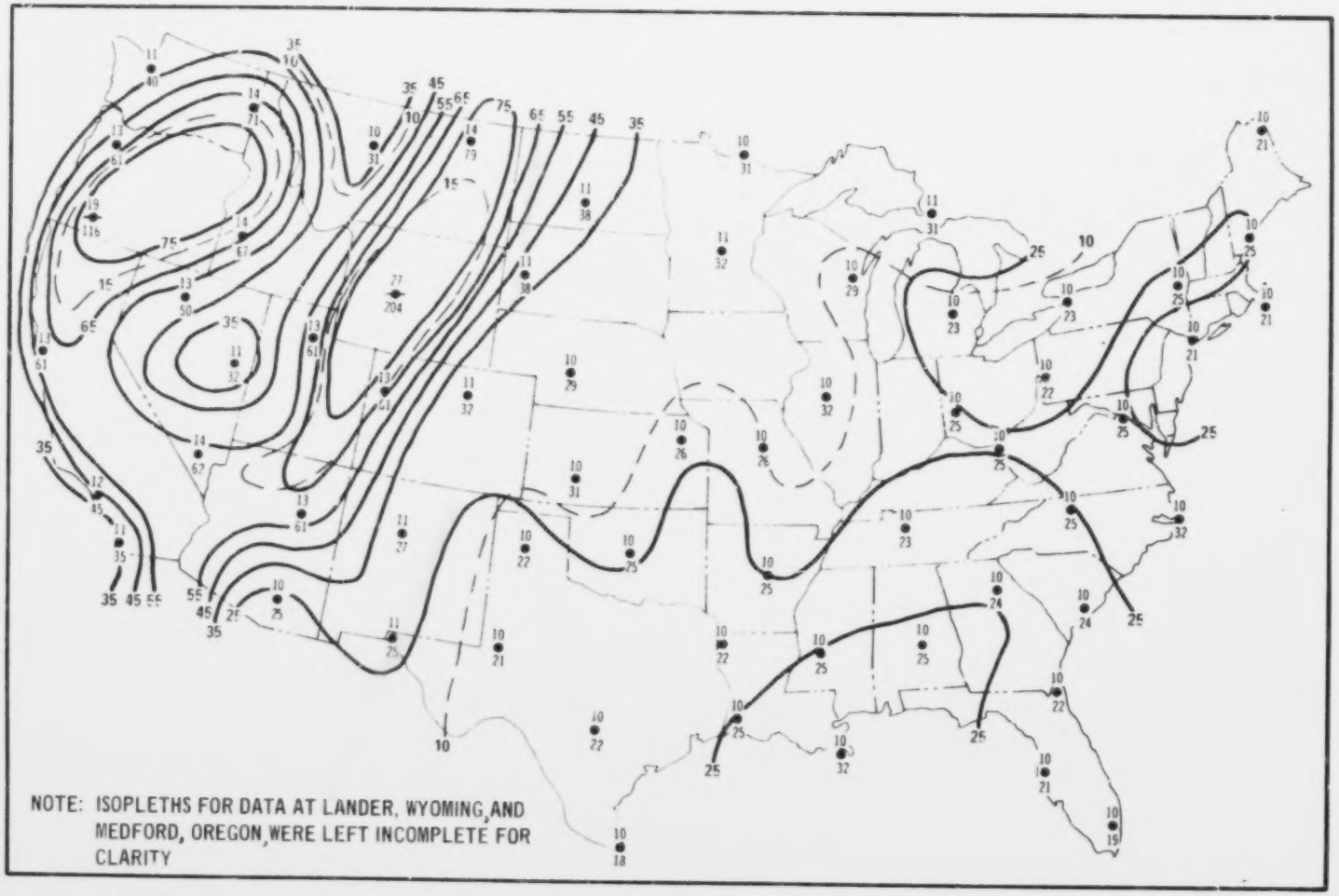

Figure 37. Data and isopleths (sec m^{-1}) of upper quartile winter afternoon $\bar{\chi}/\bar{Q}$ values (see text) for 10- (upper numerals and dashed isopleths) and 100-km (lower numerals and solid isopleths) city sizes.

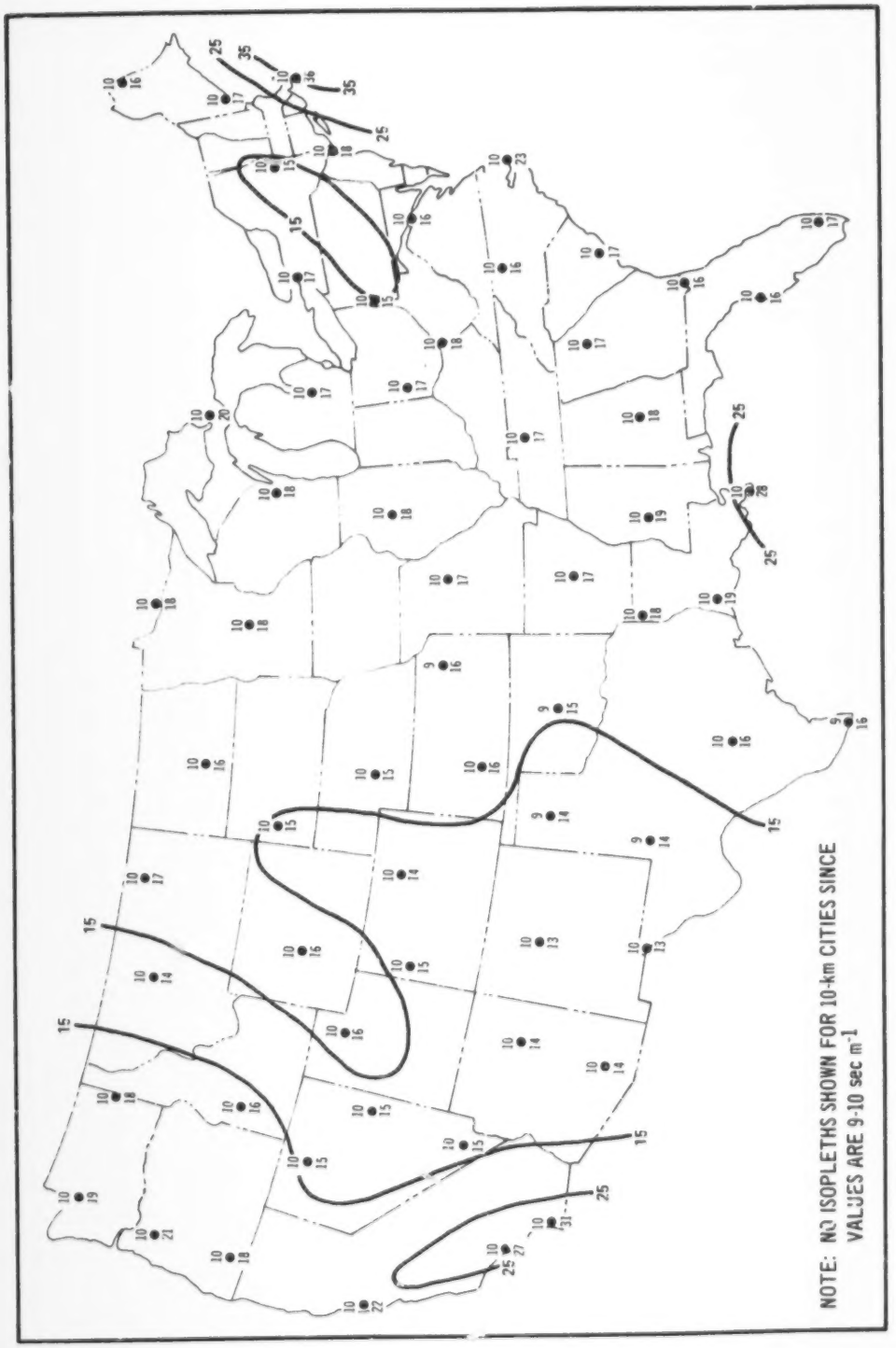

Figure 38. Data and isopleths (sec m^{-1}) of upper quartile spring afternoon $\overline{\chi}/\overline{Q}$ values (see text) for 10- (upper numerals and dashed isopleths and 100-km (lower numerals and solid isopleths) city sizes.

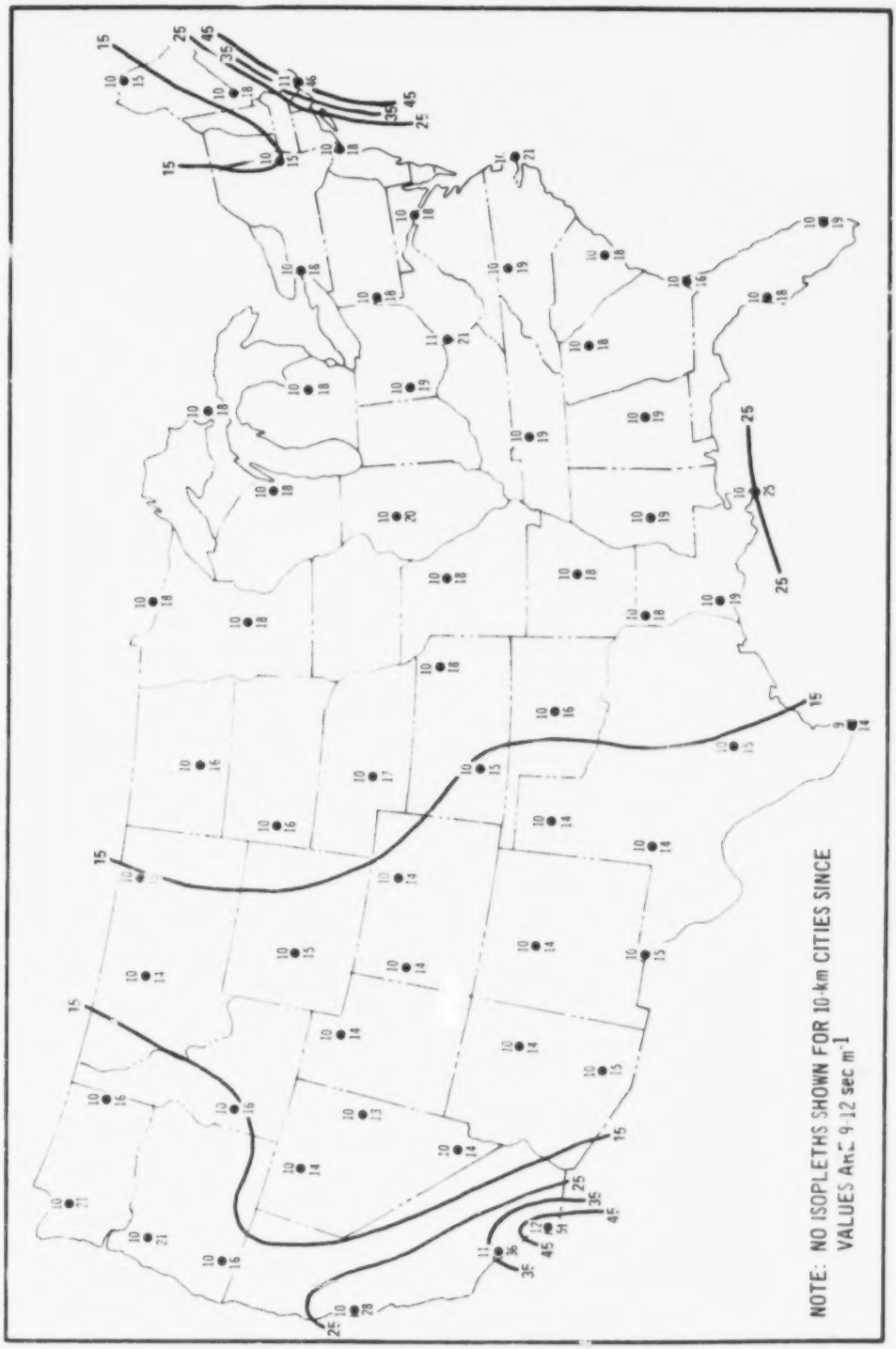

Figure 39. Data and isopleths (sec m^{-1}) of upper quartile summer afternoon $\overline{\chi}/\overline{Q}$ values (see text) for 10- (upper numerals) and 100-km (lower numerals and solid isopleths) city sizes.

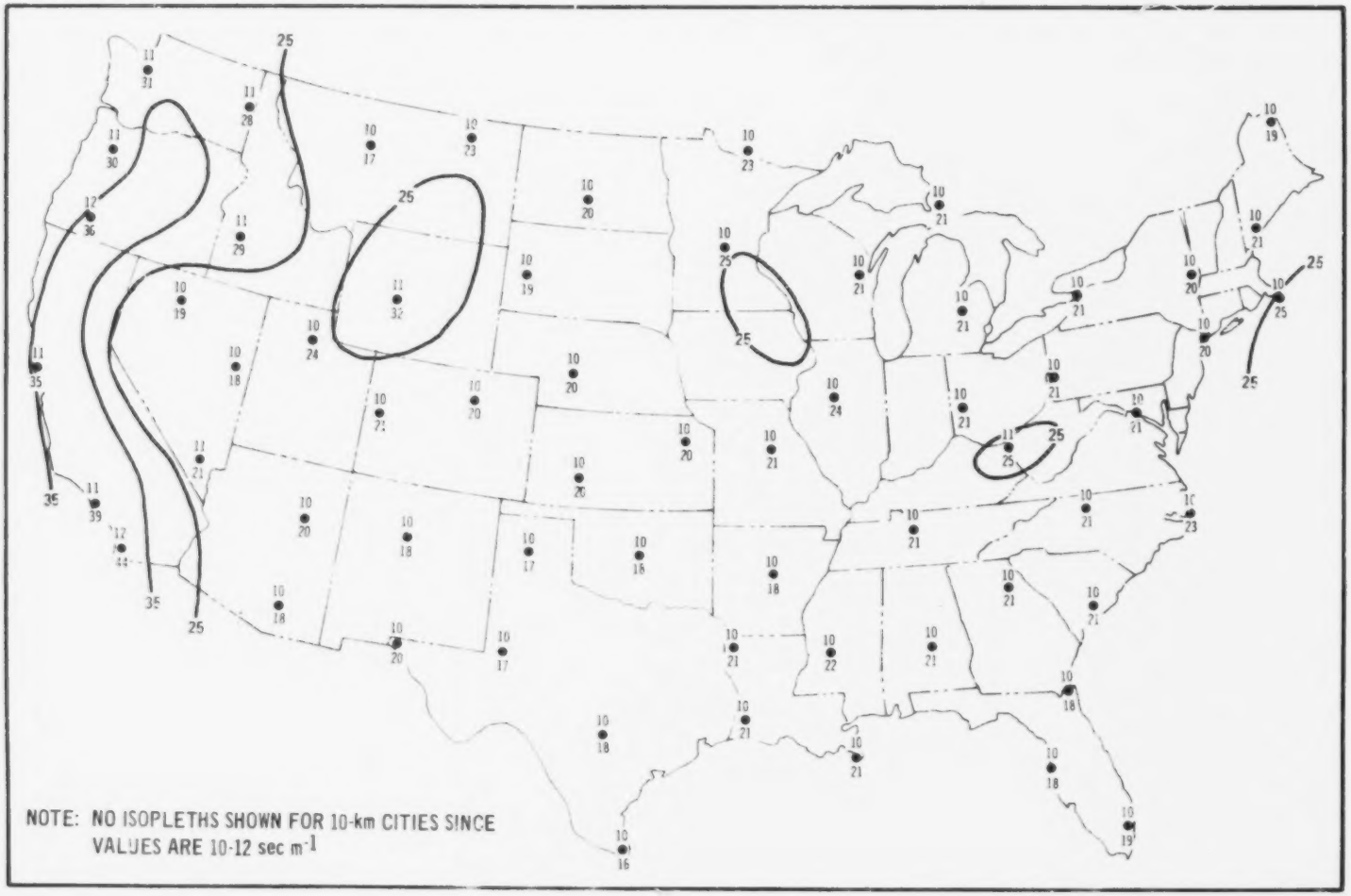

Figure 40. Data and isopleths (sec m^{-1}) of upper quartile autumn afternoon $\overline{\chi}/\overline{Q}$ values (see text) for 10- (upper numerals) and 100-km (lower numerals and solid isopleths) city sizes.

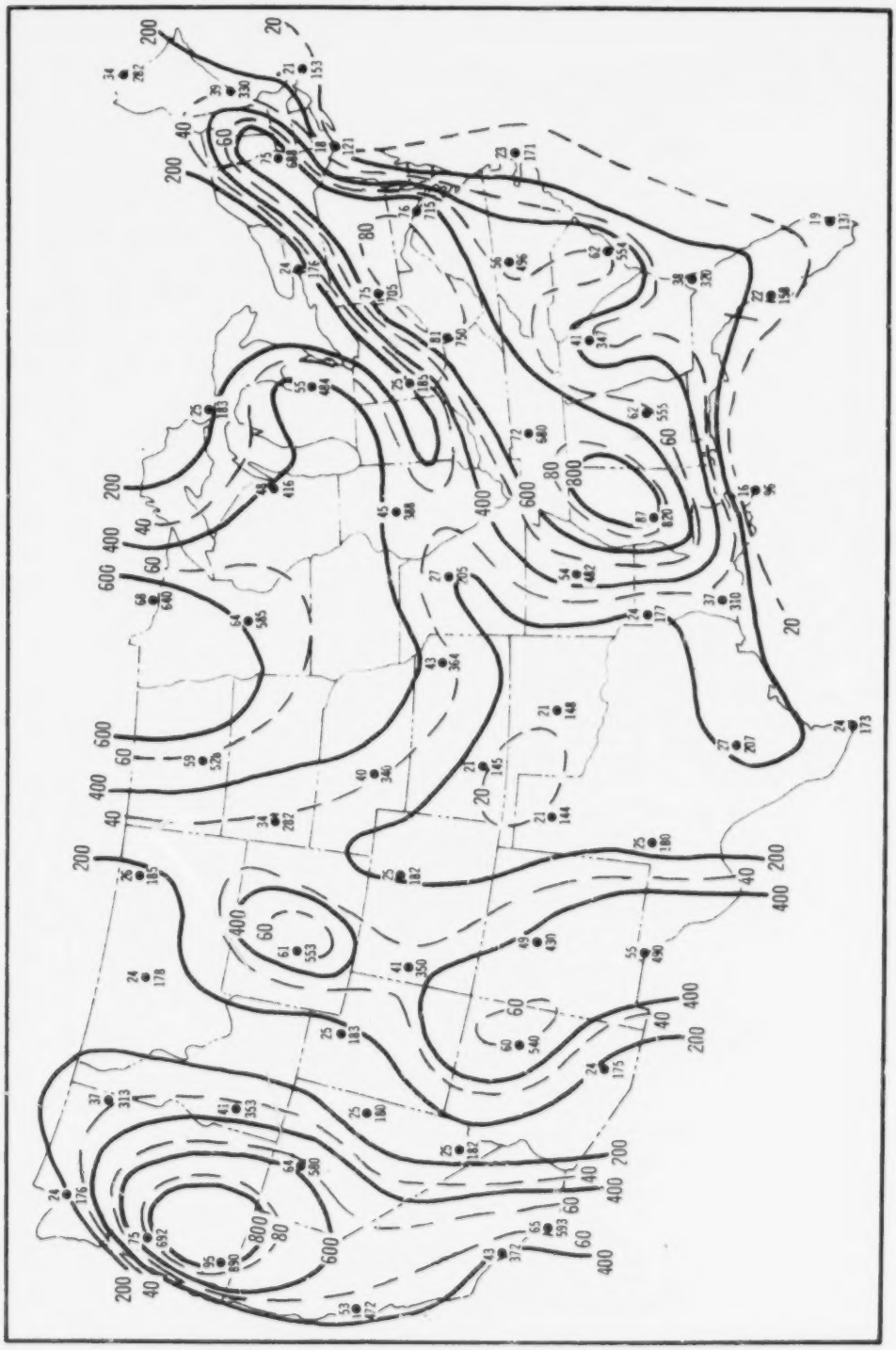

Figure 41. Data and isopleths (sec m^{-1}) of upper decile annual morning $\overline{\chi}/\overline{Q}$ values (see text) for 10- (upper numerals and dashed isopleths) and 100-km (lower numerals and solid isopleths) city sizes.

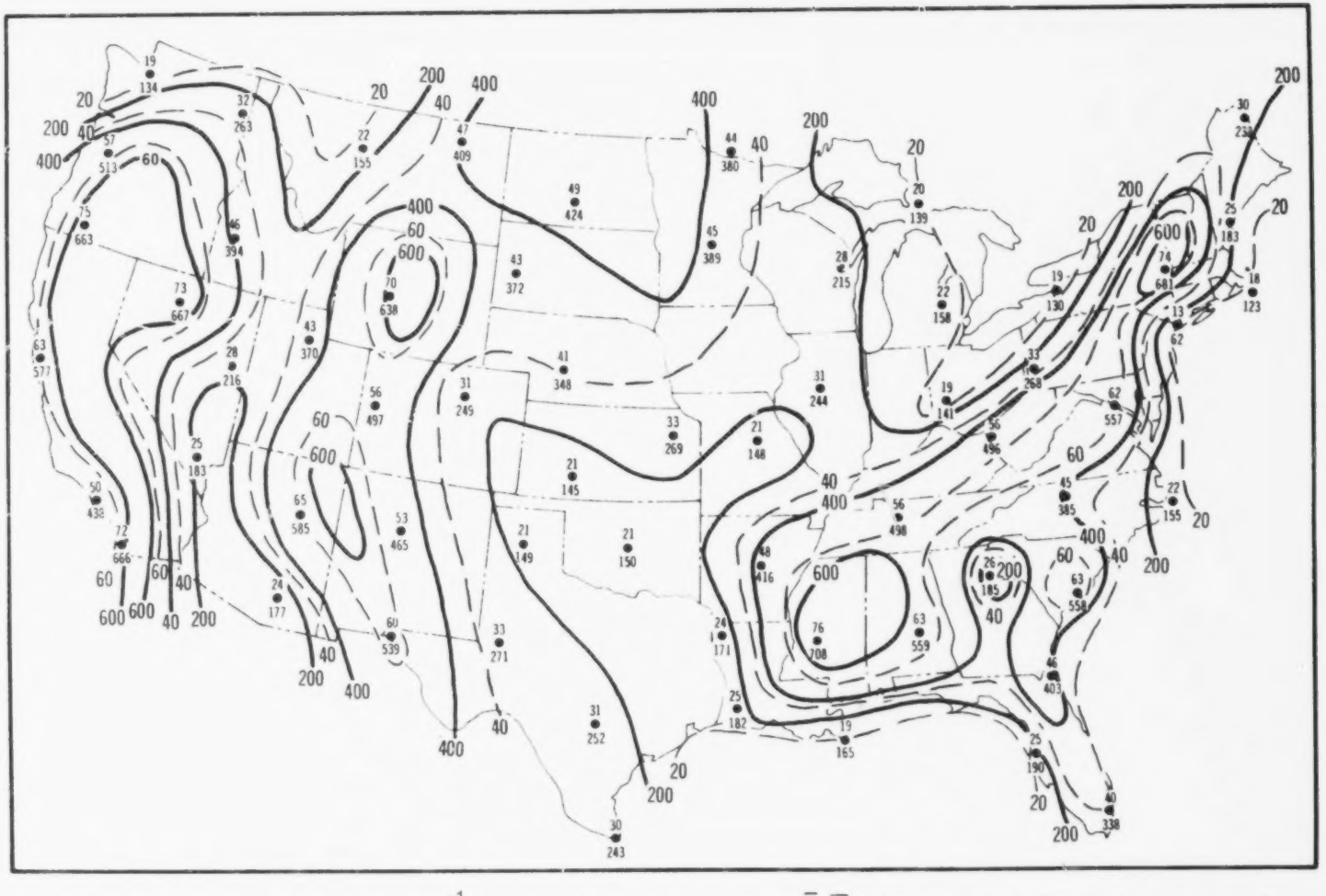

Figure 42. Data and isopleths (sec m^{-1}) of upper decile winter morning $\overline{\chi}/\overline{Q}$ values (see text) for 10- (upper numerals and dashed isopleths) and 100-km (lower numerals and solid isopleths) city sizes.

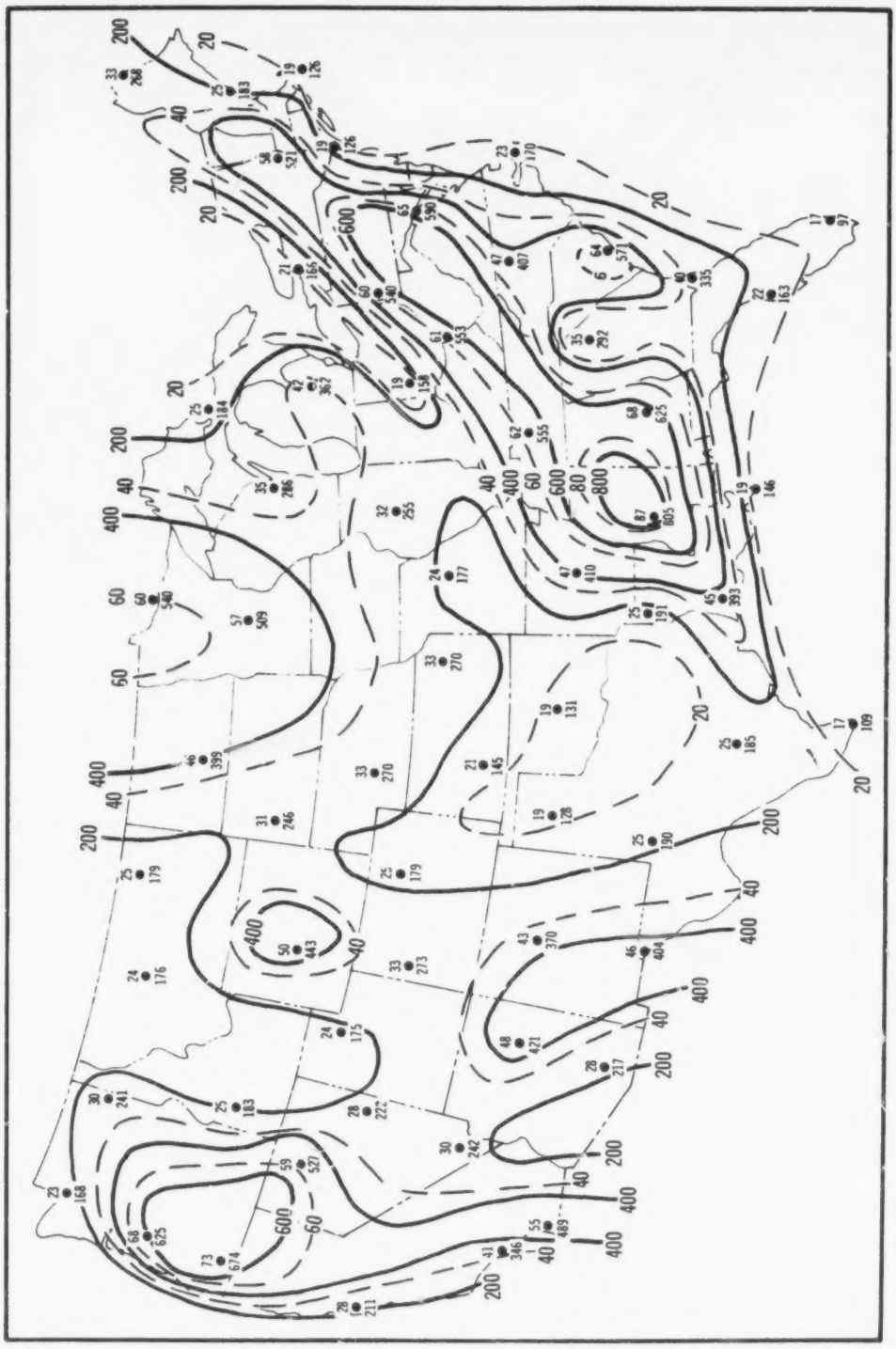

Figure 43. Data and isopleths (sec m^{-1}) of upper decile spring morning $\bar{\chi}/\bar{Q}$ values (see text) for 10- (upper numerals and dashed isopleths) and 100-km (lower numerals and solid isopleths) city sizes.

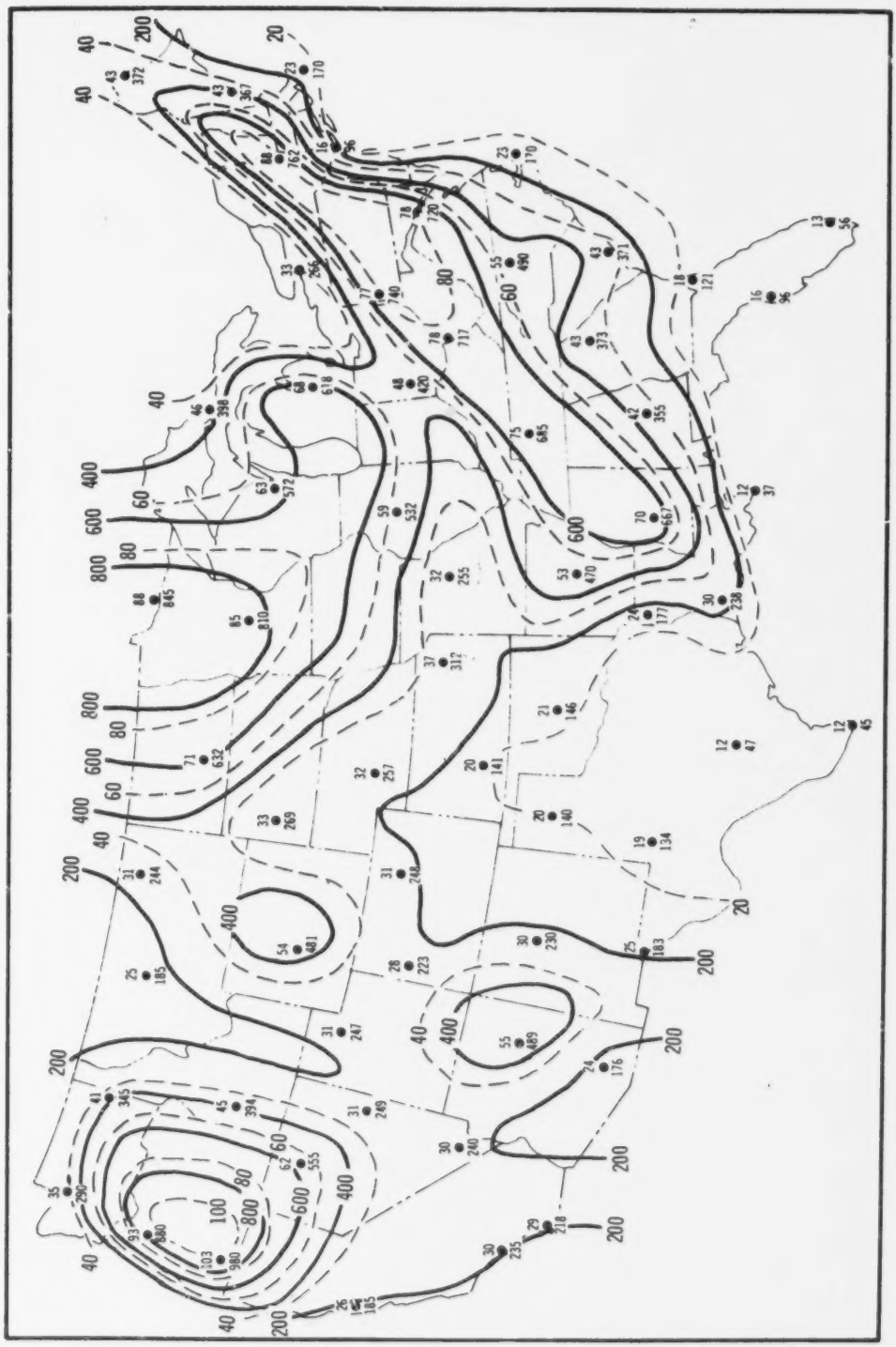

Figure 44. Data and isopleths (sec m^{-1}) of upper decile summer morning $\bar{x}/\bar{Q}$ values (see text) for 10- (upper numerals and dashed isopleths) and 100-km (lower numerals and solid isopleths) city sizes.

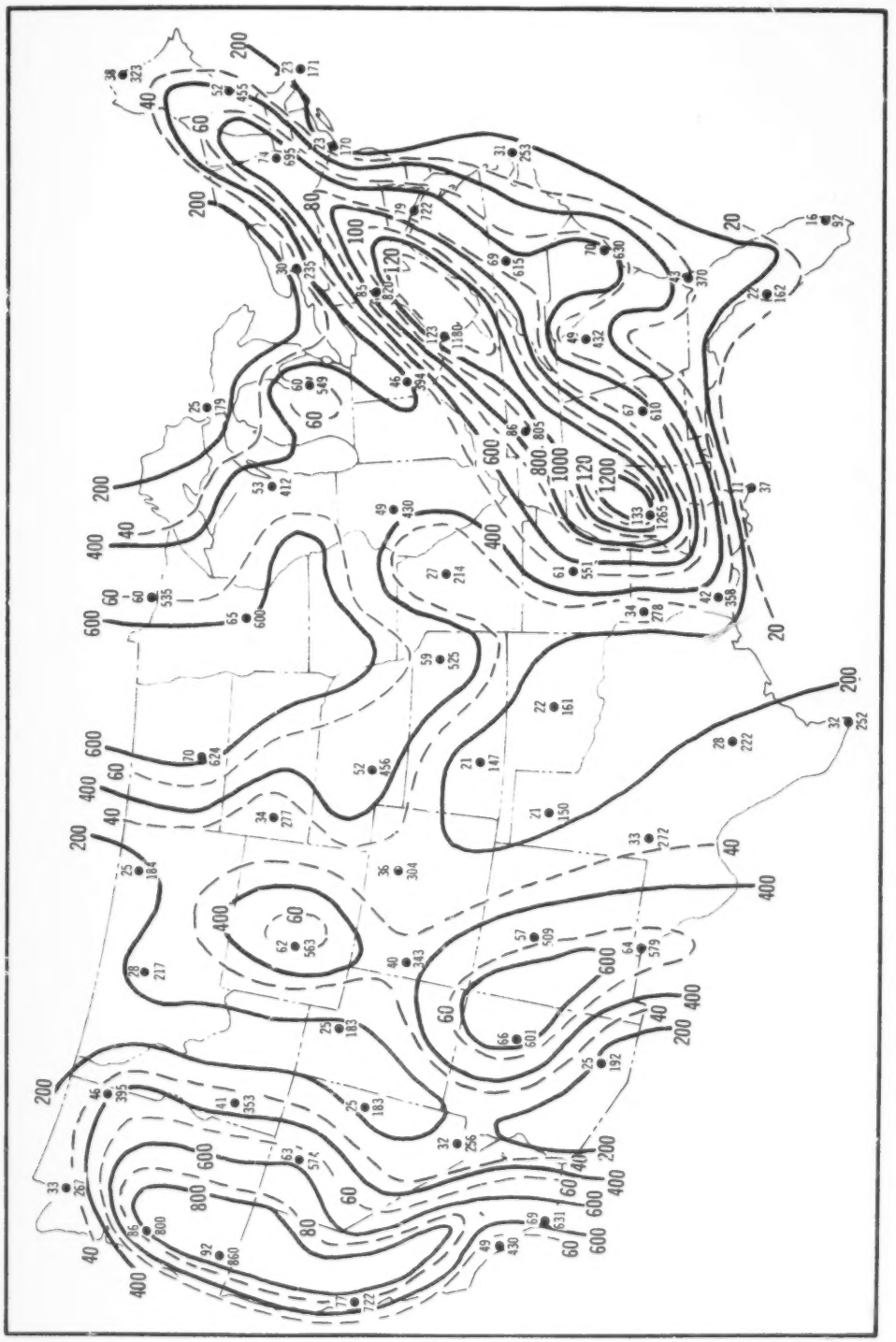

Figure 45. Data and isopleths (sec m^{-1}) of upper decile autumn morning $\overline{\chi}/\overline{Q}$ values (see text) for 10- (upper numerals and dashed isopleths) and 100-km (lower numerals and solid isopleths) city sizes.

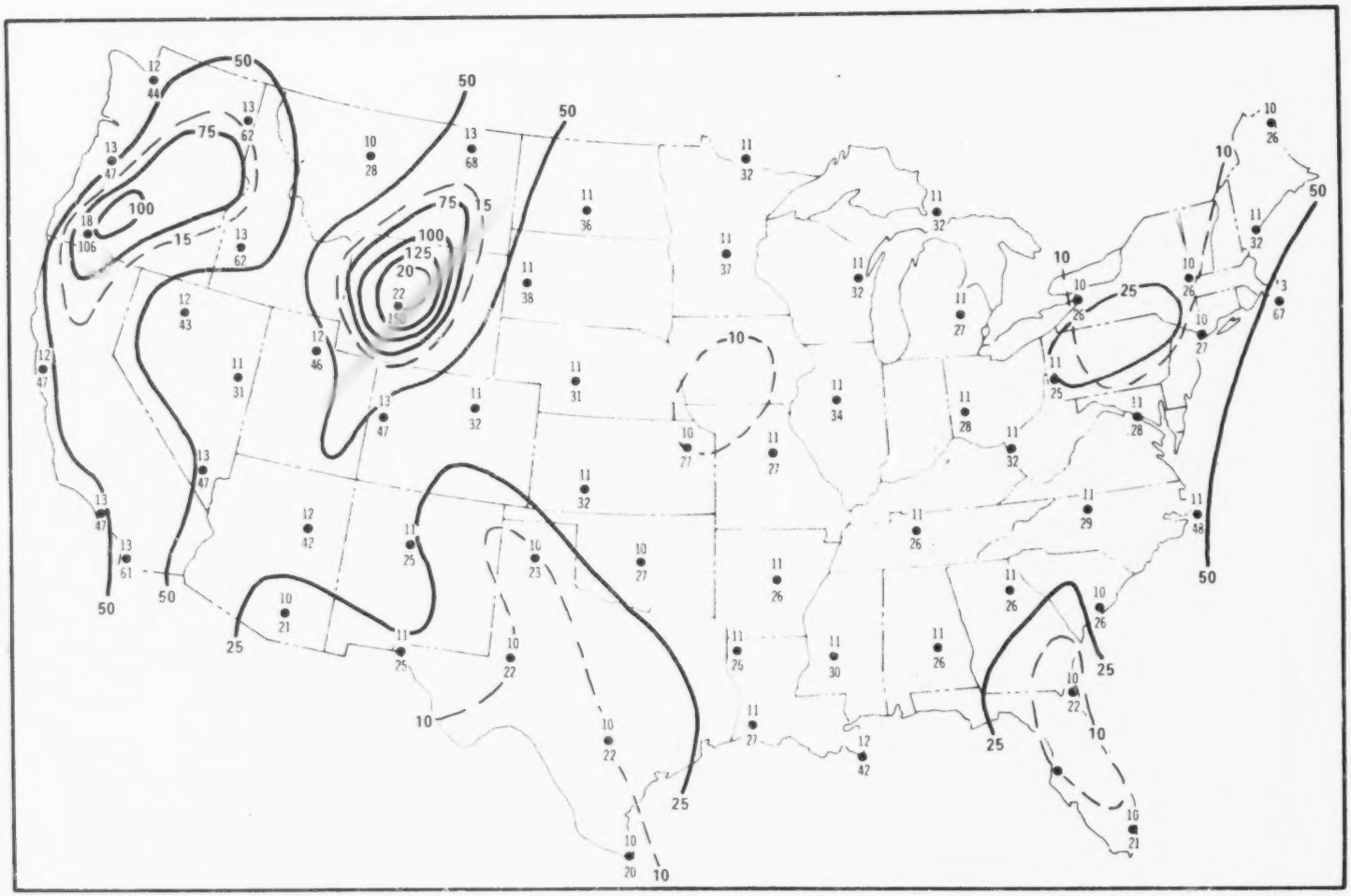

Figure 46. Data and isopleths (sec m^{-1}) of upper decile annual afternoon $\overline{\chi}/\overline{Q}$ values (see text) for 10- (upper numerals and dashed isopleths) and 100-km (lower numerals and solid isopleths) city sizes.

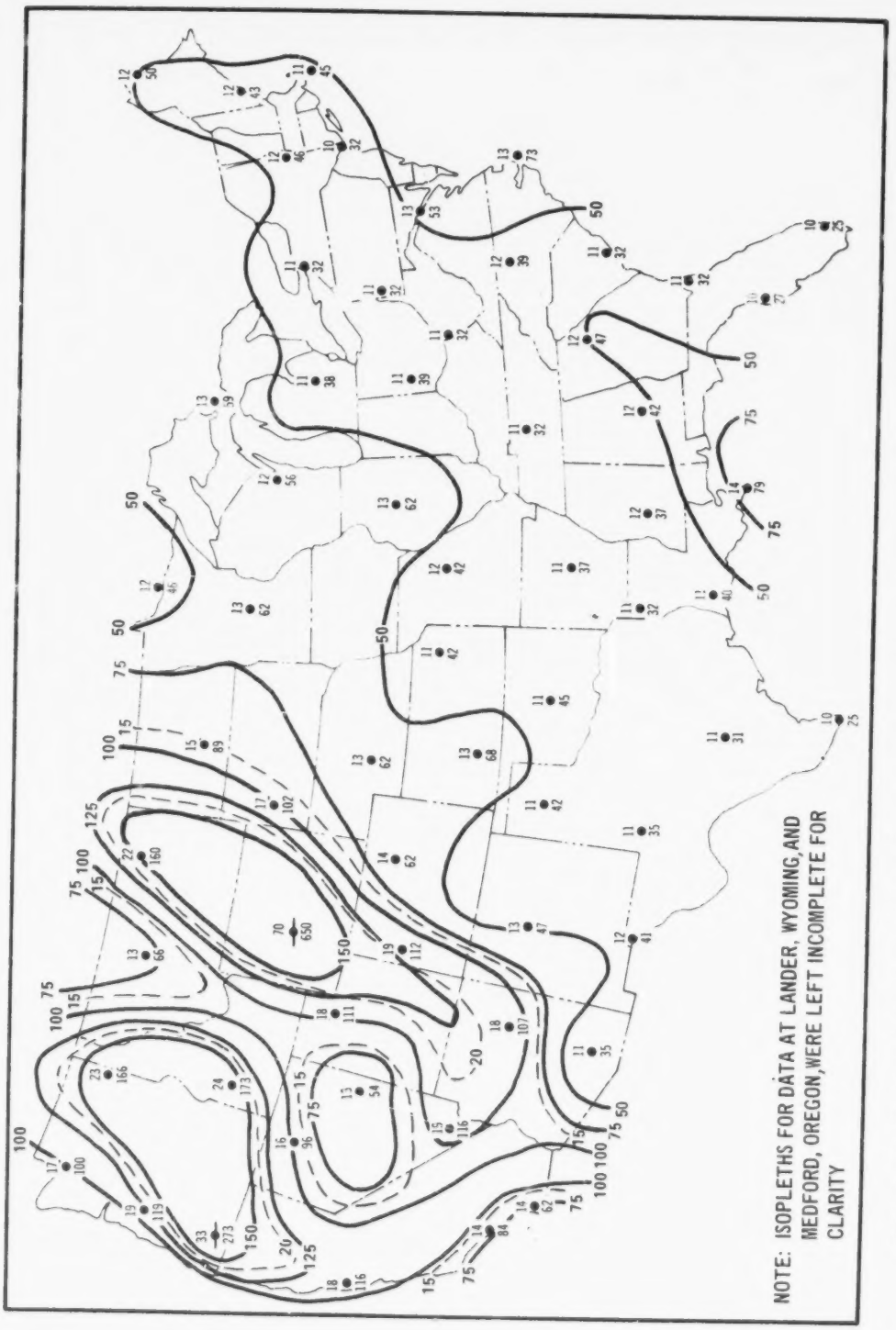

Figure 47. Data and isopleths (sec m^{-1}) of upper decile winter afternoon $\bar{\chi}/\bar{Q}$ values (see text) for 10- (upper numerals and dashed isopleths) and 100-km (lower numerals and solid isopleths) city sizes.

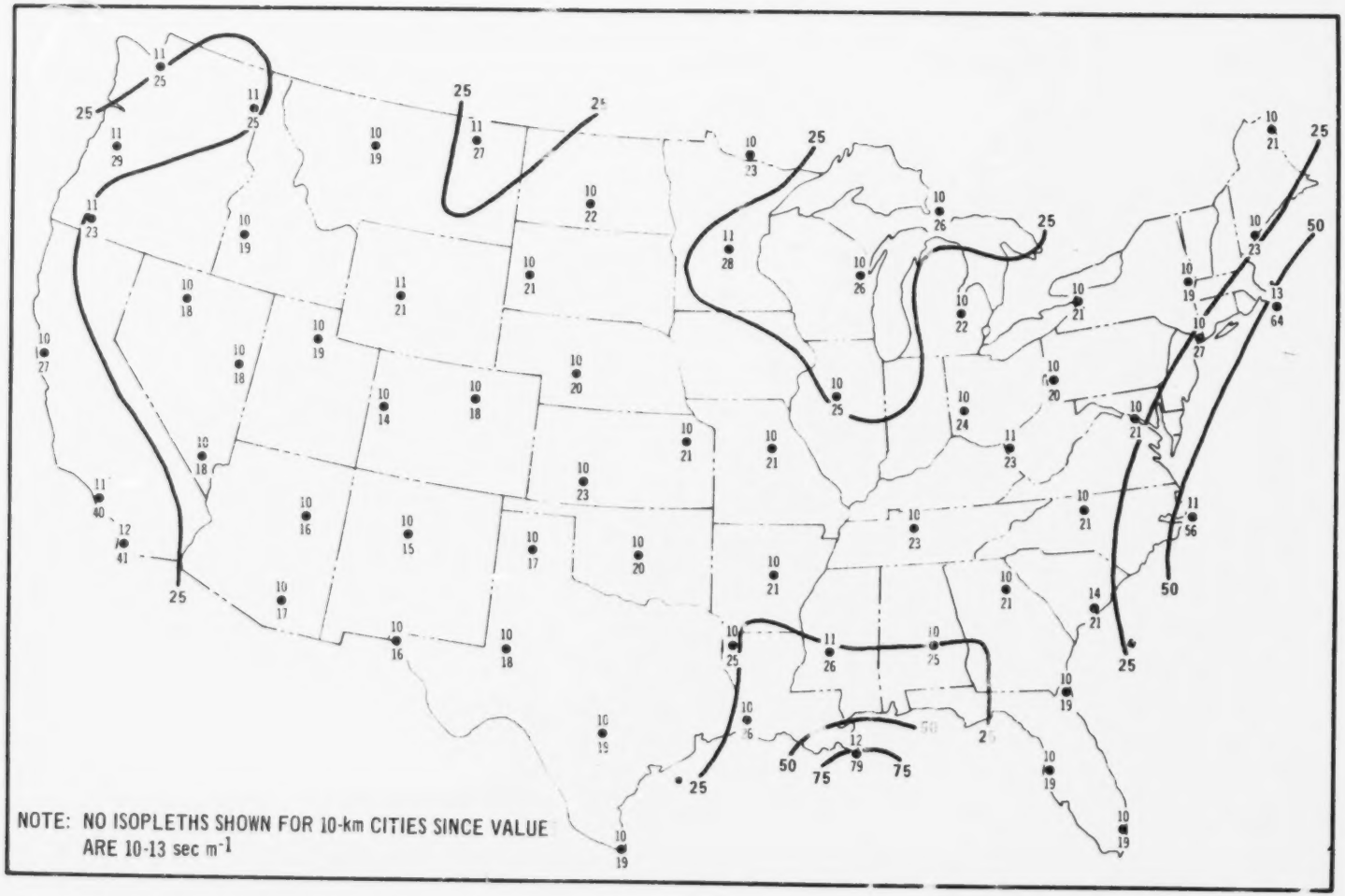

Figure 48. Data and isopleths (sec m^{-1}) of upper decile spring afternoon $\bar{\chi}/\bar{Q}$ values (see text) for 10- (upper numerals) and 100-km (lower numerals and solid isopleths) city sizes.

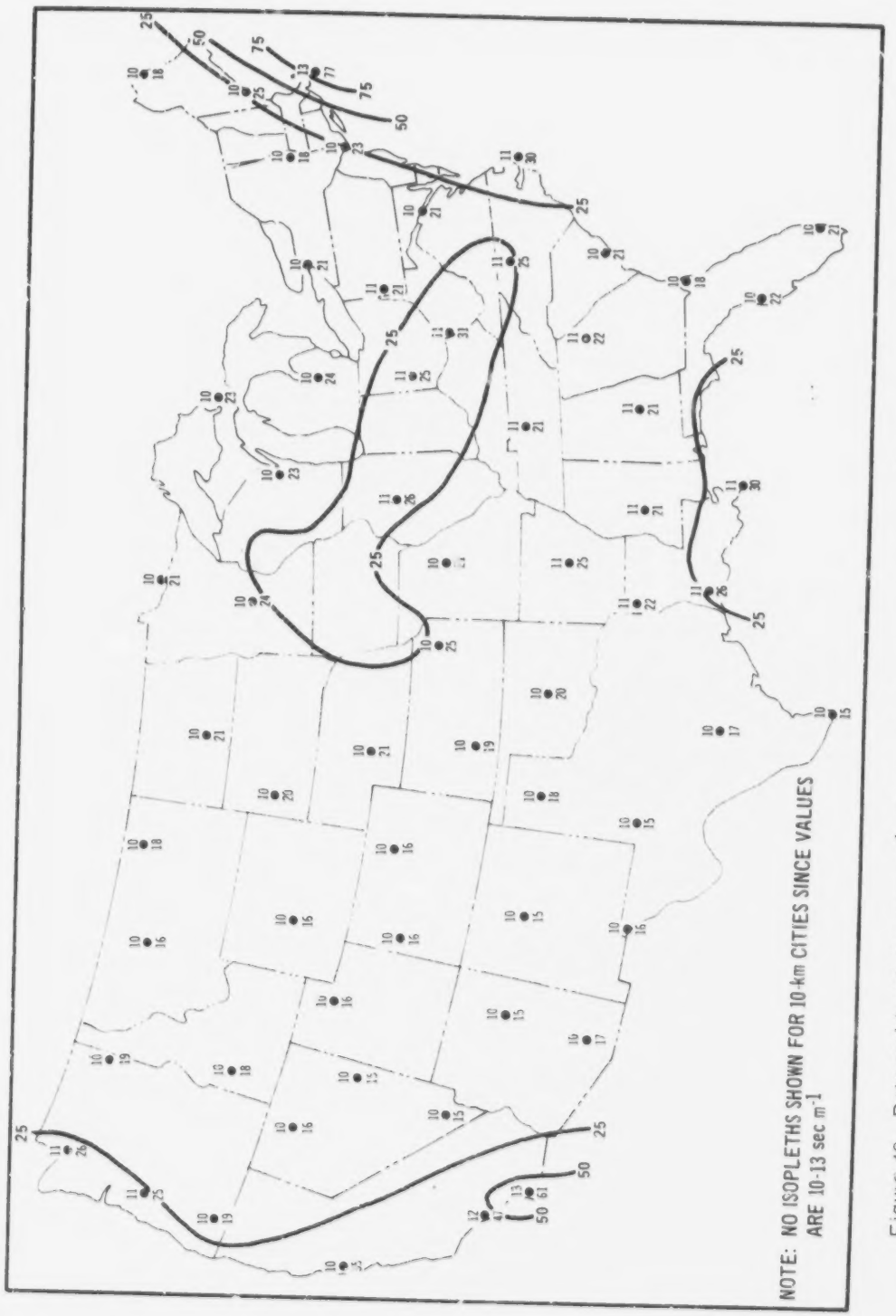

Figure 49. Data and isopleths (sec m^{-1}) of upper decile summer afternoon $\bar{\chi}/\bar{Q}$ values (see text) for 10- (upper numerals) and 100-km (lower numerals and solid isopleths) city sizes.

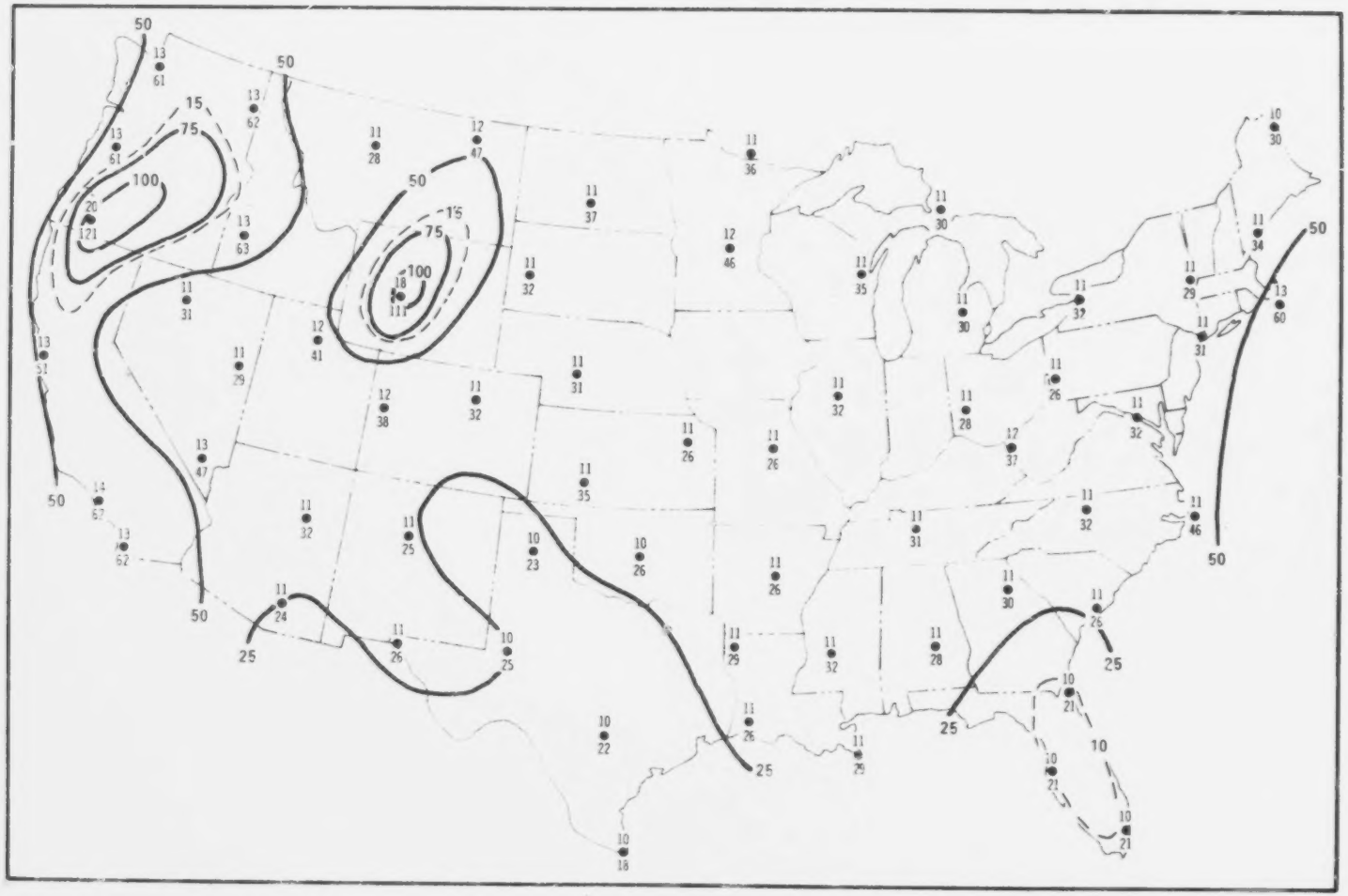

Figure 50. Data and isopleths (sec m^{-1}) of upper decile autumn afternoon $\bar{\chi}/\bar{Q}$ values (see text) for 10- (upper numerals and dashed isopleths) and 100-km (lower numerals and solid isopleths) city sizes.

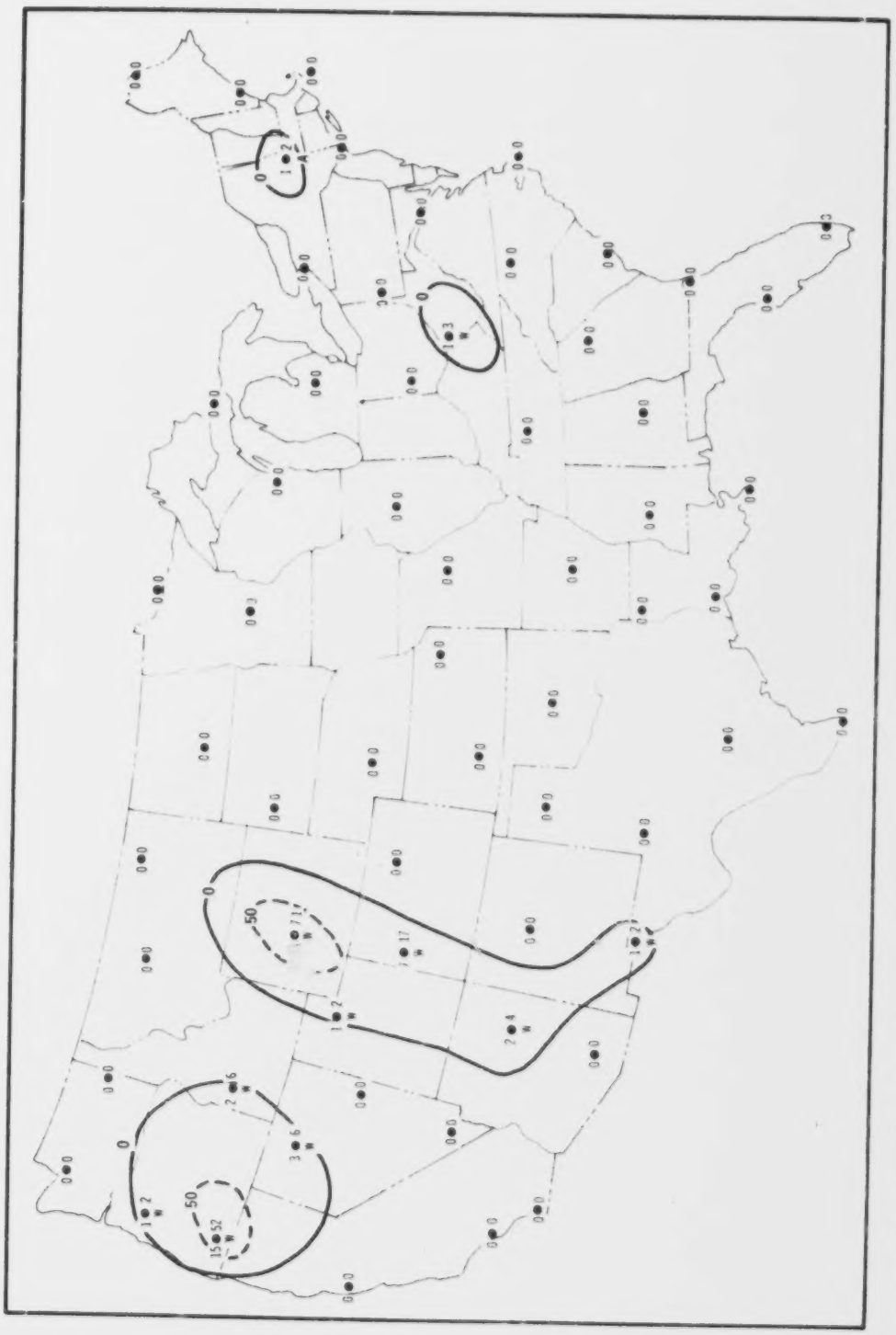

Figure 51. Isopleths of total number of episode-days in 5 years with mixing heights ≤ 500 m, wind speeds ≤ 2.0 m sec^{-1}, and no significant precipitation (see text) - - for episodes lasting at least 2 days. Numerals on left and right give total number of episodes and episode-days, respectively. Season with greatest number of episode-days indicated as W (winter), SP (spring), SU (summer), or A (autumn).

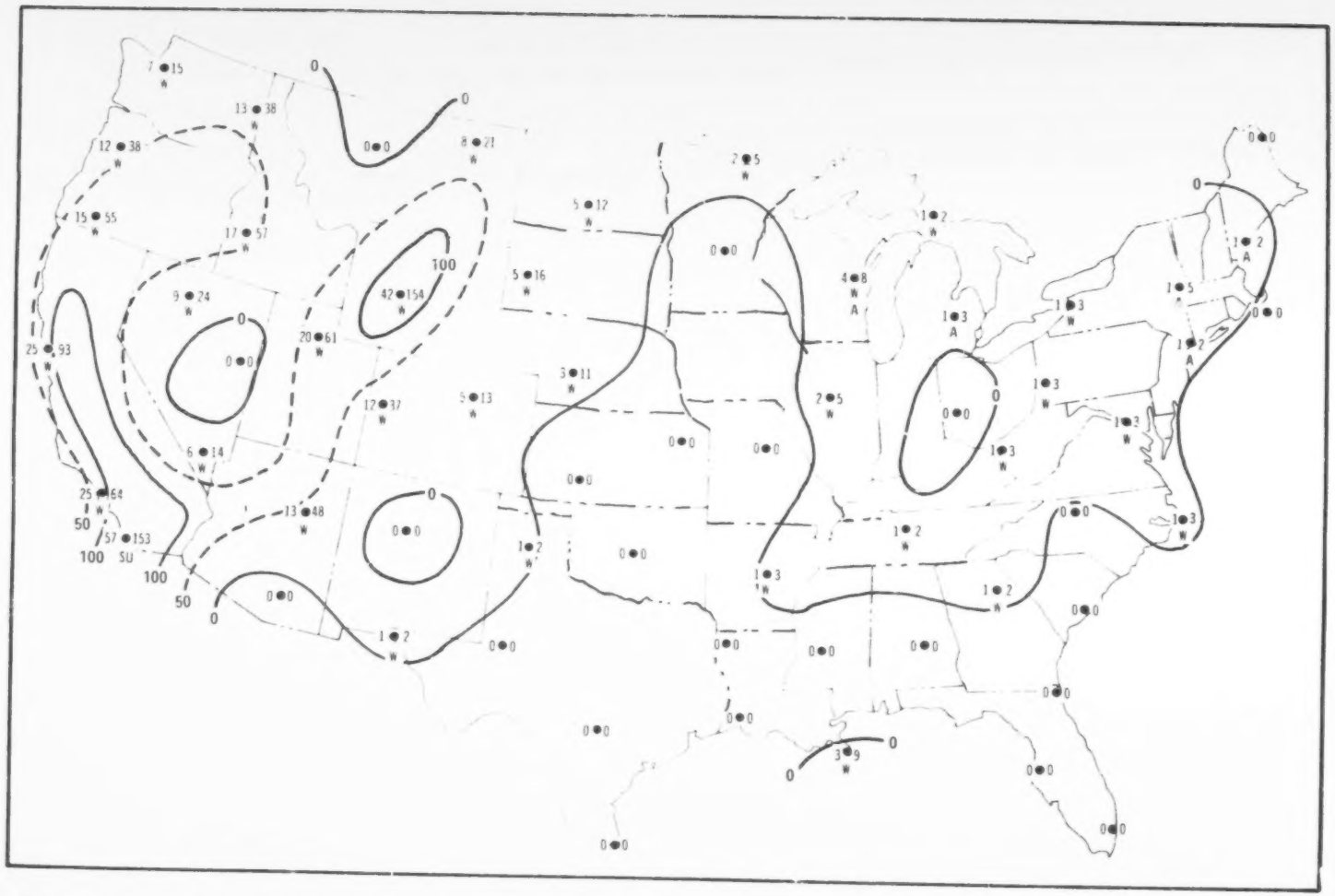

Figure 52. Isopleths of total number of episode-days in 5 years with mixing heights ≤ 500 m, wind speeds ≤ 4.0 m sec^{-1}, and no significant precipitation (see text) - - for episodes lasting at least 2 days. Numerals on left and right give total number of episodes and episode-days, respectively. Season with greatest number of episode-days indicated as W (winter), SP (spring), SU (summer), or A (autumn).

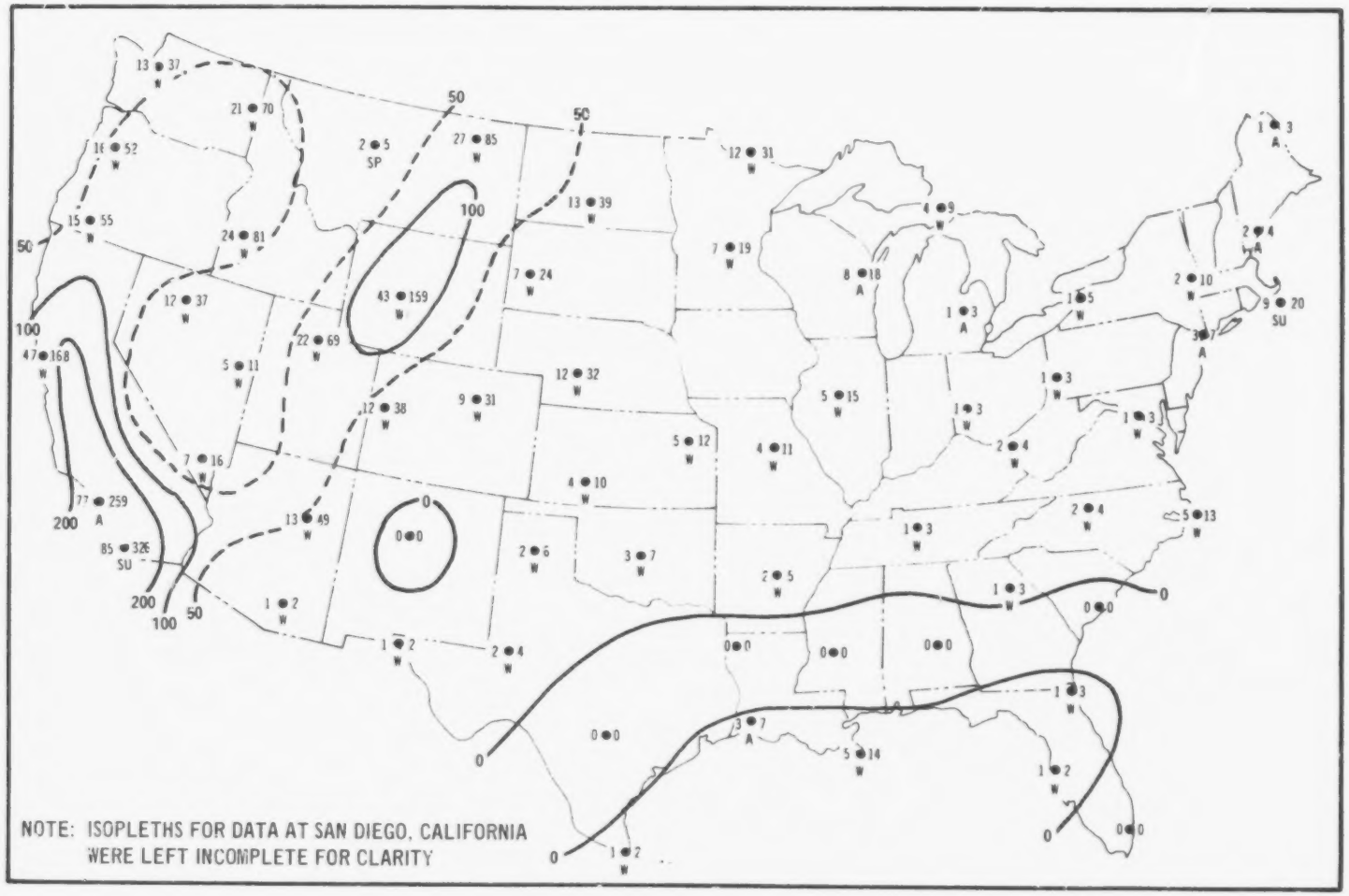

Figure 53. Isopleths of total number of episode-days in 5 years with mixing heights ≤ 500 m, wind speeds ≤ 6.0 m sec^{-1}, and no significant precipitation (see text) - - for episodes lasting at least 2 days. Numerals on left and right give total number of episodes and episode-days, respectively. Season with greatest number of episode-days indicated as W (winter), SP (spring), SU (summer), or A (autumn).

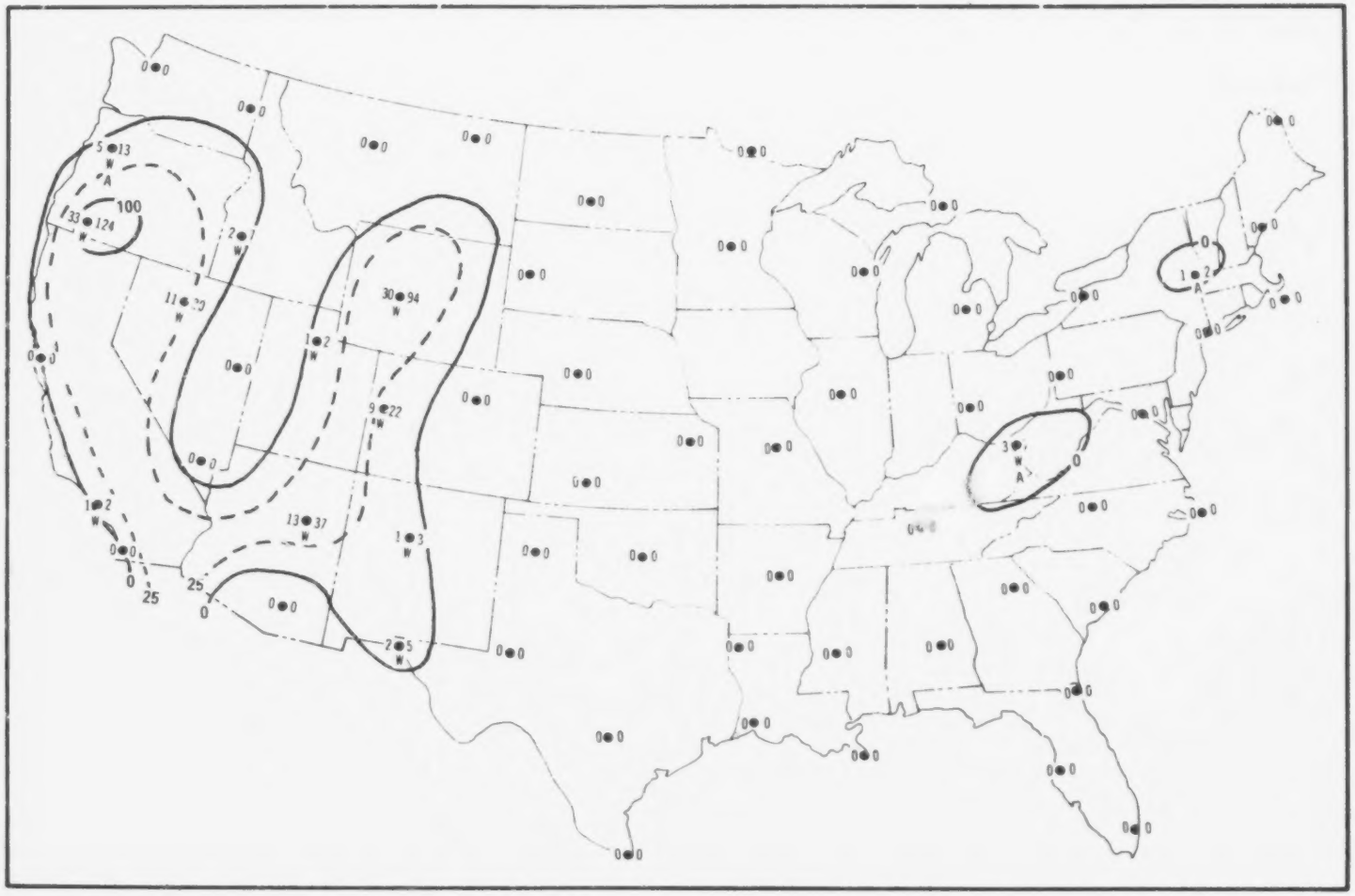

Figure 54. Isopleths of total number of episode-days in 5 years with mixing heights ≤ 1000 m, wind speeds ≤ 2.0 m sec^{-1}, and no significant precipitation (see text) - - for episodes lasting at least 2 days. Numerals on left and right give total number of episodes and episode-days, respectively. Season with greatest number of episode-days indicated as W (winter), SP (spring), SU (summer), or A (autumn).

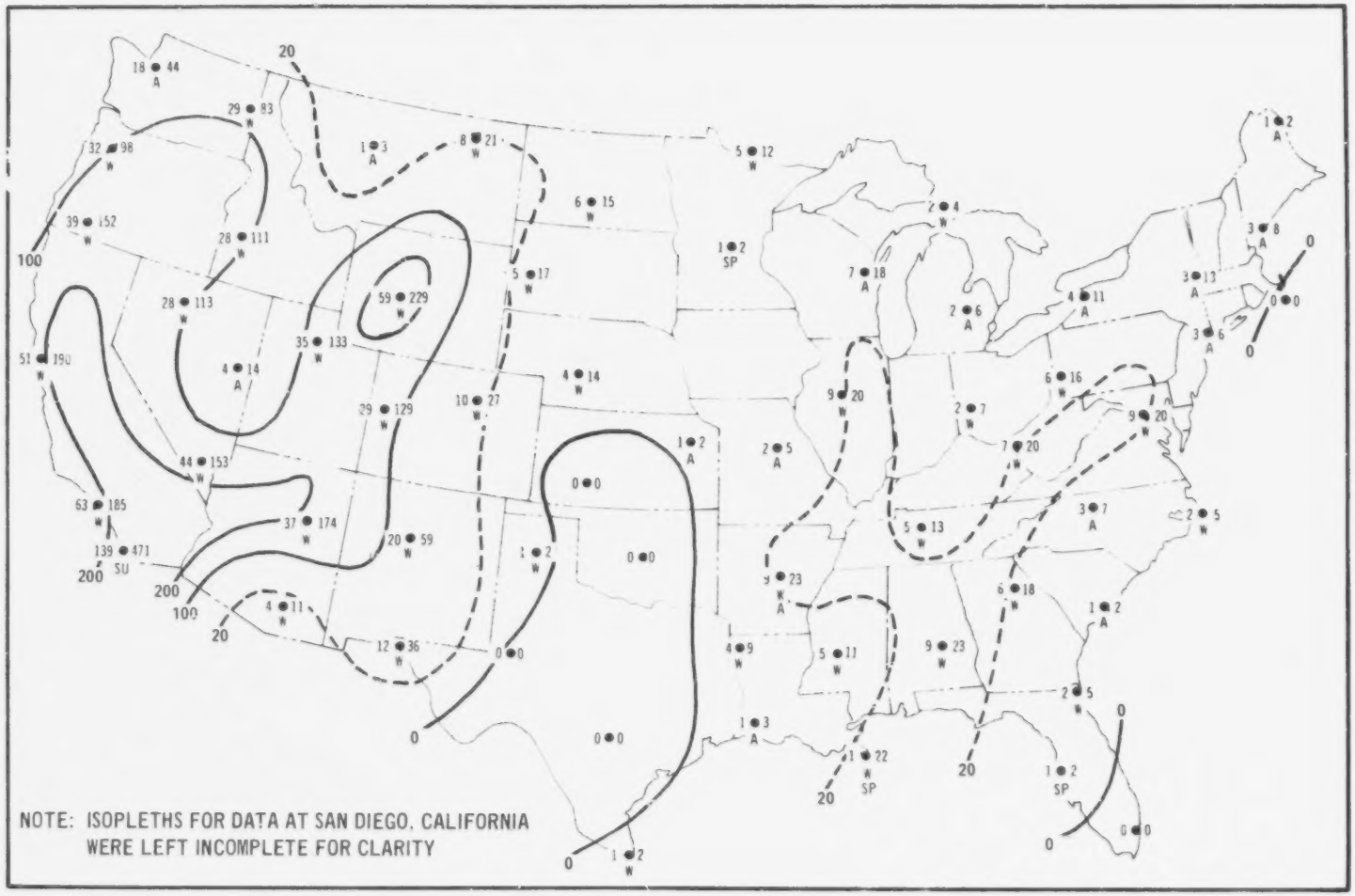

Figure 55. Isopleths of total number of episode-days in 5 years with mixing heights ≤ 1000 m, wind speeds ≤ 4.0 m sec^{-1}, and no significant precipitation (see text) - - for episodes lasting at least 2 days. Numerals on left and right give total number of episodes and episode-days, respectively. Season with greatest number of episode-days indicated as W (winter), SP (spring), SU (summer), or A (autumn).

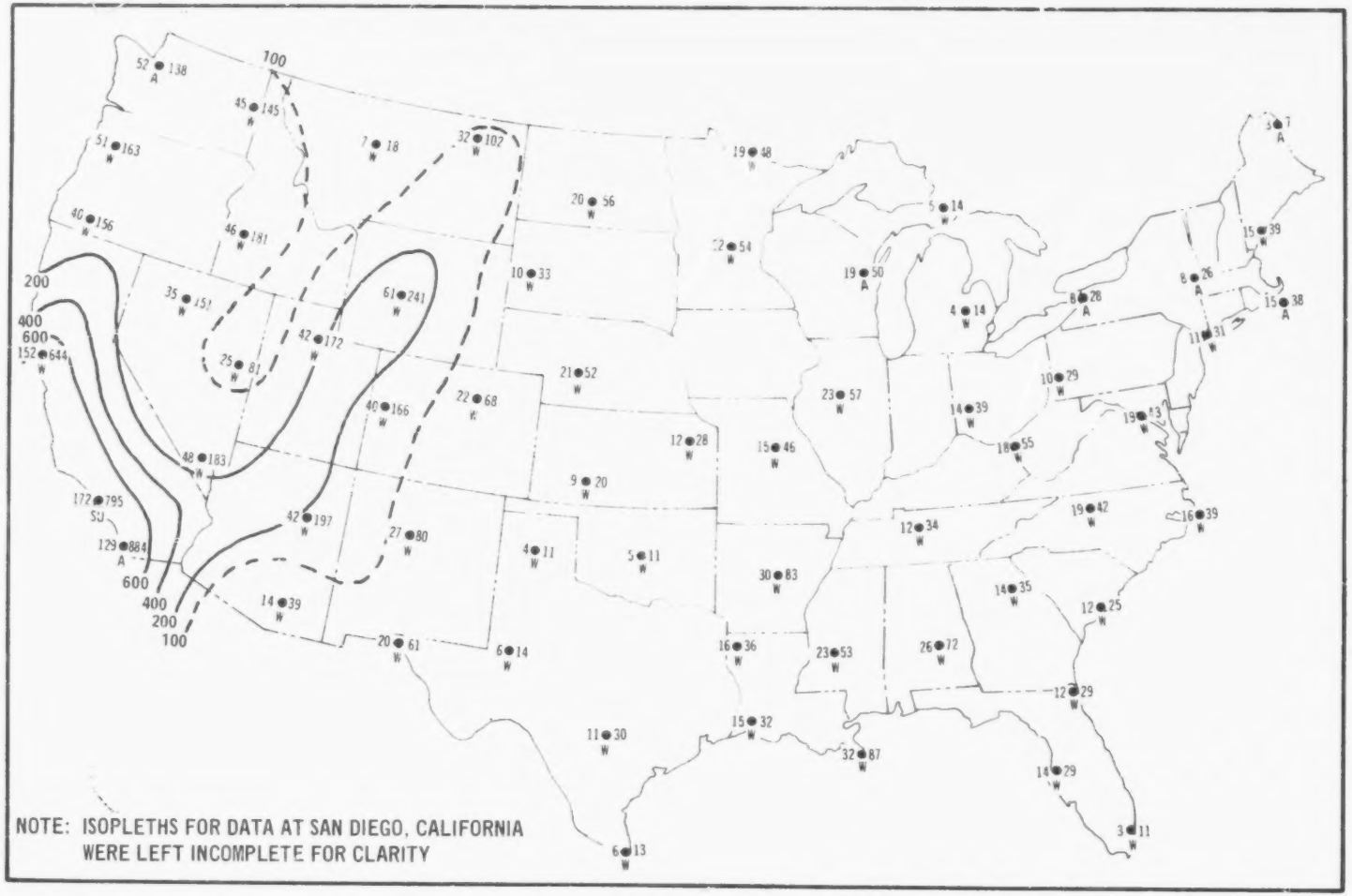

Figure 56. Isopleths of total number of episode-days in 5 years with mixing heights ≤ 1000 m, wind speeds ≤ 6.0 m sec^{-1}, and no significant precipitation (see text) - - for episodes lasting at least 2 days. Numerals on left and right give total number of episodes and episode-days, respectively. Season with greatest number of episode-days indicated as W (winter), SP (spring), SU (summer), or A (autumn).

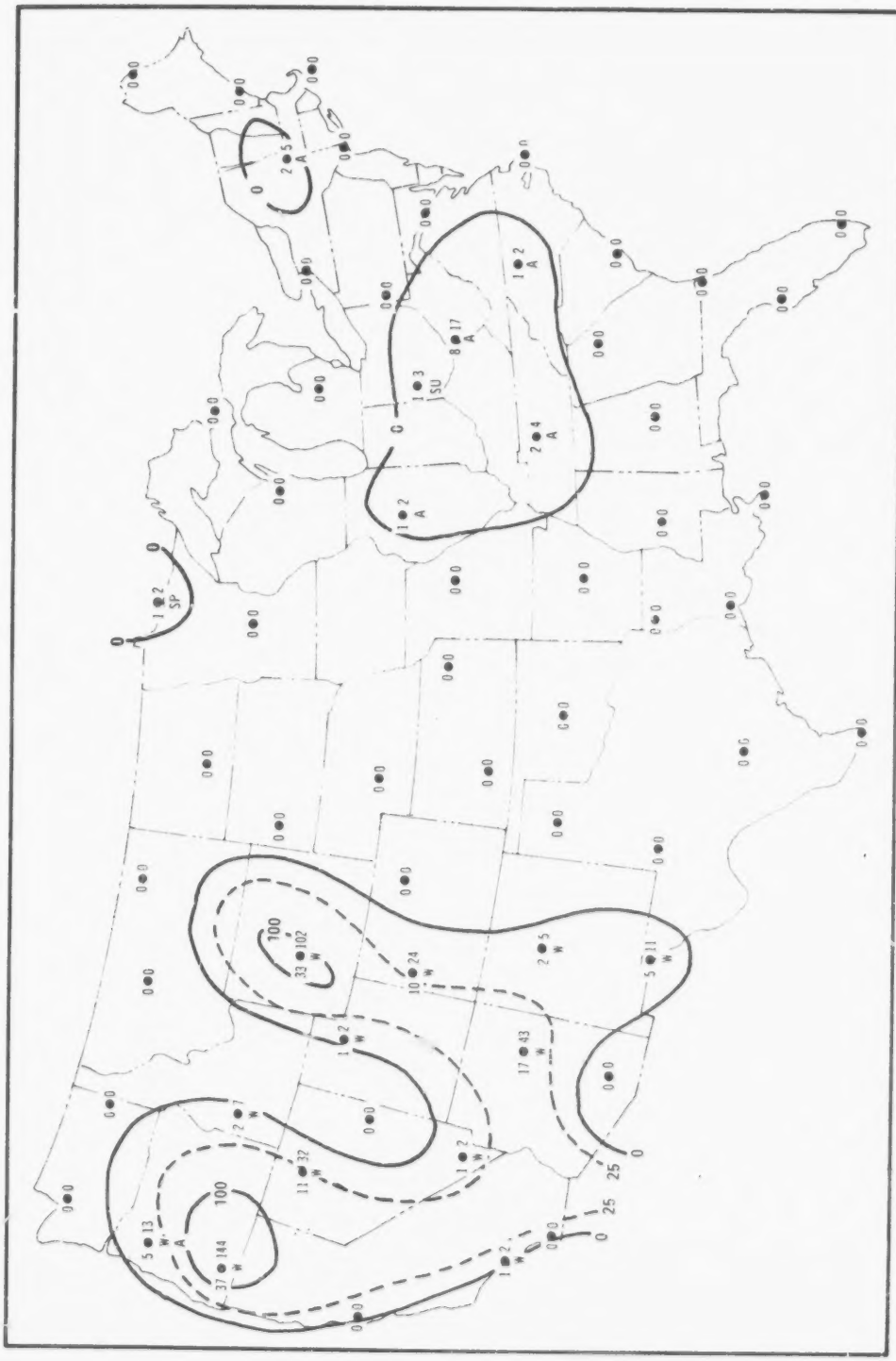

Figure 57. Isopleths of total number of episode-days in 5 years with mixing heights ≤ 1500 m, wind speeds ≤ 2.0 m sec^{-1}, and no significant precipitation (see text) - - for episodes lasting at least 2 days. Numerals on left and right give total number of episodes and episode-days, respectively. Season with greatest number of episode-days indicated as W (winter), SP (spring), SU (summer), or A (autumn).

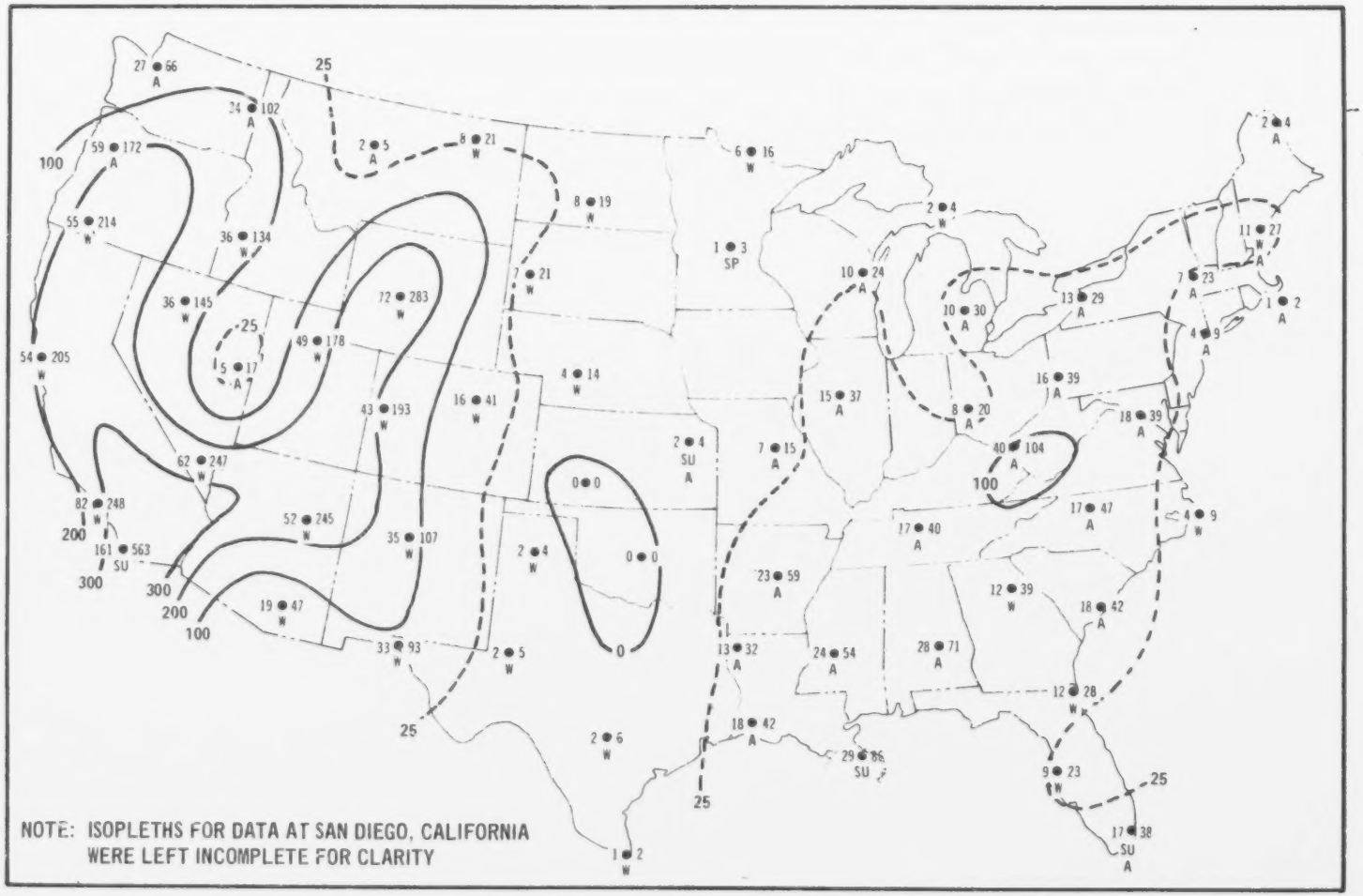

Figure 58. Isopleths of total number of episode-days in 5 years with mixing heights $\leq$ 1500 m, wind speeds $\leq$ 4.0 m sec^{-1}, and no significant precipitation (see text) - - for episodes lasting at least 2 days. Numerals on left and right give total number of episodes and episode-days, respectively. Season with greatest number of episode-days indicated as W (winter), SP (spring), SU (summer), or A (autumn).

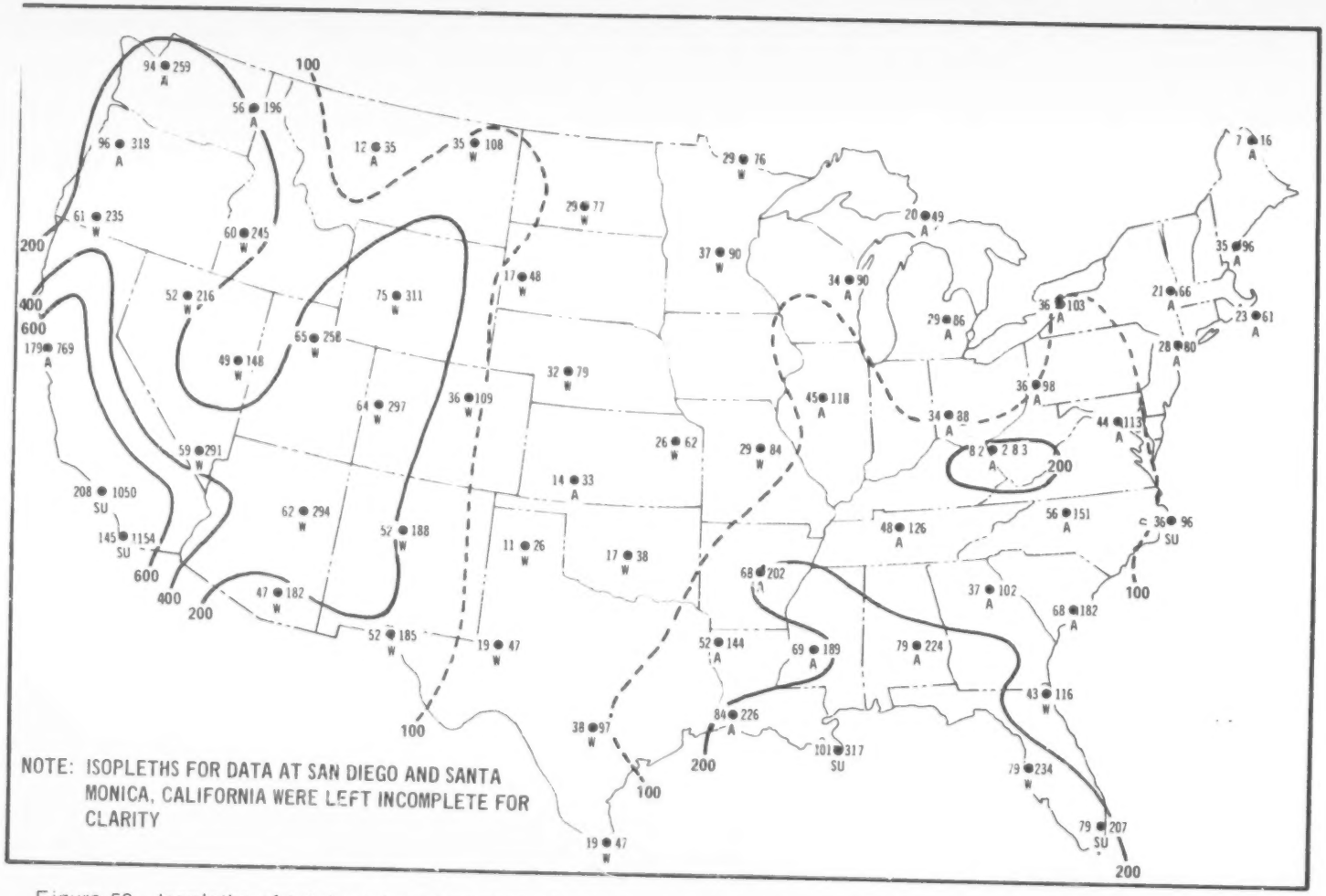

Figure 59. Isopleths of total number of episode-days in 5 years with mixing heights ≤ 1500 m, wind speeds ≤ 6.0 m sec^{-1}, and no significant precipitation (see text) - - for episodes lasting at least 2 days. Numerals on left and right give total number of episodes and episode-days, respectively. Season with greatest number of episode-days indicated as W (winter), SP (spring), SU (summer), or A (autumn).

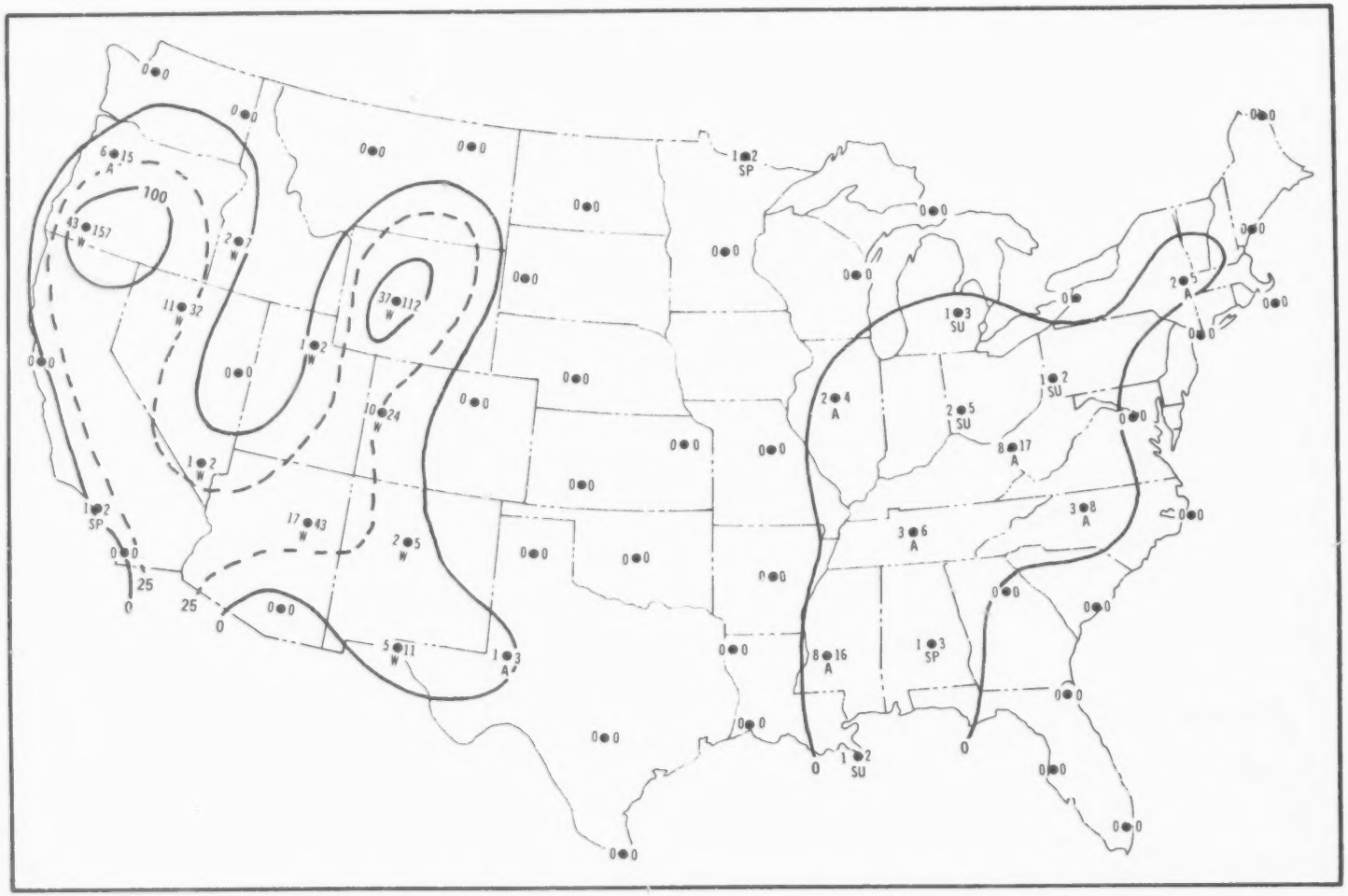
100
25
25
0
0
0

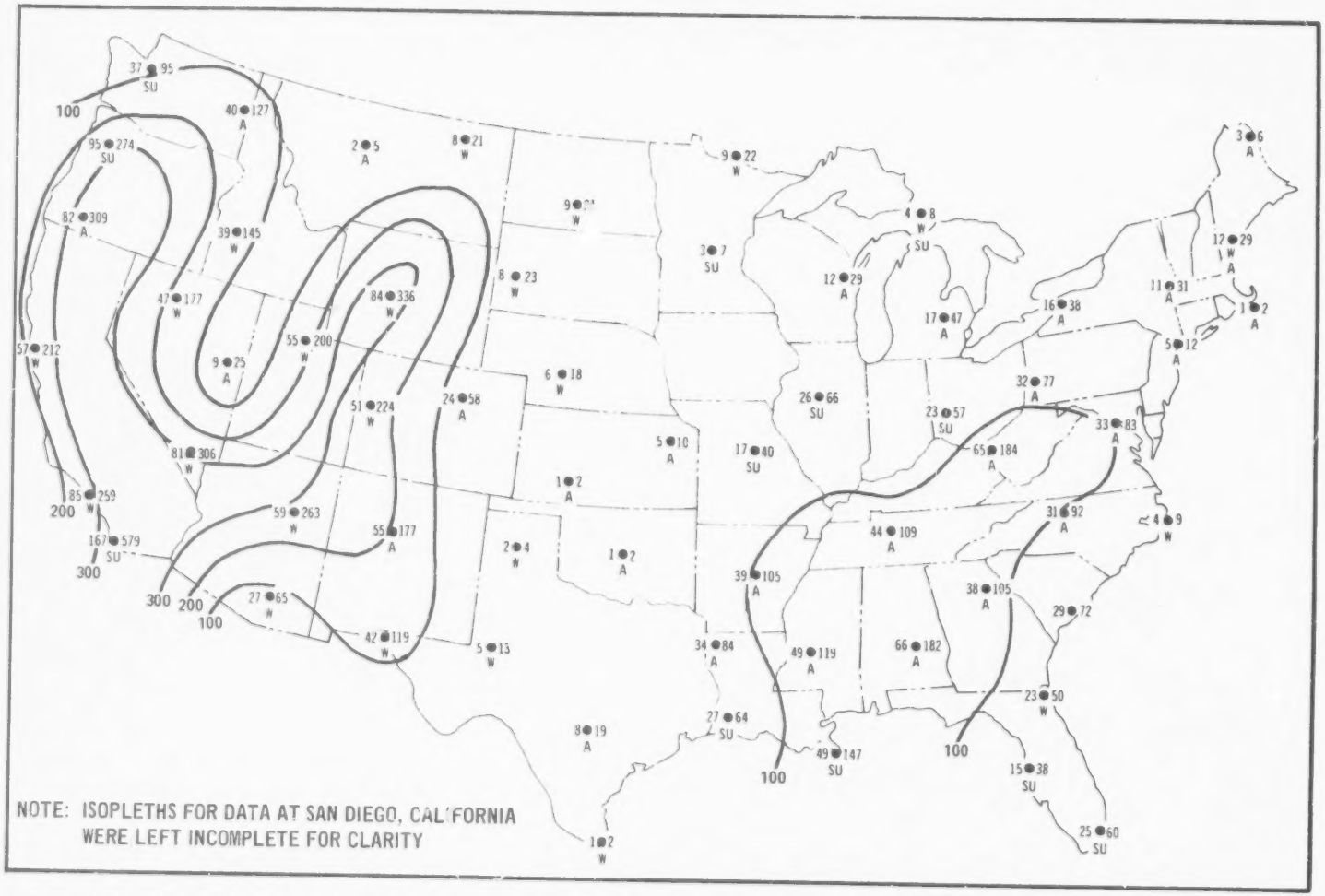

Figure 61. Isopleths of total number of episode-days in 5 years with mixing heights ≤ 2000 m, wind speeds ≤ 4.0 m sec^{-1}, and no significant precipitation (see text) - - for episodes lasting at least 2 days. Numerals on left and right give total number of episodes and episode-days, respectively. Season with greatest number of episode-days indicated as W (winter), SP (spring), SU (summer), or A (autumn).

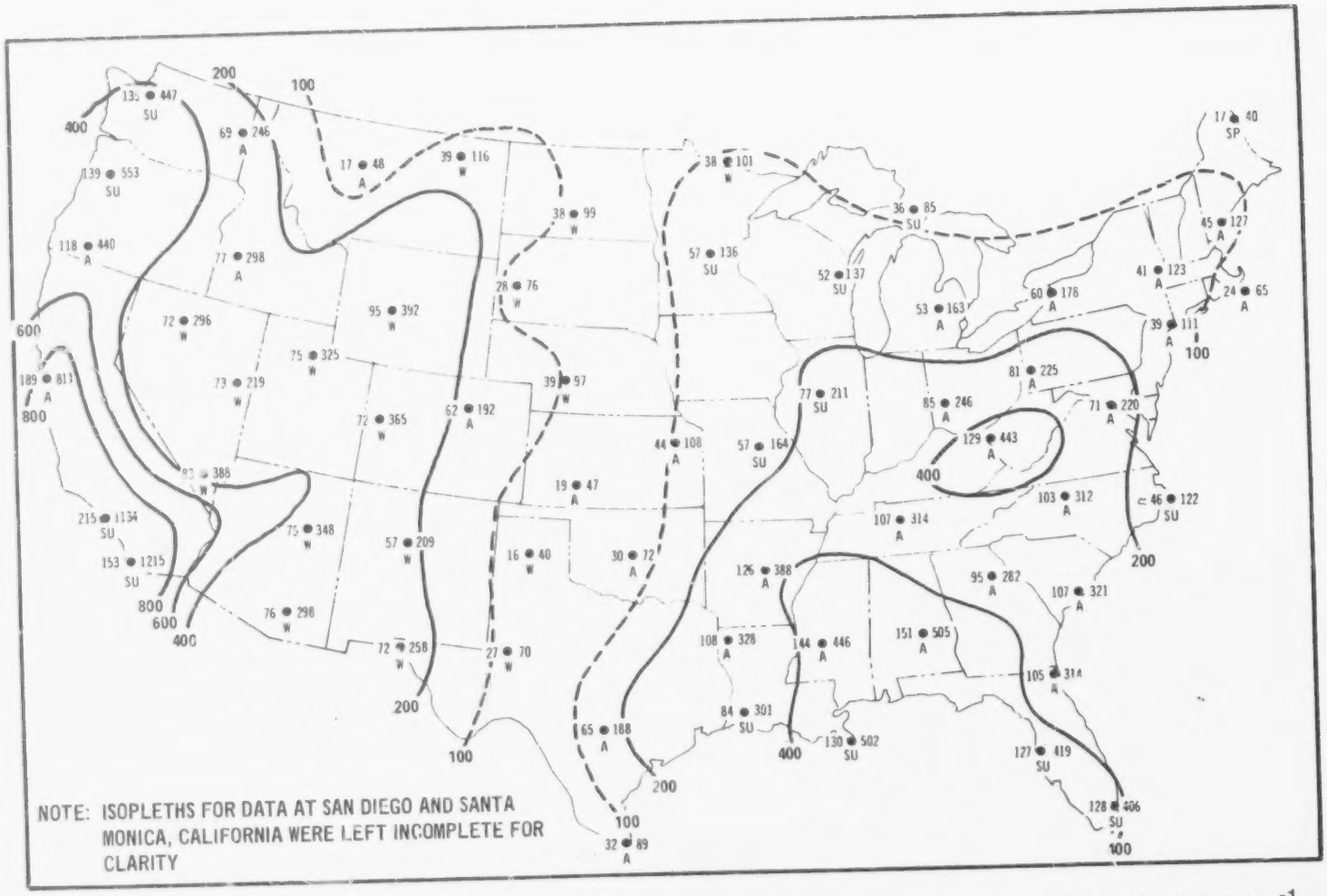

Figure 62. Isopleths of total number of episode-days in 5 years with mixing heights ≤ 2000 m, wind speeds ≤ 6.0 m sec^{-1}, and no significant precipitation (see text) - - for episodes lasting at least 2 days. Numerals on left and right give total number of episodes and episode-days, respectively. Season with greatest number of episode-days indicated as W (winter), SP (spring), SU (summer), or A (autumn).

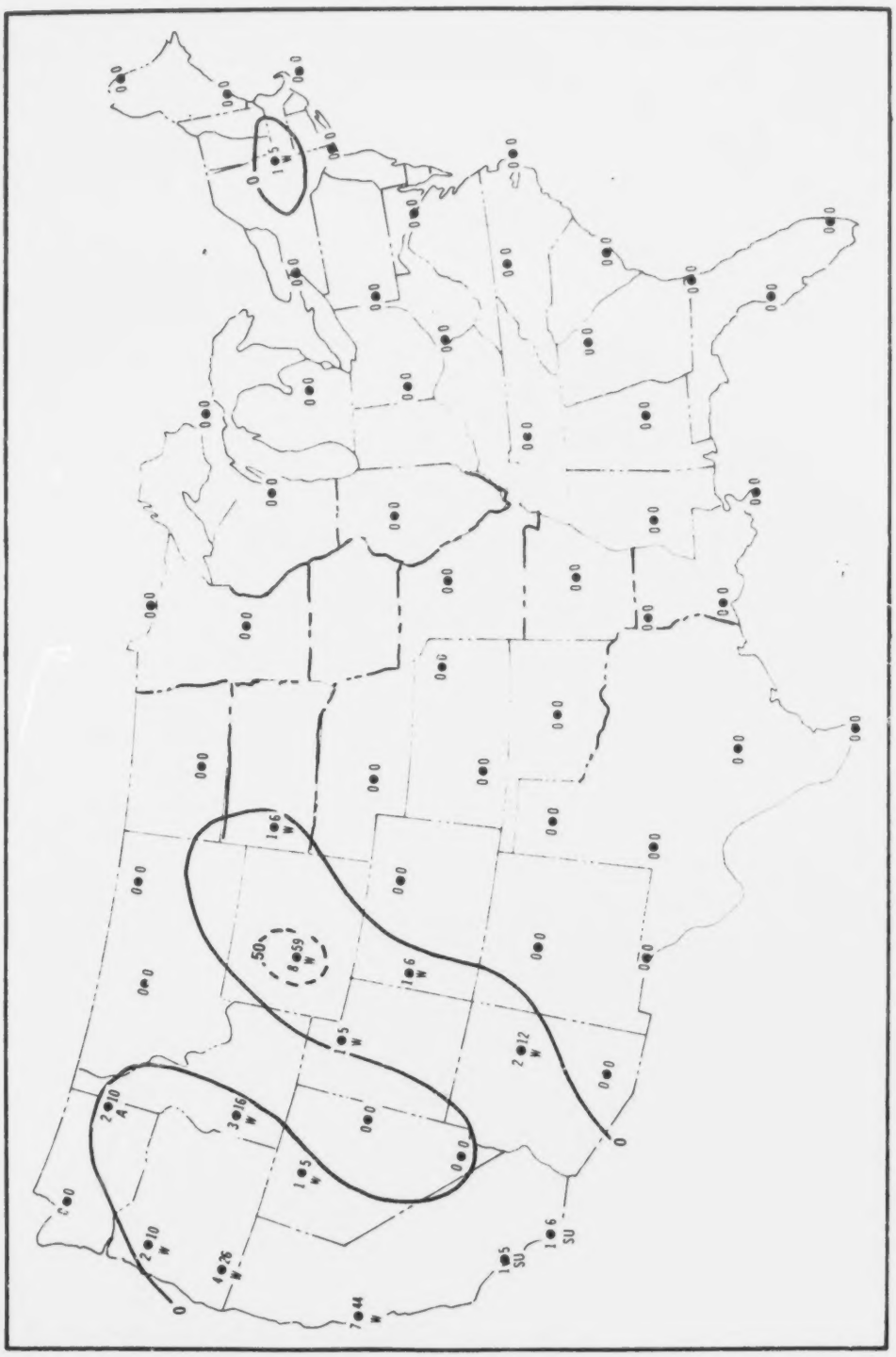

Figure 63. Isopleths of total number of episode-days in 5 years with mixing heights ≤ 500 m, wind speeds ≤ 4.0 m sec^{-1}, and no significant precipitation (see text) - - for episodes lasting at least 5 days. Numerals on left and right give total number of episodes and episode-days, respectively. Season with greatest number of episode-days indicated as W (winter), SP (spring), SU (summer), or A (autumn).

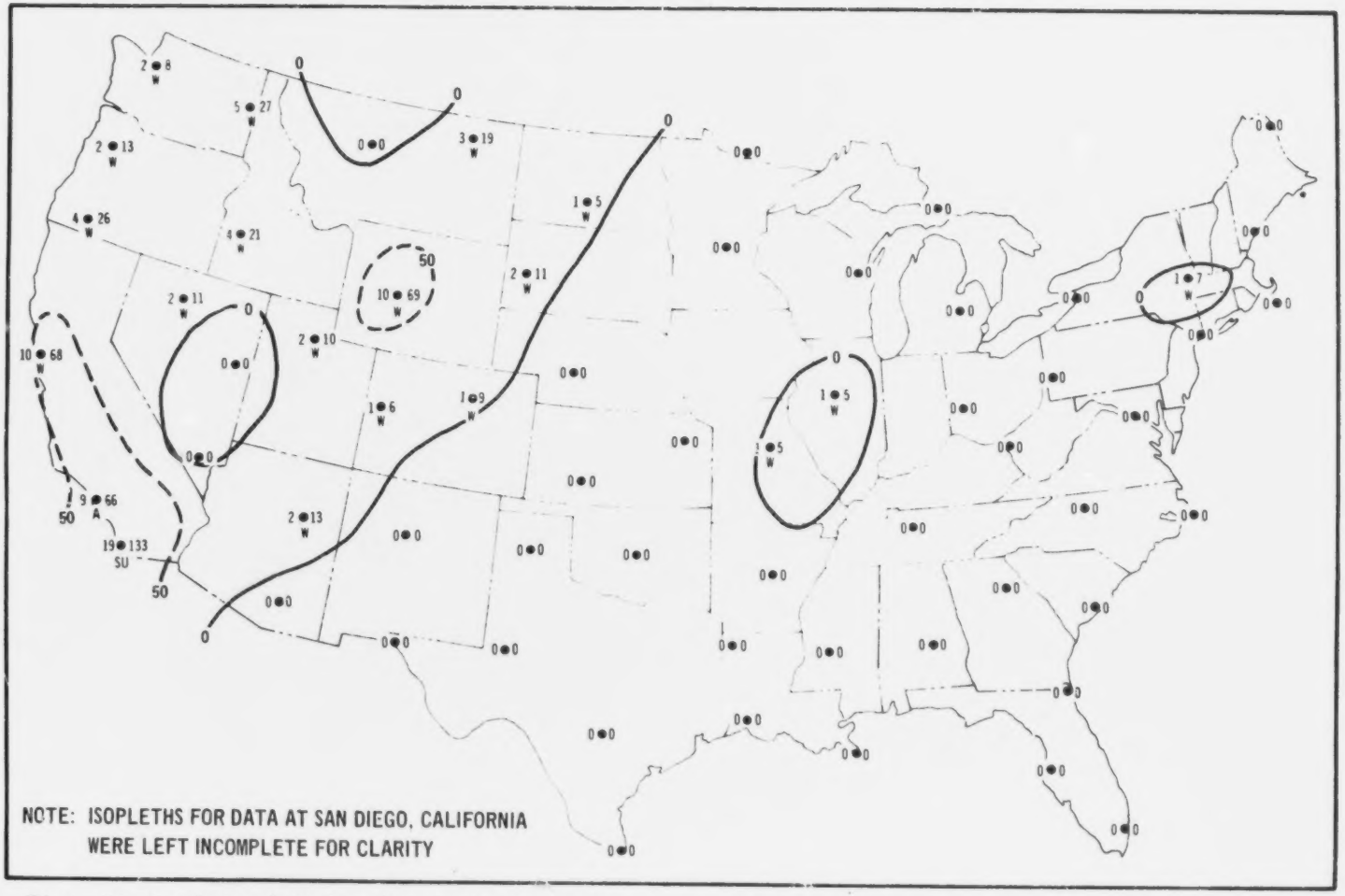

Figure 64. Isopleths of total number of episode-days in 5 years with mixing heights ≤ 500 m, wind speeds ≤ 6.0 m sec^{-1}, and no significant precipitation (see text) - - for episodes lasting at least 5 days. Numerals on left and right give total number of episodes and episode-days, respectively. Season with greatest number of episode-days indicated as W (winter), SP (spring), SU (summer), or A (autumn).

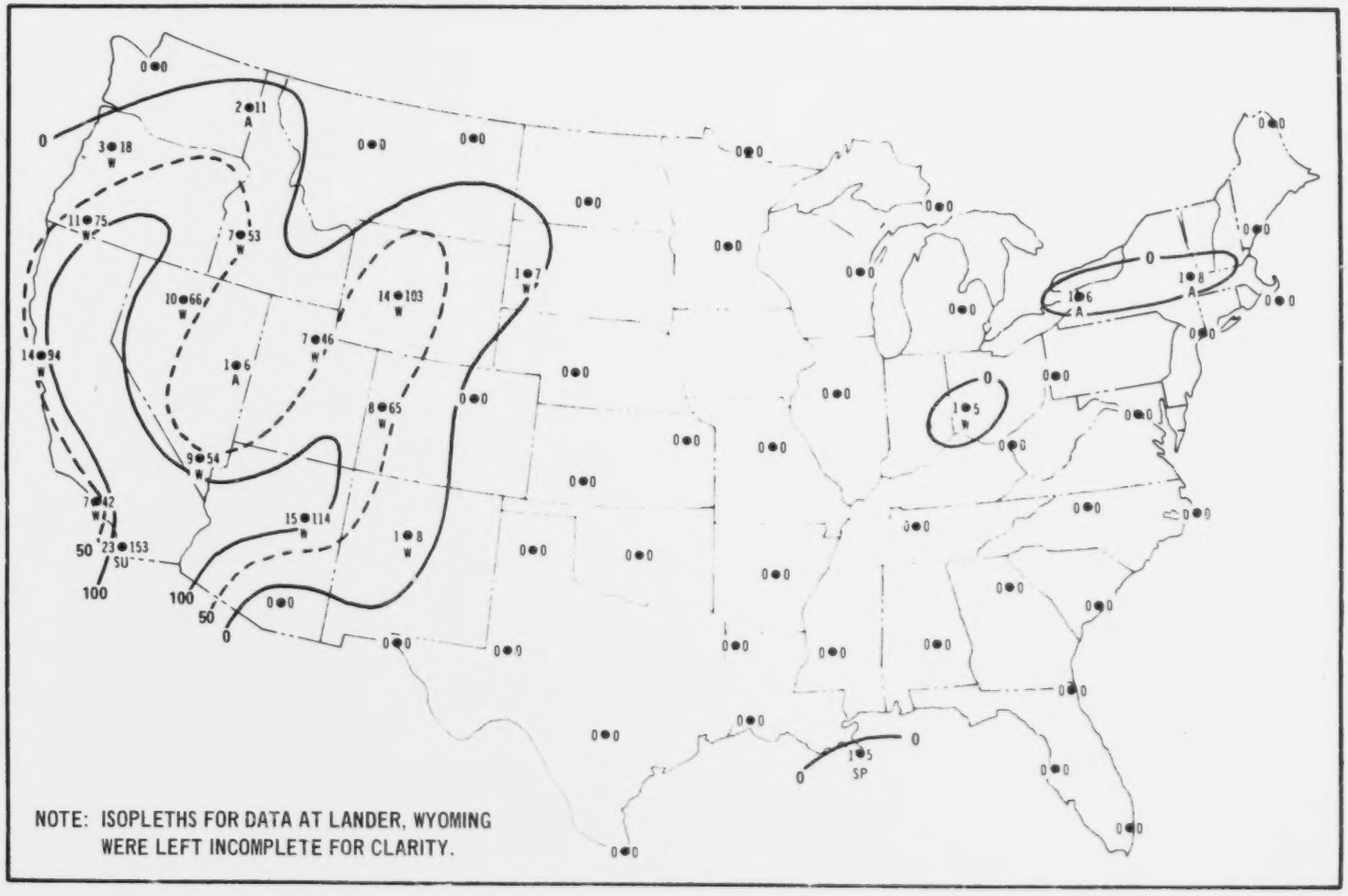

Figure 65. Isopleths of total number of episode-days in 5 years with mixing heights $\leq$ 1000 m, wind speeds $\leq$ 4.0 m sec^{-1}, and no significant precipitation (see text) - - for episodes lasting at least 5 days. Numerals on left and right give total number of episodes and episode-days, respectively. Season with greatest number of episode-days indicated as W (winter), SP (spring), SU (summer), or A (autumn).

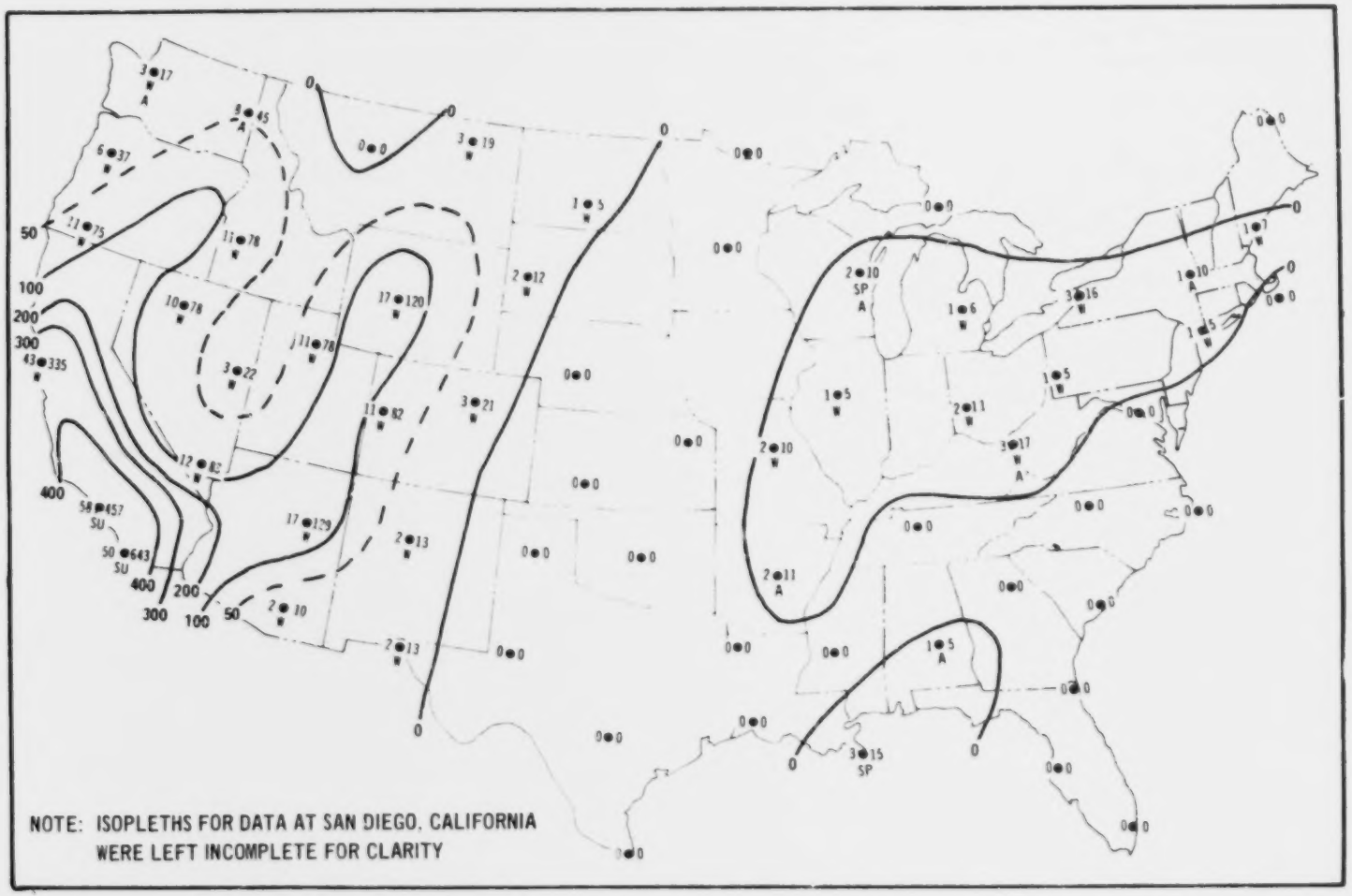

Figure 66. Isopleths of total number of episode-days in 5 years with mixing heights ≤ 1000 m, wind speeds ≤ 6.0 m sec^{-1}, and no significant precipitation (see text) - - for episodes lasting at least 5 days. Numerals on left and right give total number of episodes and episode-days, respectively. Season with greatest number of episode-days indicated as W (winter), SP (spring), SU (summer), or A (autumn).

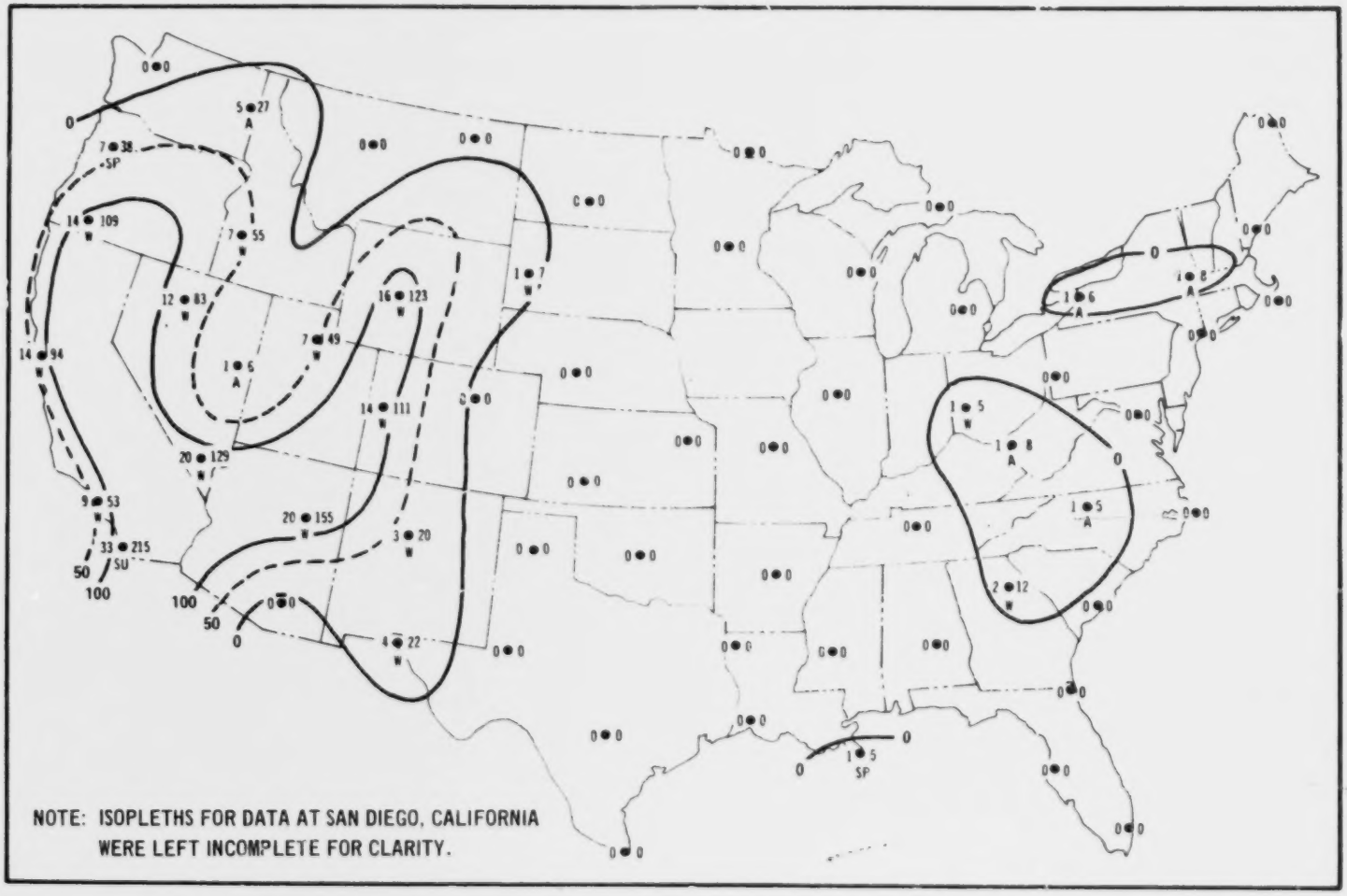

Figure 67. Isopleths of total number of episode-days in 5 years with mixing heights $\leq$ 1500 m, wind speeds $\leq$ 4.0 m sec^{-1}, and no significant precipitation (see text) - - for episodes lasting at least 5 days. Numerals on left and right give total number of episodes and episode-days, respectively. Season with greatest number of episode-days indicated as W (winter), SP (spring), SU (summer), or A (autumn).

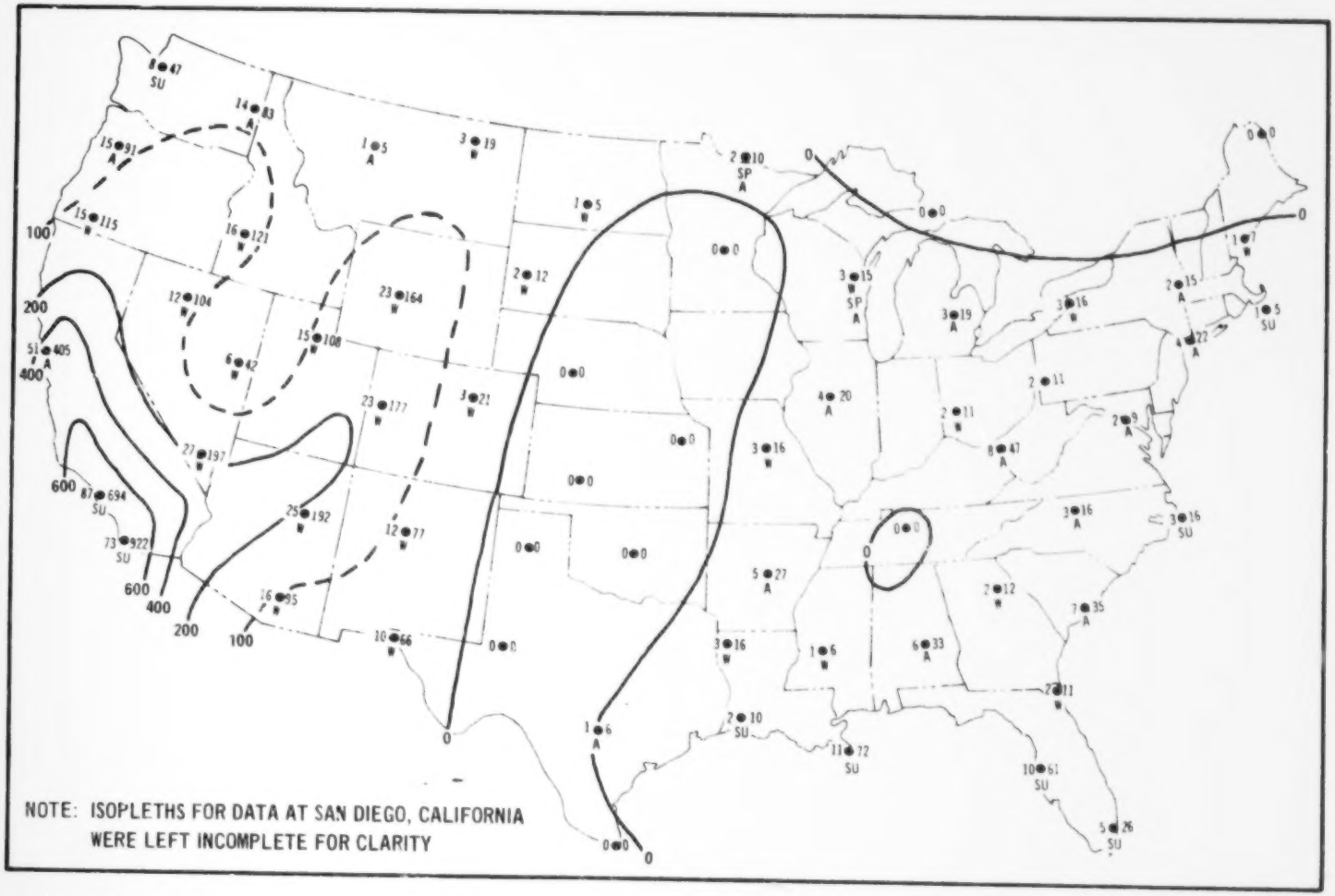

Figure 68. Isopleths of total number of episode-days in 5 years with mixing heights ≤ 1500 m, wind speed ≤ 6.0 m sec^{-1}, and no significant precipitation (see text) - - for episodes lasting at least 5 days. Numerals on left and right give total number of episodes and episode-days, respectively. Season with greatest number of episode-days indicated as W (winter), SP (spring), SU (summer), or A (autumn).

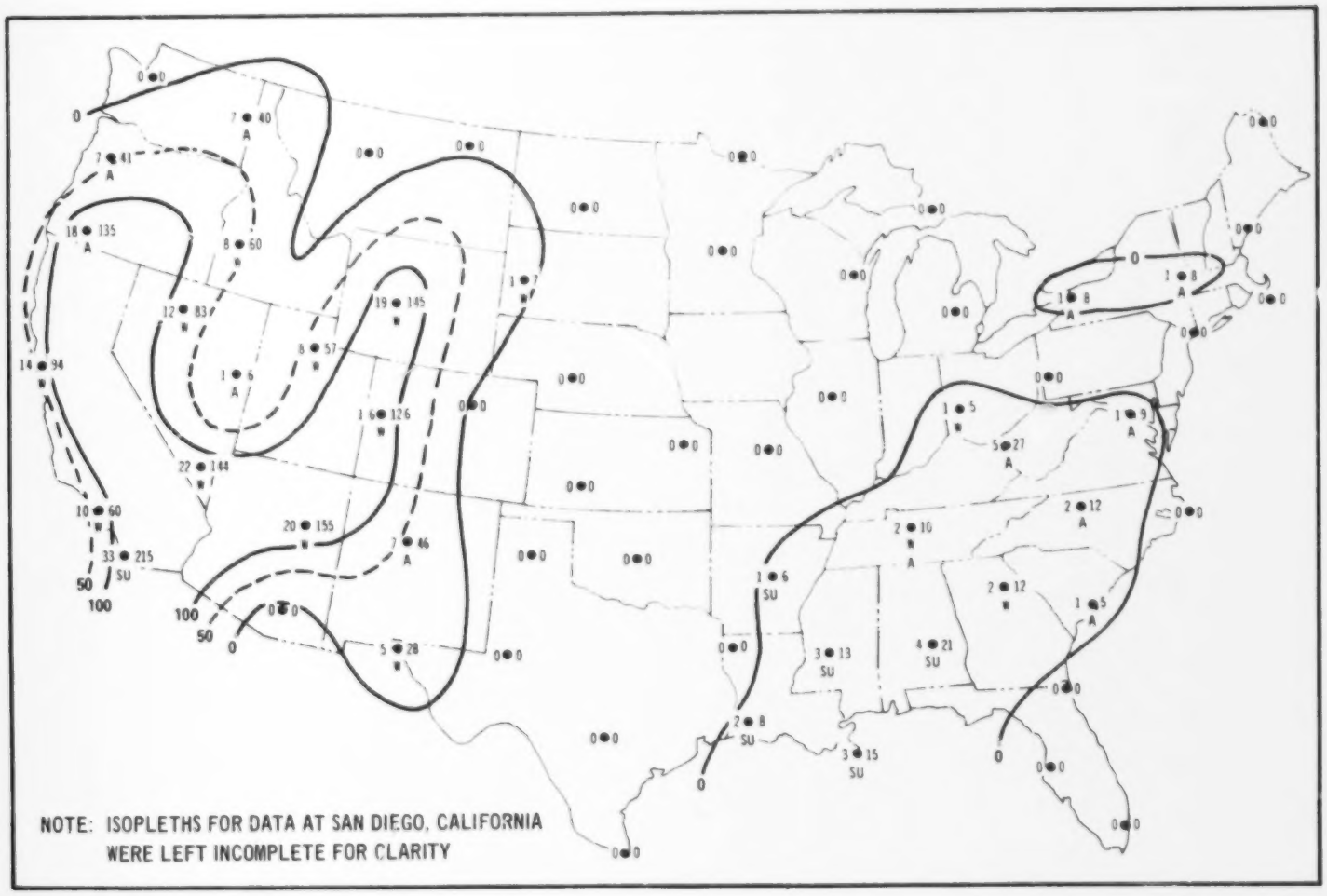

Figure 69. Isopleths of total number of episode-days in 5 years with mixing heights ≤ 2000 m, wind speeds ≤ 4.0 m sec^{-1}, and no significant precipitation (see text) - - for episodes lasting at least 5 days. Numerals on left and right give total number of episodes and episode-days, respectively. Season with greatest number of episode-days indicated as W (winter), SP (spring), SU (summer), or A (autumn).

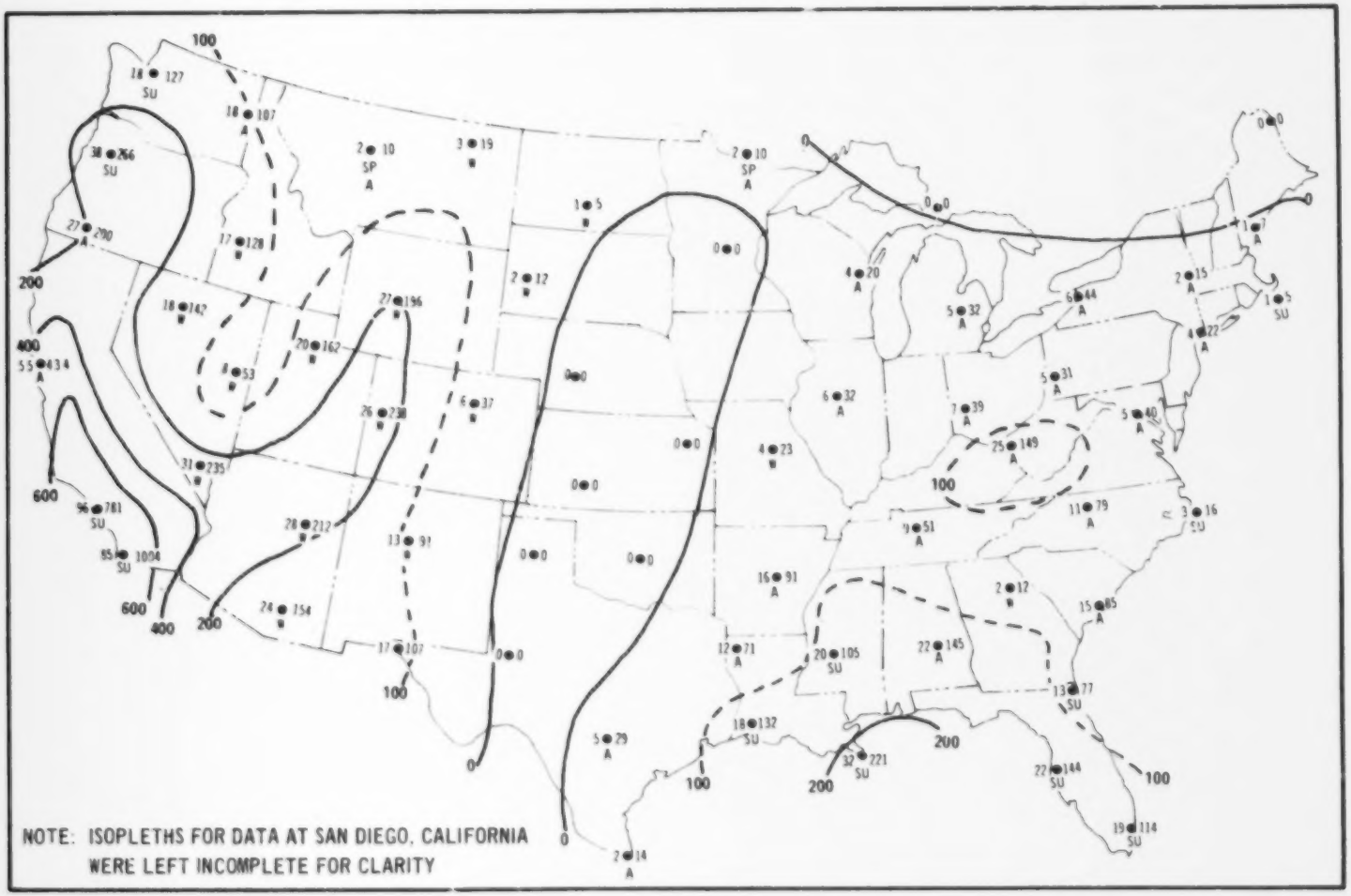

Figure 70. Isopleths of total number of episode-days in 5 years with mixing heights ≤ 2000 m, wind speeds ≤ 6.0 m sec^{-1}, and no significant precipitation (see text) - - for episodes lasting at least 5 days. Numerals on left and right give total number of episodes and episode-days, respectively. Season with greatest number of episode-days indicated as W (winter), SP (spring), SU (summer), or A (autumn).

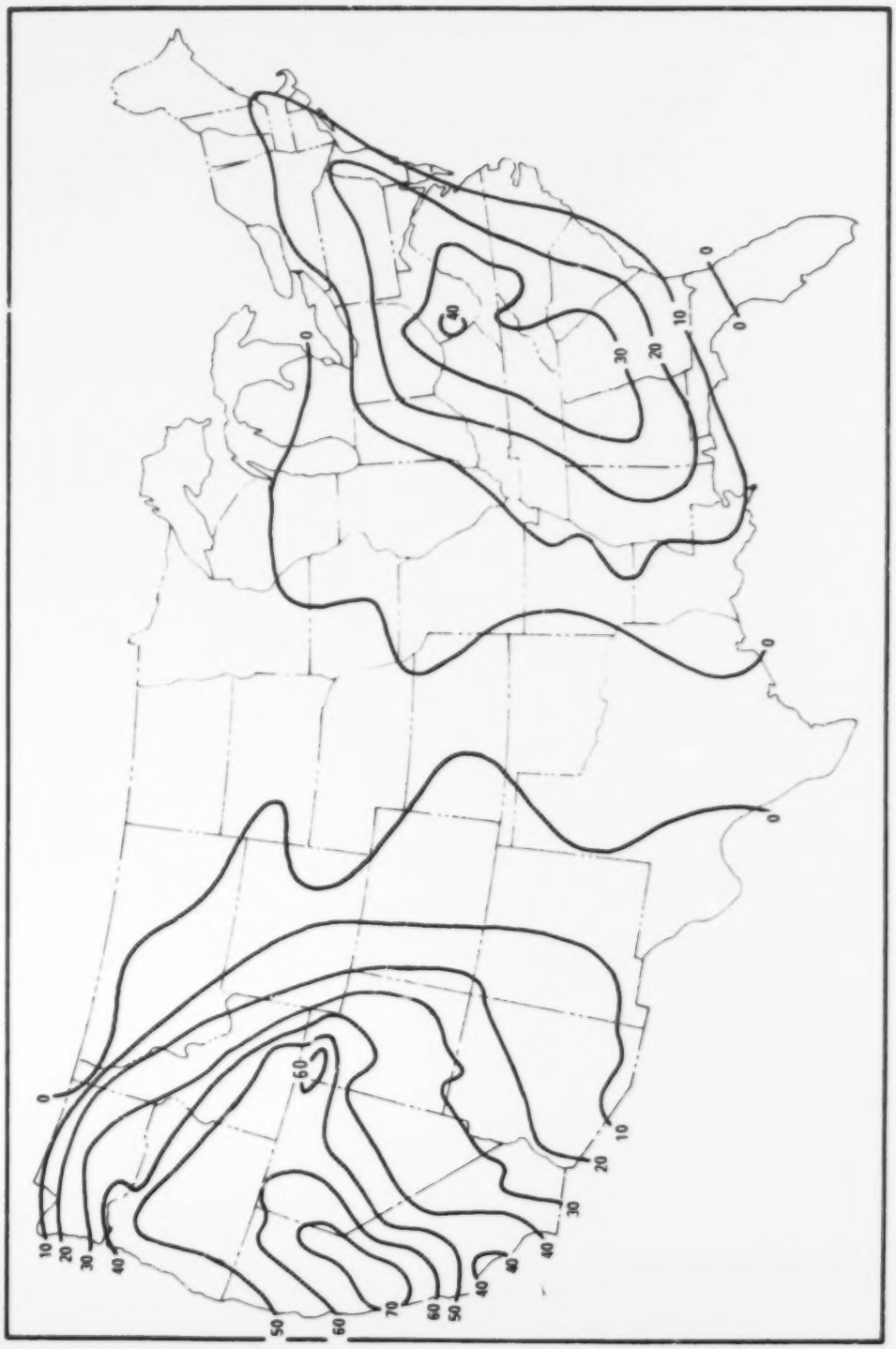

Figure 71. Isopleths of total number of forecast-days of high meteorological potential for air pollution in a 5-year period. Data are based on forecasts issued since the program began, 1 August 1960 and 1 October 1963 for eastern and western parts of the United States, respectively, through 3 April 1970.

APPENDIX A. NCC TABULATIONS OF MIXING HEIGHT AND WIND SPEED

This appendix provides a detailed description of the subject tabulations for the benefit of those interested in obtaining copies. The 62 NWS upper-air (combined radiosonde and rawinsonde) stations for which tabulations of mixing height and vertically averaged wind speed were prepared are listed in Table A-1 along with pertinent information. Station locations may be seen in Figures 21 through 70. All tabulations were accomplished by the National Climatic Center (NCC) (formerly the National Weather Records Center) under Job Order 6234, except those for Washington, D.C., which were under Job Order 7717. With few exceptions, each upper-air and corresponding surface (airways) observing station was at the same location (e.g., airport). For each station, there are three tabulations. The cover page of each tabulation includes the tabulation number (I, II, or III), upper-air station name and WBAN number, and period of record. Each tabulation is prefaced by an explanation page. (For clarity the tabulations are described in reverse numerical order, i.e., III, II, and I.)

TABULATION III

Table A-2 is an example of NCC Tabulation III. The station is Peoria, Illinois (WBAN number 14842), the year is 1960 (60), the month is April (04), and the data for mornings are indicated on the left and for afternoons on the right.

Column T gives the classification of a mixing-height calculation. If the regular hourly airways observations from 2200 through 0900 LST included at least two occurrences of light precipitation or one of moderate or heavy, the morning calculation is classified as P. A similar classification is employed for afternoons considering hourly observations from 1000 through 2100 LST. P cases are of interest because the assumption of a dry adiabatic lapse rate in the mixing layer may not be valid. If the surface temperature that is to be extended dry adiabatically (the morning minimum plus 5°C or the afternoon maximum) is less than the surface temperature of the 1200 GMT vertical temperature profile observation, no mixing height can be calculated. This condition is indicated by a letter C. Such cases occurred especially in the afternoon with strong cold air advection after the 1200 GMT upper air observation but before noon LST. For C cases the speeds are averaged through 4000 m above the station. "M" indicated missing. A blank in the T-column indicates that none of the foregoing types occurred (i.e., the conditions of greatest interest in this study).

Column 1 gives the mixing height in meters (m); column 2, the vertically averaged wind speed through the mixing layer in m sec^{-1}, based on surface winds and on winds aloft observed at 1200 GMT for morning and 0000 GMT for afternoons; column 3, the average surface wind speed (used in the vertically averaged speed) in m sec^{-1}, based on the five regular hourly airways reports from 0200 through 0600 LST for mornings, and from 1200 through 1600 LST for afternoons; column 4 gives the number of wind levels used to calculate the vertically averaged speed of column 2. Column 4 is not included for some stations.

As illustrated in Table A-3 for the seasons, Tabulation III also gives the monthly and seasonal mean mixing heights (column 1), means of vertically averaged speeds (column 2), mean surface speeds (column 3), and total number of occurrences (column N), all by classification of the mixing-height calculation (column T). A blank in the T-column designates the non-P and non-C cases.

Five years of records are processed for most stations. Tabulation III consists of 63 pages; one page of explanations, one page for each month of each year, one page for all monthly means, and one page for all seasonal means.

TABULATION II

NCC Tabulation II is a temporal analysis of the daily morning and afternoon mixing heights and wind speeds of Tabulation III (columns 1 and 2 therein). By month and season, it gives the frequencies of episodes of specified duration *or longer* during which consecutive calculations of non-P mixing height and wind speed did not exceed specified values. Table A-4 is an example of NCC Tabulation II. The letters A, B, C, D, E, F, G specify the upper limits of the mixing height as 250, 500, 750, 1000, 1500, 2000, 3000 m, and in the next column the numbers 2, 4, 6, 8 for each mixing height specify the upper limits of the vertically averaged wind speed as 2.0, 4.0, 6.0, 8.0 m sec^{-1}. The column headings 2, 3, 4, ... , 121 are the prescribed minimum number of consecutive calculations (e.g., morning to afternoon of day 1 to morning to afternoon of day 2, etc.) during which the meteorological criteria were satisfied. Thus, if the criteria were met in eight consecutive computations, that episode contributes a frequency count of one to each of the appropriate cells for 8, 7, 6, 5, 4, 3 and 2 *or more* consecutive computations. However, it does *not* contribute a frequency count of two to a duration of four or more consecutive calculations or a frequency count of four to a duration of two or more consecutive calculations. Table A-4 is for all Januarys (01) of the years considered; for mixing heights not greater than 500 m (B) and wind speeds not greater than 4.0 m sec^{-1} (4), there were seven separate episodes that lasted through at least two consecutive computations, three that lasted through at least three, one through at least four, and one that lasted through at least five consecutive computations. On the other hand, for these same conditions one episode persisted through exactly five consecutive computations, none through exactly four consecutive computations, two through exactly three consecutive computations, and four through exactly two consecutive computations. In Table A-4 the column at the far right gives the total number of occurrences of specified conditions without regard to consecutiveness. For example, in Table A-4 there were 62 occurrences (morning and afternoon) of a mixing height 500 m or less (B) with a wind speed of 4.0 m sec^{-1} or less (4); P cases are not included. It was assumed that the mixing height and wind speed computations were separated by 12-hour intervals and that the duration of an episode lasting through exactly two consecutive computations was 12 hours; the duration of an episode lasting through exactly three consecutive computations was 24 hours; etc.

For each station Tabulation II consists of 17 pages, which comprise one page of explanations, one page for each month of all years, and one page for each season of all years.

TABULATION I

An example of NCC Tabulation I is shown as Table A-5. It gives frequency counts of mixing heights by vertically averaged wind speeds, both in class intervals. There are separate tables for mornings and for afternoons of each month and season for all years. The major portion of each table is for both non-P and non-C cases (both indicated as "NOP"). However, there are column and row totals of P cases, column totals of C cases, the number of missing cases, and column and row totals of all cases. Thus, in Table A-5, autumn (04) afternoons (02), there were ten occurrences of non-P mixing heights 751 to 1000 m with a wind speed of 4.1 to 5.0 m sec^{-1} (5); there were 61 occurrences of non-P and 7 of P mixing heights 751 to 1000 m for all wind speeds. The total of all mixing heights 751 to 1000 m is 68. For all speeds the total non-P cases are 381, total P cases are 53, total C cases are 18, and 3 are missing for an accumulated total of 455 calculations for 5 years of autumns.

For each station, Tabulation I consists of 33 pages, which comprise one page of explanations and one page for each time (morning or afternoon) of each month and season for all years.

Table A-1. MIXING HEIGHT AND WIND SPEED TABULATIONS PREPARED BY THE NATIONAL CLIMATIC CENTER

Upper-air observing station			Date tabulations completed	Years of tabulations (inclusive)	Remarks*
Location	NWS Abbr.	WBAN no.			
Albany, New York	ALB	14735	5/13/68	1960-1964	
Albuquerque, New Mexico	ABQ	23050	6/12/68	1960-1964	
Amarillo, Texas	AMA	23047	7/1/68	1960-1964	
Athens, Georgia	AHN	13873	7/1/68	1960-1964	
Bismarck, North Dakota	BIS	24011	5/13/68	1960-1964	
Boise, Idaho	BOI	24131	6/12/68	1960-1964	
Brownsville, Texas	BRO	12919	6/26/68	1960-1964	
Buffalo, New York	BUF	14733	7/1/68	1961-1964	
Burwood, Louisiana	BRJ	12863	7/1/68	1960-1964	
Cape Hatteras, North Carolina	HAT	93729	7/1/68	1960-1964	
Caribou, Maine	CAR	14607	7/1/68	1960-1964	a
Charleston, South Carolina	CHS	13880	12/8/67	1960-1964	
Columbia, Missouri	CBI	13983	9/12/66	1960-1964	
Dayton, Ohio	DAY	93815	5/17/66	1960-1964	b
Denver, Colorado	DEN	23062	12/8/67	1960-1964	
Dodge City, Kansas	DDC	13985	6/26/68	1960-1964	
El Paso, Texas	ELP	23044	7/1/68	1960-1964	
Ely, Nevada	ELY	23154	7/1/68	1960-1964	
Flint, Michigan	FNT	14826	10/27/67	1960-1964	
Glasgow, Montana	GGW	94008	6/12/68	1960-1964	
Grand Junction, Colorado	GJT	23066	6/12/68	1960-1964	
Great Falls, Montana	GTF	24143	7/1/68	1960-1964	
Green Bay, Wisconsin	GRB	14898	7/1/68	1960-1964	
Greensboro, North Carolina	GSO	13723	5/13/68	1960-1964	
Huntington, West Virginia	HTS	03860	10/19/67	1962-1964	c
International Falls, Minnesota	INL	14918	7/1/68	1960-1964	
Jackson, Mississippi	JAN	13956	7/1/68	1959-1962	
Jacksonville, Florida	JAX	13889	7/1/68	1960-1964	
Lake Charles, Louisiana	LCH	03937	12/8/67	1962-1964	
Lander, Wyoming	LND	24021	7/1/68	1960-1964	d
Las Vegas, Nevada	LAS	23169	7/1/68	1960-1964	
Little Rock, Arkansas	LIT	13963	5/13/68	1960-1964	
Medford, Oregon	MFR	24225	6/12/68	1960-1964	
Miami, Florida	MIA	12839	6/26/68	1960-1964	
Midland, Texas	MAF	23023	6/12/68	1960-1964	
Montgomery, Alabama	MGM	13895	12/8/67	1960-1964	
Nantucket, Massachusetts	ACK	14756	7/23/68	1960-1964	
Nashville, Tennessee	BNA	13897	9/12/66	1960-1964	
New York, New York	JFK	94789	5/17/66	1960-1964	
North Platte, Nebraska	LBF	24023	6/12/68	1960-1964	
Oakland, California	OAK	23230	12/8/67	1960-1964	
Oklahoma City, Oklahoma	OKC	13976	5/13/68	1960-1964	
Peoria, Illinois	PIA	14842	6/12/68	1960-1964	

*Letters under remarks indicate footnotes given in text at end of table.

Table A-1 (continued)

Upper-air observing station			Date tabulations completed	Years of tabulations (inclusive)	Remarks*
Location	NWS Abbr.	WBAN no.			
Pittsburgh, Pennsylvania	PIT	94823	9/12/66	1960-1964	
Portland, Maine	PWM	14764	7/23/68	1960-1964	f
Rapid City, South Dakota	RAP	24090	7/1/68	1960-1964	
St. Cloud, Minnesota	STC	14926	12/8/67	1960-1964	
Salem, Oregon	SLE	24232	6/26/68	1960-1964	
Salt Lake City, Utah	SLC	24127	9/12/66	1960-1964	
San Antonio, Texas	SAT	12921	12/8/67	1960-1964	
San Diego, California	SAN	03131	7/1/68	1960-1964	g
Santa Monica, California	SMO	93197	5/17/66	1960-1964	h
Sault Ste. Marie, Michigan	SSM	14847	7/1/68	1960-1964	
Seattle, Washington	SEA	24233	12/8/67	1959-1961	
Shreveport, Louisiana	SHV	13957	6/26/68	1960-1964	
Spokane, Washington	GEG	24157	5/13/68	1960-1964	
Tampa, Florida	TPA	12842	5/13/68	1960-1964	
Topeka, Kansas	TOP	13996	7/1/68	1960-1964	
Tucson, Arizona	TUS	23160	12/8/67	1960-1964	
Washington, D.C.	DIA	93734	3/22/67	1961-1964	i
Winnemucca, Nevada	WMC	24128	6/12/68	1960-1964	
Winslow, Arizona	INW	23194	7/1/68	1962-1964	

Footnotes for Table A-1:

a. At Caribou from 1 August 1963 through 31 December 1964, the hourly airways observations from 0000 through 0400 EST were not taken. Thus, the afternoon computations were not affected in any way. The 0500 and 0600 EST reports were deemed adequate for determining the morning minimum temperature and the average surface wind speed. The only problem arose in the determination of morning P cases, but this was solved by appraisal of hourly precipitation amounts (from automatic precipitation gage records) for the missing hourly reports. This appraisal was only necessary for those mornings when P cases were not determined in the usual manner from the available hourly reports. In order to compare the results, Tabulations I, II, and III were prepared separately for 1960 through 1962 and 1963 through 1964, as well as the complete period 1960 through 1964. None of the differences in the tabulations could be ascribed to the alternate method of determining P cases.

b. The Dayton upper-air soundings were made from Sulphur Grove (979-ft elevation), about 6 miles east-southeast of Cox-Dayton Airport (1002-ft elevation) where the hourly airways observations were made.

c. At Huntington, some of the wind reports for levels aloft within a mixing layer were occasionally missing, necessitating computation of a vertically averaged speed based on incomplete data. Investigation showed, however, that this rarely happened more than a few times a month.

d. At Lander from 1 January 1960 through 31 March 1962, many of the hourly surface observations from 1900 through 0600 MST were not taken (about eight missing per day). All observations for 1200 through 1600 MST were available, however, so that the afternoon maximum temperature and surface wind speed were determined as usual. The 0200 and 0500 MST observations were always taken and were deemed adequate for

determining morning minimum temperatures and average surface wind speeds. The main problem that arose in determining P cases was solved by evaluation of hourly precipitation amounts (from automatic precipitation gage records) for the missing hourly reports. To check these results, Tabulations I, II, and III were prepared separately for 1960 through 1961 and 1962 through 1964, in addition to the entire period of 1960 through 1964. The differences in the tabulations between periods could not be ascribed to the methods of determining P cases.

e. The New York surface and upper-air observations were made at J. F. Kennedy (formerly Idlewild) International Airport.

f. The initial set of tabulations for Portland produced a surprising number of C cases for morning mixing height in the warmer months. This was found to be due to a comparatively late release of the scheduled 1200 GMT radiosonde and an early sunrise (0358 EST on June 15), which together frequently resulted in the surface temperature of the 1200 GMT sounding being greater than the minimum surface temperature plus 5°C. To overcome this problem in computing the urban morning mixing height, the hourly temperature at 0600 EST plus 5°C was used instead of the minimum hourly temperature from 0200 to 0600 EST plus 5°C. It should be noted that upper-air soundings are permitted to begin up to an hour ahead of schedule. Most stations begin a sounding from 45 to 60 minutes prior to schedule, but at Portland the 1200 GMT sounding was seldom begun before 1130 GMT (0630 EST).

g. The San Diego upper-air soundings were made at Montgomery Field (elevation 407 ft) and were used with hourly surface reports for Lindbergh Field (elevation 19 ft). Lindbergh Field is on the shore of San Diego Bay and Montgomery Field is on the coastal plain about 7 miles to the north-northeast.

h. Hourly surface weather observations at Los Angeles International Airport (elevation 97 ft) were used with upper-air soundings at Santa Monica Municipal Airport, Clover Field (elevation 125 ft), about 7 miles to the north-northwest. Both locations are about 2 miles from the coast and in similar suburban or residential surroundings.

i. Upper-air soundings at Dulles International Airport (elevation 279 ft), located in rural surroundings about 23 miles west-northwest of the Capitol, were available for 1961 through 1964, but hourly surface observations there were only available for 1963 through 1964. However, hourly surface observations at Washington National Airport (elevation 14 ft), located in suburban surroundings on the shore of the Potomac River about 4 miles south of the Capitol, were available for 1961 through 1963. Investigation showed that minimum temperatures at National Airport averaged 4.4°F warmer than at Dulles Airport, undoubtedly due to the proximity of National Airport to the built-up area and possibly due to the proximity of the water. Therefore, all calculations of the urban morning mixing height that used hourly observations at National Airport were obtained by adding 2.5°C instead of 5.0°C to the minimum hourly temperature observed from 0200 through 0600 EST. For comparative purposes six sets of tabulations were obtained for various periods of record involving the two-surface observation stations. Comparison of the 1963 mixing heights and wind speeds based on hourly observations at Dulles Airport did not show complete agreement, but it was deemed adequate for climatological purposes. Thus, in keeping with a policy of using surface and upper-air data for the same location whenever possible, the tabulations were based on hourly observations at National Airport for 1961 through 1962, hourly observations at Dulles Airport for 1963 through 1964, and upper-air soundings at Dulles Airport for 1961 through 1964. The user who is only interested in the 4 years of data used in this report should specifically request only the F_1, F_2, and F_3 special tabulations of regular Tabulations I, II, and III, respectively. These mixing-depth and wind-speed tabulations were prepared by the NCC under Job Number 7717.

Table A-2. EXAMPLE OF NATIONAL CLIMATIC CENTER TABULATION III, DAILY $\bar{\chi}/Q$ VALUES

Station	Yr	Mo	Day	Daily mixing depths and average wind speeds									
				Morning					Afternoon				
				T	1	2	3	4	T	1	2	3	4
14842	60	04	01		498	9.7	5.9	3	P	811	17.8	10.3	4
			02	P	1237	11.8	5.7	4		304	13.7	11.0	3
			03		1084	6.5	3.8	4		1038	8.8	6.7	4
			04	P	784	3.0	2.3	3	P	1116	9.8	4.9	4
			05		424	8.0	5.5	3		1644	11.4	10.1	5
			06		151	7.5	4.7	2		1200	15.0	11.3	4
			07		300	9.0	5.4	3		1545	13.4	10.5	5
			08		461	9.0	4.7	3	P	342	12.7	11.5	3
			09		1825	9.2	6.5	6		1867	6.8	6.4	6
			10		123	2.2	2.2	1		1728	9.2	6.2	5
			11	P	582	13.7	9.0	3		909	13.8	10.3	4
			12		86	1.5	1.5	1		1715	10.0	6.7	5
			13		151	7.0	4.5	2		1518	12.4	8.5	5
			14	P	608	8.3	4.2	3	P	469	2.0	2.9	3
			15		413	6.3	3.5	3		1799	7.0	5.1	5
			16	P	234	8.5	6.5	2	P	165	8.5	7.4	2
			17	P	562	7.0	4.3	3	C	–	19.6	12.7	9
			18		153	3.5	2.7	2		1671	2.6	4.0	5
			19		254	6.5	5.3	2		1762	12.8	9.5	5
			20		213	10.0	8.3	2	P	1034	14.0	9.7	4
			21	P	238	4.5	4.0	2		1628	8.0	5.8	5
			22		180	6.5	5.1	2		335	13.3	9.8	3
			23		189	6.5	4.6	2		1394	11.6	8.4	5
			24		103	5.1	5.1	1		1982	11.7	7.5	6
			25		130	3.0	3.0	1		1188	8.5	5.1	4
			26		484	12.7	7.4	3		1021	8.0	7.7	4
			27		59	1.5	1.5	1		1374	5.2	4.7	5
			28		278	4.5	3.7	2		1406	8.4	5.3	5
			29	P	830	14.8	7.3	4		778	5.0	5.7	3
			30	P	1145	15.3	6.9	4	C	–	15.8	10.0	9

Table A-3. EXAMPLE OF NATIONAL CLIMATIC CENTER TABULATION III, SEASONAL MEAN VALUES

Station	Season	Seasonal means of daily mixing depths and average wind speed									
		Morning					Afternoon				
		T	1	2	3	N	T	1	2	3	N
14842	01		327	5.2	3.8	313		533	6.8	5.4	290
		P	675	7.9	5.4	128	P	388	6.6	5.4	110
		C		14.5	4.4	2	C		13.3	7.3	43
14842	02		361	5.7	3.9	327		1353	8.2	6.2	332
		P	695	8.1	5.4	129	P	718	8.3	6.1	105
		C					C		12.6	8.1	19
14842	03		272	3.8	2.6	383		1498	5.8	4.7	391
		P	548	5.9	4.0	70	P	1034	5.8	4.4	61
		C					C		5.6	5.1	1
14842	04		273	4.4	3.1	374		1068	6.7	5.1	381
		P	690	8.1	5.0	78	P	608	7.8	5.8	53
		C					C		12.6	6.6	18

Table A-4. EXAMPLE OF NATIONAL CLIMATIC CENTER TABULATION II, EPISODES

Station	Month	Mix depth, m	Avg wind speed through mix depth, m sec^{-1}	Frequency of episodes, Number of consecutive computations ≥: 2	3	4	5	6	7	8	9	10	11	13	15	17	19	21	25	31	41	51	61	91	121	Total
14842	01	A	2																							15
			4	3																						47
			6	6	2	2																				63
			8	7	4	3																				71
		B	2																							16
			4	7	3	1	1																			62
			6	18	6	3	3	1	1	1																98
			8	26	14	9	6	3	1	1	1	1														127
		C	2																							16
			4	8	3	1	1																			63
			6	25	10	3	3	1	1	1																109
			8	33	19	12	7	3	3	2	1	1														146
		D	2																							16
			4	8	3	1	1																			65
			6	27	10	3	3	1	1	1																113
			8	35	20	13	8	4	3	2	1	1														153
		E	2																							16
			4	8	3	1	1																			65
			6	27	10	3	3	1	1	1																113
			8	35	20	13	8	4	3	2	1	1														153
		F	2																							16
			4	8	3	1	1																			65
			6	27	10	3	3	1	1	1																113
			8	35	20	13	8	4	3	2	1	1														153
		G	2																							16
			4	8	3	1	1																			65
			6	27	10	3	3	1	1	1																113
			8	35	20	13	8	4	3	2	1	1														153

Table A-5. EXAMPLE OF NATIONAL CLIMATIC CENTER TABULATION I, MIXING HEIGHTS BY WIND SPEEDS

Station	Season	Time	Mixing depth, m	Frequency of occurrence: Average wind speed through mixing depth for NOP cases 1	2	3	4	5	6	7	8	9	10	Totals NOP	P	M	
14842	04	02	250*		2	1	2	2	3	6	1			17	14		31
			251-500		2	3	4	3	6	18	4	3		43	12		55
			501-750		2	3	8	4	6	21	7	2	1	54	11		65
			751-1000		2	8	2	10	6	15	9	5	4	61	7		68
			1001-1500		2	15	15	16	14	29	9	16	14	130	6		136
			1501-2000		4	6	8	6	9	12	8	6	5	64	3		67
			2001-2500					1	1	3	5			10			10
			2501-3000										2	2			2
			3001-3500														
			3501-4000														
			>4000														
			NOP Total		14	36	39	42	45	104	43	32	26	381			381
			Total P		1	1	5	5	8	13	9	6	5		53		53
			Total C							4	1	5	8				18
			Missing													3	3
			Total		15	37	44	47	53	121	53	43	39	381	53	3	455

APPENDIX B. ALLOWANCE FOR P-, C-, AND M-TYPE MIXING HEIGHTS AND WIND SPEEDS

NCC tabulations of mean mixing heights and wind speeds are given separately for precipitation (P) and non-precipitation (non-P) cases. These tabulations show a distinct tendency for P mixing heights to be higher in the morning and lower in the afternoon than non-P heights. In the calculations, this happens because of the effects of dense cloudiness. Actually, morning and afternoon mixing heights with precipitation may be expected to be higher than without because in the mixing layer above the condensation level the (lower) pseudoadiabatic lapse rate would be more appropriate than the dry adiabatic lapse rate. However, the effectiveness of this consideration is highly dependent on such assumptions as the water vapor content of the initially lifted parcel, the amount of entrainment as the parcel rises, etc. In view of such complexities and the intended climatological use of the derived data, it was decided to allow for all mixing-height and wind-speed cases other than non-P in an arbitrary manner. C cases (Appendix A, Tabulation III) were treated as P cases since marked cold air advection was assumed to be generally indicative of a comparatively deep mixing layer. Wind speeds for P and C cases were assumed faster than otherwise. The number of missing (M) cases was insignificant.

In allowing for P, C, and M cases, it was assumed that the morning and afternoon mixing heights and wind speeds generally were greater than for non-P cases. The allowance was made through use of NCC Tabulation I (see Table A-5), frequencies of mixing-height classes by wind speed classes. One-half of the total P, C, and M frequencies were proportionately redistributed among the non-P frequencies for mixing-height classes above the mean height (for all speed classes). The remaining one-half of P, C, and M frequencies were redistributed among the non-P frequencies for wind speed classes above the mean speed (for all mixing height classes). Thus, the non-P part of each table of mixing-height class by wind-speed class (see Table A-5) was divided into four sections according to the mean height and mean speed. Approximately one-fourth of the P, C, and M frequencies was redistributed in the upper-right section of the frequency table (i.e. in the non-P section with speeds above the mean and heights below the mean); one-fourth was redistributed in the lower left section (i.e., non-P heights above the mean and speeds below); and one-half was redistributed in the lower-right section (i.e., non-P heights and speeds both above the mean). In the redistributions each individual (cell) frequency of non-P mixing height by wind speed was increased in proportion of its frequency to the total non-P frequency of all cells being considered. The total frequencies of all non-P cells above the mean mixing height and above the mean wind speed each was considered separately. Cells with zero non-P frequencies were unaffected by redistributions as were cells below both the mean mixing height and mean wind speed. Due allowance was made for mean heights and wind speeds that fell within a class interval.

Mean mixing heights and wind speeds given in NCC Tabulation III (see Table A-3) are based on averages of the actual values. The means finally arrived at after the redistributions are the NCC Tabulation III means plus the increase in mean value between the mean based on frequency counts by class intervals before (non-P cases only) and after (all cases) the redistributions. Table B-1 gives mean seasonal and annual values of mixing height and wind speed for both before and after allowance for P, C, and M cases. Percentage frequencies of non-P cases are given also.

Preceding page blank

Table B 1. MEAN SEASONAL AND ANNUAL MORNING AND AFTERNOON MIXING HEIGHTS (U) AND WIND SPEEDS (U) FOR NOP[a] AND ALL[b] CASES

Station	Time[c]	Winter					Spring					Summer					Autumn					Annual				
		H, m			U, m sec^{-1}		H, m			U, m sec^{-1}		H, m			U, m sec^{-1}		H, m			U, m sec^{-1}		H, m			U, m sec^{-1}	
		NOP	All	% NOP	NOP	All	NOP	All	% NOP	NOP	All	NOP	All	% NOP	NOP	All	NOP	All	% NOP	NOP	All	NOP	All	% NOP	NOP	All
Albany, New York	M	576	804	58.0	5.0	6.7	613	786	66.3	5.0	6.1	474	527	83.0	3.7	4.1	491	583	81.1	4.2	4.8	538	675	72.1	4.5	5.4
	A	862	967	60.8	6.9	7.6	1663	1753	69.4	8.3	8.7	1896	1943	79.1	6.8	7.0	1231	1272	80.2	6.9	7.2	1414	1484	72.3	7.2	7.6
Albuquerque, New Mexico	M	345	391	88.9	3.7	4.0	498	553	92.4	4.2	4.5	560	582	93.7	3.6	3.7	377	414	90.3	3.3	3.5	445	485	91.3	3.7	3.9
	A	1402	1464	88.3	5.5	5.8	3426	3452	94.4	8.8	8.9	3902	3941	88.5	5.8	6.0	2247	2295	90.1	5.3	5.5	2744	2788	90.3	6.4	6.5
Amarillo, Texas	M	237	273	83.9	6.5	6.9	311	337	88.7	7.8	8.1	353	379	83.5	7.0	7.4	296	323	87.0	6.5	6.8	299	328	85.7	7.0	7.3
	A	1101	1171	83.0	8.2	8.5	2447	2507	89.6	9.9	10.1	2475	2520	88.9	7.3	7.4	1648	1693	88.4	7.4	7.6	1917	1973	87.4	8.2	8.4
Athens, Georgia	M	328	407	71.2	5.1	6.0	328	383	78.7	4.7	5.3	363	390	82.6	3.6	3.8	278	314	85.5	4.0	4.4	324	374	79.5	4.4	4.9
	A	970	1042	72.4	6.5	7.0	1707	1754	77.8	6.9	7.2	1876	1918	75.7	4.7	4.9	1428	1455	85.3	5.5	5.7	1495	1542	77.8	5.9	6.2
Bismarck, North Dakota	M	272	380	59.7	5.0	6.5	378	474	68.7	5.5	6.5	239	282	80.2	3.9	4.5	255	301	84.4	4.4	5.0	286	359	73.2	4.7	5.6
	A	528	625	60.8	7.0	7.8	1756	1880	74.6	8.7	9.2	2015	2078	84.4	7.0	7.2	1299	1368	83.5	7.8	8.1	1399	1488	75.8	7.6	8.1
Boise, Idaho	M	327	407	68.1	3.6	4.2	342	424	76.7	4.5	5.0	185	193	90.4	3.3	3.4	224	279	79.8	3.8	4.2	269	326	78.7	3.8	4.2
	A	631	754	67.9	4.3	4.9	2244	2329	78.0	6.4	6.7	2511	2540	92.2	5.8	5.9	1320	1409	81.5	5.0	5.3	1676	1758	79.9	5.4	5.7
Brownsville, Texas	M	365	438	74.6	6.4	7.4	722	746	88.9	8.1	8.3	788	794	96.5	7.1	7.2	530	561	89.2	5.6	5.9	601	635	87.3	6.8	7.2
	A	1043	1084	78.3	8.2	8.6	1113	1127	89.4	9.5	9.6	1533	1540	93.0	8.7	8.7	1369	1385	85.8	7.7	7.8	1264	1284	86.8	8.5	8.7
Buffalo, New York	M	595	869	36.6	6.3	8.2	476	627	62.5	5.4	6.4	391	458	80.7	4.2	4.6	462	571	76.7	4.7	5.3	481	631	64.1	5.1	6.1
	A	727	857	34.4	7.2	8.5	1333	1431	56.8	7.5	8.1	1575	1616	81.0	6.5	6.7	1135	1196	73.1	6.5	6.9	1192	1275	61.3	6.9	7.6
Burrwood, Louisiana	M	535	593	81.6	7.0	7.5	701	720	92.6	6.4	6.6	1282	1300	87.8	4.1	4.2	1090	1113	87.5	6.2	6.4	902	932	87.3	5.9	6.2
	A	637	681	76.1	6.8	7.1	804	816	91.3	6.1	6.2	1238	1252	83.7	4.2	4.3	1053	1073	83.1	6.0	6.2	933	956	83.5	5.8	5.9
Cape Hatteras, North Carolina	M	630	725	73.2	7.8	8.5	643	736	78.3	7.6	8.2	780	848	77.4	6.2	6.7	761	846	78.2	6.6	7.2	703	789	76.7	7.0	7.6
	A	701	769	71.5	7.7	8.2	878	945	77.2	8.5	8.8	988	1021	78.7	7.1	7.3	923	962	78.7	7.0	7.3	872	924	76.5	7.6	7.8
Caribou, Maine	M	447	596	54.0	6.1	7.5	475	610	62.8	5.6	6.7	417	508	68.7	4.4	5.1	472	603	65.5	5.3	6.3	452	579	62.7	5.4	6.4
	A	706	823	49.6	7.8	8.9	1511	1618	62.0	7.7	8.2	1817	1883	69.8	7.6	8.0	1099	1191	62.4	7.7	8.3	1283	1379	60.9	7.7	8.3
Charleston, South Carolina	M	296	363	74.8	4.9	5.8	339	385	82.6	4.8	5.3	411	437	84.4	4.2	4.5	264	297	85.7	4.2	4.6	327	371	81.8	4.5	5.1
	A	951	1004	75.0	6.7	7.1	1519	1562	82.4	7.2	7.4	1447	1510	70.7	5.7	6.0	1222	1243	84.8	6.1	6.3	1284	1330	78.2	6.4	6.7
Columbia, Missouri	M	390	448	74.3	6.0	6.5	409	477	73.9	6.6	7.3	294	321	83.3	4.7	5.0	317	358	83.1	5.5	5.9	352	401	78.6	5.7	6.2
	A	797	872	71.5	7.0	7.5	1523	1599	75.8	8.4	8.8	1689	1723	83.9	5.6	5.8	1349	1395	82.2	6.5	6.7	1339	1397	78.3	6.9	7.2
Dayton, Ohio	M	461	557	58.6	6.2	7.1	462	555	67.2	5.9	6.6	349	375	87.4	3.8	4.0	360	417	82.4	4.5	5.0	408	476	73.9	5.1	5.7
	A	749	836	56.4	7.2	7.9	1570	1670	68.3	7.5	8.0	1661	1685	83.9	5.3	5.5	1315	1346	82.6	6.3	6.5	1323	1384	72.8	6.6	7.0

[a] NOP excludes type P, C, and M cases (see text).
[b] ALL includes all cases, with allowances for types P, C, and M (see text).
[c] M, morning, A, afternoon.

Table B-1 (continued). MEAN SEASONAL AND ANNUAL MORNING AND AFTERNOON MIXING HEIGHTS (H) AND WIND SPEEDS (U) FOR NOP[a] AND ALL[b] CASES

Station	Time[c]	Winter					Spring					Summer					Autumn					Annual				
		H, m			U, m sec^{-1}		H, m			U, m sec^{-1}		H, m			U, m sec^{-1}		H, m			U, m sec^{-1}		H, m			U, m sec^{-1}	
		NOP	All	% NOP	NOP	All	NOP	All	% NOP	NOP	All	NOP	All	% NOP	NOP	All	NOP	All	% NOP	NOP	All	NOP	All	% NOP	NOP	All
Denver, Colorado	M	178	219	78.5	4.5	4.8	360	423	82.6	4.3	4.6	243	255	92.6	3.6	3.7	163	174	87.0	3.5	3.6	236	268	85.1	4.0	4.2
	A	1357	1482	80.3	5.8	6.3	2951	3070	80.7	7.2	7.6	3358	3458	79.6	5.9	6.1	2085	2161	86.8	5.1	5.3	2437	2543	81.8	6.0	6.3
Dodge City, Kansas	M	224	266	80.5	6.7	7.3	316	354	81.7	7.7	8.2	302	328	79.6	7.1	7.5	255	283	85.5	6.6	7.0	274	308	81.8	7.0	7.5
	A	811	879	81.4	8.0	8.2	1783	1872	82.8	9.6	9.9	2028	2086	86.1	8.3	8.5	1267	1323	87.3	8.2	8.4	1472	1540	84.4	8.5	8.8
El Paso, Texas	M	360	405	90.7	4.2	4.5	660	690	96.1	5.5	5.7	718	758	89.8	4.0	4.2	385	429	90.3	3.3	3.5	530	571	91.7	4.3	4.5
	A	1421	1460	91.6	5.9	6.1	3211	3222	97.0	8.4	8.4	3696	3721	91.7	5.1	5.2	2118	2148	91.9	4.4	4.5	2611	2638	93.0	5.9	6.1
Ely, Nevada	M	157	193	78.8	4.8	5.1	427	489	83.3	4.7	5.1	108	109	95.0	4.2	4.2	146	161	88.8	4.3	4.5	209	238	86.4	4.5	4.7
	A	1020	1072	30.8	5.2	5.5	2630	2708	79.1	7.1	7.4	3583	3624	87.8	6.9	7.0	2116	2179	88.1	5.9	6.1	2337	2396	83.9	6.3	6.5
Flint, Michigan	M	518	674	49.1	6.0	7.2	429	527	69.6	5.3	6.1	280	328	83.5	3.5	4.0	400	494	77.1	4.5	5.2	406	506	69.8	4.8	5.6
	A	762	862	45.6	7.0	7.8	1496	1608	66.1	7.6	8.2	1697	1734	81.1	6.1	6.3	1213	1268	75.6	6.7	7.1	1292	1368	67.1	6.8	7.4
Glasgow, Montana	M	220	283	73.7	4.7	5.5	347	391	82.6	5.9	6.3	277	304	86.5	5.4	5.7	232	262	88.8	5.0	5.3	269	310	82.9	5.3	5.7
	A	428	524	67.3	6.2	6.9	1855	1971	77.6	7.7	8.1	2409	2454	88.0	7.1	7.2	1257	1307	88.6	7.5	7.7	1487	1564	80.3	7.1	7.5
Grand Junction, Colorado	M	276	329	81.9	3.1	3.4	550	628	86.5	5.1	5.4	290	307	90.4	4.6	4.7	239	273	86.6	3.7	3.9	338	384	86.3	4.1	4.3
	A	1075	1160	83.0	3.1	3.4	3087	3166	86.1	6.3	6.6	3895	3940	87.8	5.9	6.1	2048	2133	86.4	4.4	4.6	2526	2600	85.8	4.9	5.2
Great Falls, Montana	M	447	562	73.5	8.8	9.7	527	643	76.7	6.5	7.3	359	399	89.1	4.4	4.7	422	491	84.2	7.0	7.5	438	524	80.8	6.7	7.3
	A	874	1003	70.8	9.9	10.5	2318	2439	72.2	8.4	8.9	2984	3040	83.3	6.9	7.2	1641	1707	83.3	9.0	9.3	1954	2047	77.4	8.6	9.0
Green Bay, Wisconsin	M	442	573	59.7	5.8	6.9	433	534	70.9	5.4	6.2	323	372	81.7	4.0	4.5	465	543	79.6	4.9	5.5	415	506	72.9	5.0	5.8
	A	632	704	59.7	7.3	7.9	1389	1492	73.3	7.8	8.2	1607	1648	84.1	6.5	6.7	1067	1127	78.0	7.1	7.5	1173	1243	73.7	7.2	7.6
Greensboro, North Carolina	M	389	480	74.8	4.7	5.4	402	492	76.1	4.7	5.4	400	445	80.9	3.8	4.2	290	343	82.4	3.8	4.3	370	440	78.5	4.3	4.8
	A	926	992	71.9	6.4	6.8	1708	1765	78.7	7.1	7.4	1674	1710	78.5	4.9	5.1	1306	1334	84.6	5.6	5.8	1403	1450	78.4	6.0	6.3
Huntington, West Virginia	M	482	634	57.9	4.2	5.3	575	721	70.7	4.6	5.5	300	338	83.0	2.4	2.7	332	403	82.1	2.6	3.1	442	524	73.4	3.4	4.2
	A	963	1079	58.3	5.7	6.4	1872	1986	72.5	6.0	6.5	1596	1641	81.9	4.1	4.3	1300	1340	81.7	4.6	4.9	1432	1511	73.6	5.1	5.5
International Falls, Minn.	M	251	347	54.0	4.3	5.6	319	411	66.3	4.6	5.6	266	337	75.2	3.3	4.1	406	513	70.6	5.1	6.0	310	402	66.5	4.3	5.3
	A	584	656	52.7	6.3	7.0	1540	1646	68.3	7.1	7.5	1688	1747	78.9	6.6	6.9	1054	1146	69.9	7.0	7.4	1216	1299	67.4	6.8	7.2
Jackson, Mississippi	M	379	470	68.8	4.0	4.9	417	467	81.3	4.4	4.9	408	421	91.9	3.0	3.1	305	343	83.0	3.2	3.6	377	425	81.2	3.7	4.1
	A	1014	1088	69.1	5.4	5.9	1503	1543	81.8	6.0	6.2	1803	1830	76.4	4.3	4.5	1319	1349	31.3	4.9	5.1	1409	1453	77.1	5.2	5.4
Jacksonville, Florida	M	345	403	79.4	5.2	5.9	447	477	90.4	5.3	5.6	567	583	91.1	4.3	4.4	418	458	85.9	4.7	5.0	444	480	86.7	4.9	5.2
	A	1058	1104	80.1	6.7	7.0	1639	1667	86.1	7.1	7.2	1681	1712	68.0	5.6	5.8	1321	1342	80.4	6.5	6.5	1424	1456	78.6	6.5	6.7
Lake Charles, Louisiana	M	319	394	71.2	5.8	6.7	418	459	87.3	5.3	5.7	493	506	92.4	4.0	4.1	290	308	90.8	4.3	4.5	380	417	85.4	4.9	5.3
	A	812	867	74.5	7.1	7.5	1164	1179	86.2	6.9	7.0	1365	1392	80.4	5.0	5.2	1299	1315	86.5	5.7	5.8	1162	1188	81.9	6.2	6.4

Table B.1 (continued). MEAN SEASONAL AND ANNUAL MORNING AND AFTERNOON MIXING HEIGHTS (H) AND WIND SPEEDS (U) FOR NOP[a] AND ALL[b] CASES

Station		Winter					Spring					Summer					Autumn					Annual				
		H, m			U, m sec^{-1}		H, m			U, m sec^{-1}		H, m			U, m sec^{-1}		H, m			U, m sec^{-1}		H, m			U, m sec^{-1}	
		NOP	All	% NOP	NOP	All	NOP	All	% NOP	NOP	All	NOP	All	% NOP	NOP	All	NOP	All	% NOP	NOP	All	NOP	All	% NOP	NOP	All
Portland, Maine	M	481	618	70.4	5.6	6.6	533	689	68.5	5.4	6.4	435	501	78.9	4.3	4.8	395	506	74.1	4.7	5.6	461	578	72.0	5.0	5.9
	A	879	945	69.0	7.2	7.8	1384	1479	70.9	8.2	8.7	1414	1476	80.4	7.3	7.6	1083	1141	76.3	7.0	7.4	1190	1260	74.1	7.4	7.8
Rapid City, South Dakota	M	226	363	65.5	4.7	6.2	362	466	73.7	5.8	6.7	298	330	85.4	4.5	4.8	264	314	86.6	5.0	5.5	287	368	77.8	5.0	5.8
	A	848	982	67.7	7.2	7.9	2032	2166	74.6	8.4	8.8	2419	2510	83.5	6.7	6.9	1559	1615	87.0	7.6	7.8	1714	1810	78.2	7.5	7.9
St. Cloud, Minnesota	M	338	393	74.8	5.4	6.1	404	469	77.6	5.6	6.3	328	351	89.4	3.9	4.2	389	429	87.0	5.1	5.5	364	411	82.2	5.0	5.5
	A	537	607	59.7	6.6	7.3	1344	1432	75.7	7.7	8.0	1595	1646	82.8	6.6	6.9	952	1006	80.7	7.4	7.7	1107	1173	74.7	7.1	7.5
Salem, Oregon	M	325	431	56.2	3.0	3.8	432	627	55.4	2.3	2.9	379	424	89.1	2.0	2.2	292	404	68.1	2.2	2.8	357	471	67.2	2.4	2.9
	A	622	787	50.4	3.7	4.5	1614	1733	56.3	4.3	4.8	1655	1632	86.1	4.4	4.5	1115	1212	67.9	4.2	4.6	1251	1354	65.1	4.1	4.6
Salt Lake City, Utah	M	254	329	71.9	3.7	4.3	317	419	73.7	4.8	5.4	198	216	88.9	4.4	4.6	198	238	84.8	4.3	4.6	241	300	79.8	4.3	4.7
	A	808	944	67.9	4.0	4.6	2548	2675	74.9	6.2	6.6	3673	3737	85.9	6.0	6.2	1821	1933	83.7	5.2	5.5	2212	2322	78.0	5.2	5.7
San Antonio, Texas	M	370	459	71.7	5.0	5.8	678	748	78.9	6.0	6.5	897	915	92.0	5.6	5.7	595	654	84.0	5.1	5.5	635	694	81.6	5.4	5.9
	A	1065	1112	79.0	6.5	6.8	1529	1552	88.7	7.1	7.2	2108	2119	91.7	5.9	6.0	1542	1572	87.5	6.0	6.1	1561	1589	86.7	6.4	6.5
San Diego, California	M	468	534	88.1	2.0	2.2	807	851	91.1	2.6	2.7	531	538	95.4	2.0	2.0	558	578	95.0	2.0	2.1	591	625	92.4	2.2	2.2
	A	989	1021	91.4	4.2	4.3	1056	1085	92.6	5.1	5.2	564	566	93.5	4.1	4.1	819	834	95.8	4.3	4.3	857	877	94.5	4.4	4.5
Santa Monica, California	M	376	422	85.4	2.8	3.0	651	676	92.6	2.7	2.8	552	562	94.1	1.9	1.9	487	510	91.9	2.3	2.4	516	542	91.0	2.4	2.5
	A	863	893	91.6	4.4	4.5	946	963	95.0	5.9	6.0	603	603	99.4	5.1	5.1	785	798	95.8	4.8	4.8	799	814	95.4	5.1	5.1
Sault Ste. Marie, Michigan	M	385	532	33.9	4.8	6.1	390	493	66.1	4.7	5.5	278	322	76.1	3.7	4.2	519	675	64.2	4.9	5.8	393	508	60.0	4.5	5.4
	A	582	700	33.4	5.9	7.0	1152	1243	66.3	7.3	7.7	1394	1433	79.1	6.9	7.1	1024	1125	60.7	7.0	7.6	1038	1125	59.8	6.8	7.3
Seattle, Washington	M	626	824	49.8	5.1	6.2	681	838	55.1	4.6	5.5	552	576	85.1	4.0	4.2	476	585	61.5	4.3	5.0	578	705	62.8	4.5	5.2
	A	585	718	45.8	4.7	5.4	1490	1577	56.5	5.7	6.2	1358	1419	89.5	4.8	4.9	898	987	66.3	4.6	5.0	1092	1175	64.5	4.9	5.4
Shreveport, Louisiana	M	430	508	72.4	5.7	6.3	555	566	83.9	6.3	6.7	469	482	92.2	4.7	4.8	391	430	86.2	4.5	4.8	451	497	83.6	5.3	5.7
	A	1016	1088	72.8	6.2	6.7	1441	1484	82.4	6.8	7.1	1802	1823	85.4	4.7	4.8	1385	1414	85.3	5.2	5.4	1411	1452	81.4	5.7	6.0
Spokane, Washington	M	336	414	60.2	4.7	5.7	341	401	74.1	5.2	5.8	234	259	88.3	4.1	4.4	218	266	75.0	3.8	4.3	282	335	74.4	4.4	5.1
	A	430	523	56.9	4.8	5.6	1661	1943	72.0	6.1	6.5	2533	2559	87.8	5.2	5.3	1261	1362	74.7	5.0	5.4	1521	1597	72.8	5.3	5.7
Tampa, Florida	M	394	436	85.8	5.8	6.1	503	526	91.7	5.6	5.8	656	678	91.1	4.2	4.3	419	439	89.2	5.4	5.6	493	519	89.4	5.3	5.4
	A	1052	1079	81.4	6.4	6.6	1523	1544	87.8	6.7	6.8	1460	1526	68.9	5.0	5.3	1401	1429	84.4	6.4	6.8	1359	1394	80.6	6.2	6.4
Topeka, Kansas	M	381	448	73.7	5.9	6.6	454	529	75.9	7.0	7.8	371	406	80.4	5.2	5.6	317	361	81.3	5.0	5.6	380	436	77.8	5.6	6.4
	A	801	876	74.6	7.4	7.9	1441	1512	77.2	9.3	9.6	1503	1542	86.1	6.8	7.0	1228	1267	82.2	7.5	7.8	1243	1299	80.0	7.8	8.1
Tucson, Arizona	M	216	247	90.7	4.3	4.5	244	260	96.5	4.2	4.3	335	356	90.0	3.8	3.9	225	241	93.0	4.4	4.5	255	276	92.5	4.2	4.3
	A	1390	1424	88.3	5.0	5.2	2659	2664	97.8	6.8	6.8	3040	3110	82.2	5.3	5.5	2073	2110	89.5	4.9	5.0	2290	2347	89.4	5.5	5.6

Table B.1 (continued). MEAN SEASONAL AND ANNUAL MORNING AND AFTERNOON MIXING HEIGHTS (H) AND WIND SPEEDS (U) FOR NOP[a] AND ALL[b] CASES

Station	Time[c]	Winter					Spring					Summer					Autumn					Annual				
		H, m			U, m sec^{-1}		H, m			U, m sec^{-1}		H, m			U, m sec^{-1}		H, m			U, m sec^{-1}		H, m			U, m sec^{-1}	
		NOP	All	% NOP	NOP	All	NOP	All	% NOP	NOP	All	NOP	All	% NOP	NOP	All	NOP	All	% NOP	NOP	All	NOP	All	% NOP	NOP	All
Lander, Wyoming	M	188	223	83.9	2.5	2.8	427	511	81.7	3.3	3.7	326	337	95.4	2.7	2.7	265	322	86.2	2.6	2.9	301	348	86.5	2.8	3.0
	A	808	926	82.1	3.6	4.1	2629	2755	79.4	6.4	6.9	3406	3490	84.4	6.3	6.6	1907	2030	85.1	4.6	5.0	2167	2380	82.7	5.2	5.6
Las Vegas, Nevada	M	266	321	92.0	4.2	4.5	405	433	95.4	5.4	5.6	283	292	97.2	4.6	4.7	242	276	94.3	4.1	4.3	299	331	94.7	4.6	4.8
	A	1123	1153	94.0	4.1	4.2	2769	2785	95.2	7.0	7.1	3672	3693	92.0	6.6	6.7	2015	2106	95.6	5.1	5.2	2410	2434	94.2	5.7	5.8
Little Rock, Arkansas	M	451	541	76.3	4.6	5.2	460	544	77.8	5.0	5.7	355	375	90.0	3.5	3.7	303	342	86.2	3.4	3.8	392	450	82.5	4.1	4.6
	A	996	1101	72.1	6.1	6.6	1554	1612	80.0	6.7	7.0	1817	1851	84.1	4.3	4.9	1360	1401	84.6	5.0	5.2	1431	1491	80.2	5.7	5.9
Medford, Oregon	M	289	387	60.6	1.5	1.9	392	535	68.0	1.8	2.2	259	285	93.7	1.2	1.3	220	293	75.0	1.1	1.3	290	375	74.3	1.4	1.7
	A	747	933	65.0	2.2	2.8	2004	2079	67.6	4.5	4.8	2332	2349	92.0	4.6	4.6	1481	1594	77.6	3.2	3.5	1641	1738	75.5	3.6	3.9
Miami, Florida	M	654	707	87.2	5.4	5.7	947	980	91.1	5.7	5.5	1041	1071	88.3	4.3	4.5	872	933	82.4	5.0	5.3	878	923	87.2	5.1	5.3
	A	1208	1221	89.2	6.4	6.5	1440	1459	87.4	6.8	6.9	1360	1383	73.7	5.3	5.5	1315	1341	78.7	6.6	6.9	1330	1351	82.2	6.3	6.5
Midland, Texas	M	249	290	83.4	5.1	5.7	405	429	90.9	7.3	7.5	583	606	90.2	7.0	7.2	388	419	87.9	5.7	6.0	406	436	88.1	6.3	6.6
	A	1222	1276	84.5	7.5	7.8	2408	2449	92.4	8.9	9.0	2716	2744	90.7	6.6	6.7	1649	1887	89.7	6.6	6.7	2048	2089	89.3	7.4	7.5
Montgomery, Alabama	M	387	484	72.1	4.2	5.0	382	431	82.6	3.9	4.3	430	444	92.0	3.4	3.5	294	323	86.8	3.3	3.6	373	420	83.3	3.7	4.1
	A	988	1060	72.1	5.8	6.3	1590	1622	84.4	5.8	6.0	1770	1801	79.6	4.1	4.4	1380	1402	86.7	4.8	4.9	1432	1471	80.4	5.2	5.4
Nantucket, Massachusetts	M	760	905	63.7	8.5	9.5	588	734	66.3	7.5	8.4	389	448	75.9	5.7	6.2	625	739	72.3	6.9	7.6	595	707	69.5	7.1	7.9
	A	791	890	59.7	9.0	9.8	746	827	74.6	8.4	8.8	609	667	77.4	7.1	7.3	765	831	70.6	7.9	8.3	727	804	70.6	8.1	8.6
Nashville, Tennessee	M	440	563	62.8	4.3	5.2	500	606	73.7	4.8	5.6	417	441	89.4	3.2	3.4	301	357	81.1	3.0	3.5	414	492	76.7	3.8	4.4
	A	1035	1123	66.6	6.2	6.8	1713	1783	75.4	6.8	7.1	1845	1874	80.9	4.6	4.8	1438	1473	80.9	5.1	5.3	1507	1563	75.9	5.7	6.0
New York, New York	M	875	986	71.5	8.3	9.1	788	918	72.0	6.9	7.7	662	711	82.0	5.5	5.8	675	741	82.6	6.6	7.1	750	839	77.0	6.8	7.4
	A	901	976	67.5	8.2	8.8	1360	1466	75.4	8.7	9.1	1512	1570	82.0	6.8	7.0	1086	1132	80.7	7.4	7.7	1214	1286	76.4	7.8	8.2
North Platte, Nebraska	M	209	284	72.1	4.3	5.3	317	383	73.0	5.9	6.8	321	361	80.9	5.4	5.9	238	287	82.0	4.3	4.9	271	329	77.0	5.0	5.7
	A	886	986	77.4	7.6	8.1	1778	1894	76.1	8.7	9.1	1717	1756	98.7	7.3	7.4	1356	1400	88.6	7.5	7.7	1434	1509	82.7	7.8	8.1
Oakland, California	M	386	453	78.3	2.9	3.3	709	763	84.6	3.9	4.2	515	527	93.3	3.2	3.3	464	508	85.3	2.7	2.9	516	563	85.3	3.2	3.4
	A	649	709	80.1	4.1	4.4	1087	1121	87.6	6.5	6.6	643	644	98.0	5.9	5.9	745	770	89.5	5.0	5.1	781	811	88.8	5.4	5.5
Oklahoma City, Oklahoma	M	296	342	78.1	6.9	7.5	409	457	82.0	8.7	9.2	344	367	83.5	6.9	7.2	309	343	83.1	6.7	7.2	339	377	81.6	7.3	7.8
	A	804	859	78.8	8.1	8.4	1447	1506	82.0	9.8	10.0	1830	1862	88.5	7.2	7.3	1256	1302	85.5	7.7	7.9	1336	1382	83.7	8.2	8.4
Peoria, Illinois	M	327	392	69.3	5.2	5.9	361	421	71.1	5.7	6.4	272	305	83.3	3.8	4.2	273	321	82.2	4.4	4.9	308	362	76.4	4.8	5.4
	A	533	594	64.2	6.8	7.3	1353	1443	72.2	8.2	8.7	1498	1532	85.0	5.8	6.0	1068	1104	83.7	6.7	6.9	1113	1168	76.2	6.9	7.2
Pittsburgh, Pennsylvania	M	419	634	42.3	4.7	6.5	404	536	61.1	4.2	5.1	333	382	82.8	3.1	3.5	404	488	79.3	3.7	4.3	390	510	66.3	3.9	4.9
	A	811	920	45.1	6.9	7.9	1753	1892	60.9	7.7	8.4	1794	1827	82.2	5.4	5.6	1365	1409	78.7	6.2	6.5	1430	1512	66.7	6.5	7.1

Table B.1 (continued) MEAN SEASONAL AND ANNUAL MORNING AND AFTERNOON MIXING HEIGHTS (H) AND WIND SPEEDS (U) FOR NOP[a] AND ALL[b] CASES

Station		Winter					Spring					Summer					Autumn					Annual				
		H, m			U, m sec^{-1}		H, m			U, m sec^{-1}		H, m			U, m sec^{-1}		H, m			U, m sec^{-1}		H, m			U, m sec^{-1}	
		NOP	All	% NOP	NOP	All	NOP	All	% NOP	NOP	All	NOP	All	% NOP	NOP	All	NOP	All	% NOP	NOP	All	NOP	All	% NOP	NOP	All
Washington, D.C.	M	539	672	74.0	5.3	6.3	481	585	77.5	4.7	5.4	378	421	84.0	3.1	3.4	359	436	83.2	3.7	4.4	439	528	79.6	4.2	4.9
	A	963	1054	71.5	6.7	7.3	1795	1890	74.5	7.5	7.9	1884	1924	83.4	5.4	5.6	1371	1412	84.3	6.2	6.4	1503	1570	78.4	6.4	6.8
Winnemucca, Nevada	M	231	301	82.2	2.8	3.3	343	434	83.6	3.6	4.1	111	129	85.2	2.6	2.7	179	255	82.6	2.9	3.4	217	280	83.5	3.0	3.4
	A	1001	1067	82.5	4.5	4.5	2489	2756	83.5	6.6	6.8	3627	3956	92.6	6.1	6.2	2095	2150	90.3	5.2	5.4	2356	2407	87.2	5.6	5.8
Winslow, Arizona	M	205	223	91.1	2.8	3.0	241	270	94.5	4.0	4.2	221	232	93.8	3.2	3.3	198	213	91.9	2.5	2.6	216	234	92.7	3.1	3.3
	A	1078	1178	91.5	5.3	5.6	3160	3175	94.6	8.8	8.9	3801	3240	87.3	6.9	7.1	2243	2303	88.3	5.0	5.2	2570	2613	90.4	6.5	6.7

APPENDIX C. DERIVATION OF URBAN DISPERSION MODEL

Following the discussion in the main body of this report, consider a city with along-wind length S (meters m) and cross-wind width 2B located in a rectangular coordinate system with the wind along the x-axis and the origin at ground-level of the midpoint along the upwind side of the city:

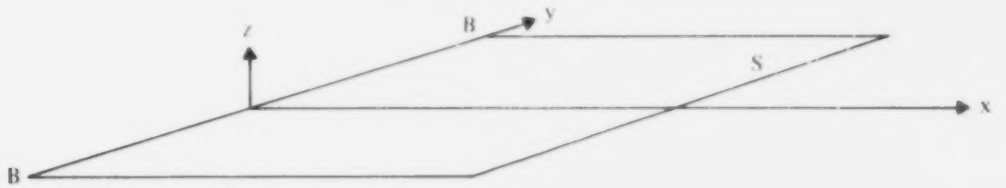

Assume a uniform average area emission rate Q (g m $^{-2}$ sec $^{-1}$) at ground-level over the city, perfect reflection from the ground, and no restriction on vertical mixing. The ground-level concentration χ(g m $^{-3}$) within the city (i.e., $o < x \leq S$) along the center-line wind through the city and at distance x from the origin may be written

$$\chi(x,o,o) = \int_{o}^{x} \int_{-B}^{B} \frac{2Q}{2\pi \sigma_y \sigma_z U} \exp\left[\frac{(y_o - b)^2}{2\sigma_y^2}\right] dy_o\, dx_o \qquad (1)$$

where x_o, y_o = downwind and lateral distances (m) of infinitesimal area source $dx_o dy_o$ from origin

σ_y, σ_z = lateral and vertical diffusion functions = lateral and vertical standard deviations (m) of Gaussian concentration distributions at downwind distance $x - x_o$ from source.

U = average wind speed (m sec $^{-1}$) through the mixing layer.

For situations where x and thus σ_y is not large compared to 2B, the error in concentration at (x,o,o) will not be large if in equation (1) -B and B are replaced by $-\infty$ and ∞, yielding

$$\chi(x,o,o) = \int_{o}^{x} \frac{2Q}{\sqrt{2\pi}\, \sigma_z U} dx_o \qquad (2)$$

In addition to he foregoing assumption, the general nature of the model being developed here suggests that it is more appropriate for large than small cities, say larger than about 10 km.

In this model, it is desirable to consider travel time t instead of travel distance x from the upwind edge of the city. The effect of this consideration is that the faster the winds, the less steep the profile of the upper edge of the pollutant plume. In terms of the travel time from the source to the place where the concentration is desired (i.e., in terms of $t - t_o = \tau$) equation (2) becomes

$$\chi(t,o,o) = \int_{o}^{t} \frac{2Q\, d\tau}{\sqrt{2\pi}\, \sigma_z} \qquad (3)$$

with σ_z now a function of τ. To integrate equation (3) a mathematical expression is needed for $\sigma_z(\tau)$. Smith and Singer (1966) have given expressions for $\sigma_z(x)$ for classes of atmospheric stability. Using the wind speeds of Singer and Smith (1966) that correspond to their stability classes, their expressions for $\sigma_z(x)$ may be converted to $\sigma_z(\tau)$. Since this model implicitly assumes that relatively vigorous vertical mixing occurs in the mixing layer, $\sigma_z(\tau)$ was derived as the average of "very unstable" and "unstable" stability classes (Brookhaven gustiness types B_2 and B_1). The resulting equation is

$$\sigma_z(\tau) = 1.558\tau^{0.885} \tag{4}$$

which substituted in equation (3) gives

$$\chi(t) = 4.453\bar{Q}t^{0.115} \tag{5}$$

Equation (5) gives the concentration at any travel time (or distance) within the city from the upwind edge of the city. The highest concentration occurs at the downwind edge of the city (i.e., at travel time $t = S/U = T$). In reality, for most cities the highest concentration does not necessarily occur at the downwind edge because actual emissions are not uniform, constant, necessarily at ground level, etc. In view of these circumstances and the assumptions of the model, the city-wide *average* concentration is considered a more appropriate output of the model. It is obtained by integrating equation (5) again. Thus, the average concentration over the city, normalized for average area emission rate, is

$$\bar{\chi}/\bar{Q} = 3.994\ T^{0.115} \tag{6}$$

Up to this point the mixing layer has been considered as unbounded above ground. If, however, the mixing layer is only of depth H (e.g., bounded aloft by a relatively stable layer), it is assumed that:

1. Vertical diffusion from each elemental source follows the Gaussian distribution out to a defined travel time t_H that is a function of H.
2. After the time t_H the vertical distribution of pollutant is uniform.

Therefore, equation (5) is valid only where $t \leq t_H$ and equation (6), only when $T \leq t_H$. For cases where $t \geq t_H$ equation (3) is modified to

$$\chi(t)/\bar{Q} = \int_0^{t_H} \frac{2\tau^{0.885}}{\sqrt{2\pi}\,1.558}\,d\tau + \int_{t_H}^{t} \frac{d\tau}{H} \tag{7}$$

t_H is the travel time where, assuming a Gaussian vertical distribution, the ground-level concentration from a source equals the concentration resulting from a uniform vertical distribution within the mixing layer. This is given by $2Q/\sqrt{2\pi}\,\sigma_z = Q/H$, or, using equation (4) with $\tau = t_H$,

$$t_H = 0.471\ H^{1.130} \tag{8}$$

To obtain the normalized concentration averaged over the city, $\bar{\chi}/Q$ (sec m^{-1}), for $T \geq t_H$ equation (7) is appropriately integrated again, yielding

$$\bar{\chi}/\bar{Q} = 1/T \left\{ 3.9994\, t_H^{1.115} + 4.453\, t_H^{0.115} (T - t_H) + \frac{(T - t_H)^2}{2H} \right\} \quad (9)$$

Equations (6) and (9) for $T \leq t_H$ and $T \geq t_H$, respectively, were used to generate values of $\bar{\chi}/\bar{Q}$ as a function of H, U, and S. For S greater than about 10 km, the variation of $\bar{\chi}/\bar{Q}$ against S is practically linear, as shown in Figure C-1, and permits simple interpolation according to S. Table 1, which is discussed in the main body of this report, gives values of $\bar{\chi}/\bar{Q}$ for S-values of 10 and 100 km as a function of various combinations of H and U. The values of H and U that were used are the mid-points of the class intervals in NCC Tabulation I (see Appendix A) with three exceptions. For the upper unbounded class intervals of H greater than 4000 m and U greater than 12.0 m sec^{-1}, values of 4500 m and 13.0 m sec^{-1} were assumed; for the U-interval of calm–1.0 m sec^{-1} a value of 0.75 m sec^{-1} was assumed.

Although the model has been presented only in terms of a uniform average area emission rate, it can be shown that the resulting average concentrations are the same as those for which the emission rate varies linearly along the wind through the city (no lateral variation) from zero at the upwind edge of the city, to a value of $2\bar{Q}$ at the center of the city (i.e., at $x = S/2$), to zero at the downwind edge of the city. In the case of the variable emission rate, the highest concentration does not necessarily occur at the downwind edge of the city, but usually near the middle of the city. Nevertheless, it view of the assumptions in the model, the average concentration over the city is considered most appropriate for applications in this study.

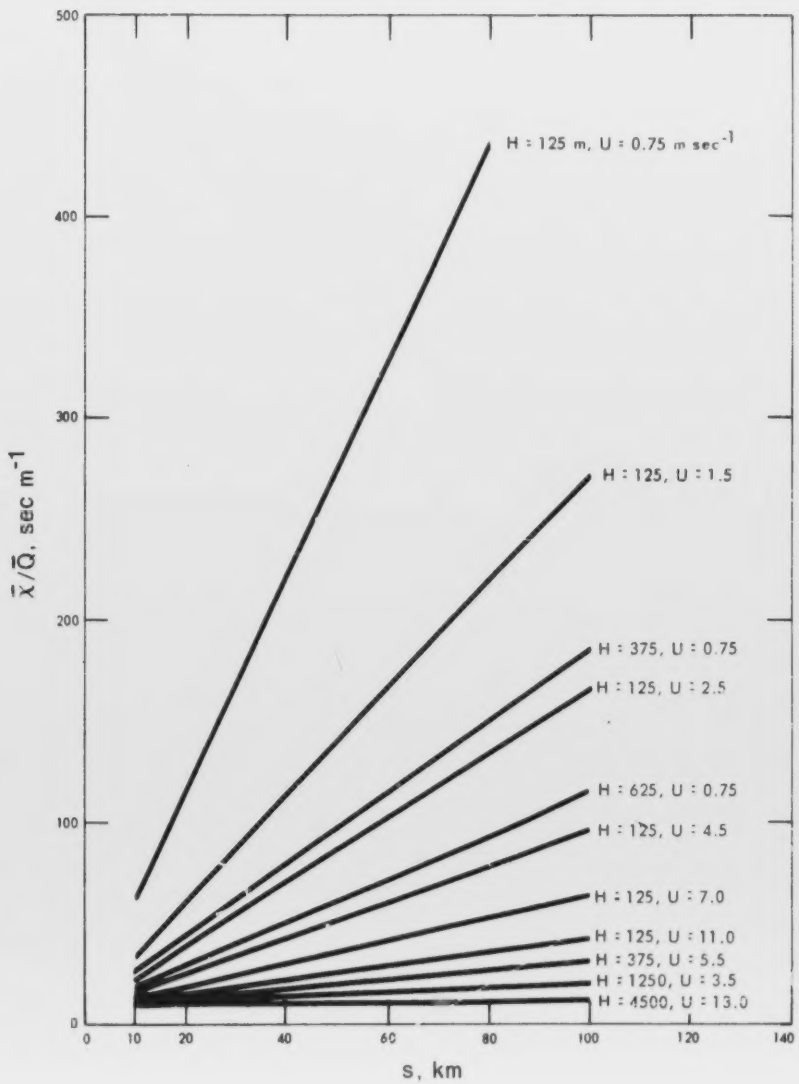

Figure C-1. Variation of $\bar{X}/\bar{Q}$ (see text) with city size (S) for various combinations of mixing height (H) and wind speed (U).

REFERENCES

Clark, J.F., 1969: Nocturnal urban boundary layer over Cincinnati, Ohio. *Mon. Weather Rev. 97:* 582-589.

DeMarrais, G.A., 1961: Vertical temperature differences observed over an urban area. *Bull. Amer. Meteor. Soc. 42:* 548-554.

Duckworth, F.S., and J.S. Sandberg, 1954: The effect of cities upon horizontal and vertical temperature gradients. *Bull. Amer. Meteor. Soc. 35:* 198-207.

Gross, E., 1970: The national air pollution potential forecast program. ESSA Tech. Memo. WBTM NMC 47. National Meteorological Center, Suitland, Maryland. 28 pp.

Hanna, S.R., 1969: The thickness of the planetary boundary layer. *Atmos. Env. 3:* 519-536.

Holzworth, G.C., 1964a: Some meteorological aspects of community air pollution. *Air Eng. 6:* 26-28 and 33-37.

Holzworth, G.C., 1964b: Estimates of mean maximum mixing depths in the contiguous United States. *Mon. Weather Rev. 92:* 235-242.

Holzworth, G.C., 1967: Mixing depths, wind speeds, and air pollution potential for selected locations in the United States. *J. Appl. Meteor. 6:* 1039-1044.

Holzworth, G.C., 1970: Meteorological potential for urban air pollution in the contiguous United States. Paper No. ME-20C. Presented at the Second International Clean Air Congress, Washington, D.C., December 6-11, 1970. 22 p.

Hosler, C.R., 1961: Low-level inversion frequency in the contiguous United States. *Mon. Weather Rev. 89:* 319-339.

Hosler, C.R., 1964: Climatological estimates of diffusion conditions in the United States. *Nuclear Safety 5:* 184-192.

Korshover, J., 1967: Climatology of stagnating anticyclones east of the Rocky Mountains, 1936-1965. Public Health Service Publication No. 999-AP-34, Cincinnati, Ohio, 15 p.

Lucas, D.H., 1958: The atmospheric pollution of cities. *Int. J. Air Poll. 1:* 71-86.

McCaldin, R.O., and R.F. Sholtes, 1970: Mixing height determinations by means of an instrumented aircraft. Paper No. ME-39G. Presented at the Second International Clean Air Congress, Washington, D.C., December 6-11, 1970. 23 p.

Miller, M.E., and G.C. Holzworth, 1967: An Atmospheric diffusion model for metropolitan areas. *J. Air Poll. Control Assoc. 17:* 46-50.

Singer, I.A., and M. E. Smith, 1966: Atmospheric dispersion at Brookhaven National Laboratory. *Int. J. Air and Water Poll. 10:* 125-135.

Smith, M.E., and I.A. Singer, 1966: An improved method of estimating concentrations and related phenomena from a point source emission. *J. Appl. Meteor. 5:* 631-639.

Stackpole, J.D., 1967: The air pollution potential forecast program. Weather Bureau Tech. Memo., WBTM-NMC 43, National Meteorological Center, Suitland, Maryland. 8 p.

Summers, P.W., 1967: An urban heat island model; its role in air pollution problems with application to Montreal. Proc. First Canadian Conf. on Micrometeorology, Toronto, Ontario, Canada. April 12-14, 1965. Dept. of Transport, Canada.

U.S. Dept. Commerce, Weather Bureau. Local climatological data (supplement). Published monthly through 1964 for selected stations.

*U.S. GOVERNMENT PRINTING OFFICE: 1972-484-482 45 1-3